NUCLEAR AND ELECTRONIC SPIN MAGNETIC RESONANCE[1]

JOHN E. WERTZ

School of Chemistry, University of Minnesota, Minneapolis 14, Minnesota

Received June 1, 1955

CONTENTS

Part I. Nuclear spin resonance

Part II. Electron spin resonance of nearly free dipoles

[1] This review was prepared at the request of and was supported by The United States Air Force under Contract AF 18(600)-479, monitored by the Office of Scientific Research, Air Research and Development Command.

Part I. Nuclear Spin Resonance

I. INTRODUCTION

The terms "nuclear magnetic resonance" and "paramagnetic resonance" are now appearing commonly in chemical journals, but to many the effects still seem mysterious. This article attempts to explain the principles, applications, and limitations of the methods to those who are interested in a qualitative understanding of the phenomena without recourse to extensive background material. A quantitative treatment of the subject would require a lengthy treatise.

The field could appropriately have been called Zeeman-level spectroscopy. The word "magnetic" is given undue prominence, for while a magnetic field is usually used, it may be considered merely as a tool to pry apart energy levels so that one may study transitions between them. Some observations have indeed been made in the absence of an externally applied field, using internal dipolar fields. "Nuclear resonance" is also a paramagnetic phenomenon, so that the term "paramagnetic resonance" is not uniquely descriptive. To focus attention on the essential nature of the phenomena, the terms "nuclear spin resonance" (NSR) and "electronic spin resonance" (ESR) will be used here. The term "nuclear induction" (used in the electromagnetic sense) is entirely appropriate for some methods of observation and will also be used. However, the term "resonance" seems peculiarly apt, for if one scans all of the radiofrequency and microwave spectrum one may see only a single line so narrow that its width cannot be plotted narrow enough except on a very restricted frequency scale.

Electron spin resonance was discovered by Zavoisky in 1945 (619). The independent discovery of nuclear induction by Bloch, Hansen, and Packard (74, 75) and of nuclear resonance absorption by Purcell, Torrey, and Pound (451) shortly thereafter was a major experimental triumph. The essential features of

the phenomena were elucidated in two masterful papers (69, 84), which have laid a solid foundation and have served to stimulate a host of experimental and theoretical investigations.

Although these are purely physical techniques, there are few aspects of the observed phenomena which have not already been shown to have chemically interesting applications. The following list is not intended to be complete but to demonstrate the variety of such applications:

1. Structure determination or analysis by observation of individual lines due to non-equivalent dipoles (NSR and ESR).
2. Determination of the nature of adjacent groups (NSR) or the extent of electron wanderings (ESR) by observation of further splitting of lines.
3. Determination of bond character (NSR and ESR).
4. Detection of association or dissociation and measurement of equilibrium constants (NSR and ESR).
5. Detection of chemical exchange and estimation of its rate (NSR).
6. Detection and interpretation of internal motion in solids (NSR).
7. Detection and characterization of defects in solids (NSR and ESR).
8. Magnetic susceptibility measurements (NSR and ESR).
9. Determination of interproton distances in solids (NSR).
10. Establishment of oxidation state (ESR).
11. Detection and identification of radical intermediates (ESR).
12. Establishment of an electronegativity scale for aromatic hydrocarbons (ESR).

This review, like others, betrays the mental astigmatism of its author, who acknowledges his indebtedness to the extensive literature of the field where specific references have not been given. Basic principles of resonance are explained in references 135 and 404. Brief accounts are given in references 57, 71, 133, 195, 446, 448, and 449. Emphasis is placed on solids in references 404, 523, and 528, on relaxation aspects in references 172, 201, and 528, on analysis in reference 510, and on nuclear and solid-state physics in reference 458. The year 1953 is covered in reference 406. A concise summary is given in reference 206. The general aspects of nuclear spin resonance and of the electron resonance of nearly free dipoles are covered here, beginning with their discovery. The area of crystalline fields has been extensively treated (66) and is slighted here, as is the determination of nuclear moments. Molecular beam methods, pure quadrupole resonance, and ferromagnetic and antiferromagnetic resonance are not included. The search of the literature was completed early in 1955.

II. THE ORIGIN OF SPIN RESONANCE

Pursuit of the details of molecular structure and molecular environment is the occupation of all chemists part of the time and of some chemists all of the time. In this pursuit it would be desirable to have some modern version of Maxwell's demon, walkie-talkie equipped, capable of following electrons and nuclei as they change their positions and energies. These demons would transmit reports

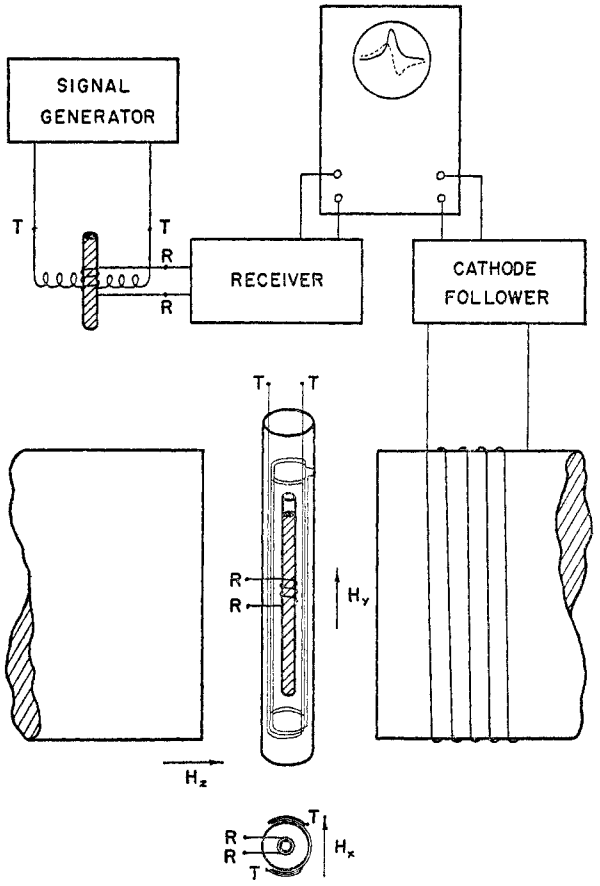

FIG. 1. Nuclear induction apparatus

on their environment upon stimulation—in code, of course. For convenience, their receiver tuning should be remotely controllable over a wide range, with transmission occurring at the same frequency. If clever enough to break the code, one would possess an embarrassing wealth of information. Fortunately it is unnecessary to invoke demonic aid, for the magnetic dipoles in nuclei and in atoms in which the electrons have not been silenced by pairing are precisely such transmitters under the proper conditions. Since they do not have their own generators, a carrier must be provided for them. The information is carried in the modulation of amplitude or frequency.

Lest the suggestion of nuclei and electrons broadcasting on their own channels be taken as unseemly levity, one hastens to adduce experimental results for the proton as a representative nucleus. Let coils at right angles both to one another and the magnetic field H_z as in figure 1 serve to transmit and receive, respectively. (The split transmitter coils attempt to preserve radial symmetry around the sample.) The source is a signal generator in the megacycle region, provided with

an attenuator to keep the transmitter power continuously at a low level. The receiver coil is connected to a communications receiver. A small tube of water is placed inside the receiver coil (inner), which is directly connected to a radio receiver. The physically trained reader will observe that the orthogonal arrangement of coils avoids saturating the receiver. To place the nuclear transmitters into a standby condition, the coils T-T are energized at a convenient frequency f and the field H_z is turned on to a value just less than H_z^* given by the expression:

$$f = 4.257 \times 10^{-3} H_z^* \tag{1}$$

where f is expressed in megacycles per second (Mcps). (This equation will later be justified.) To be specific, let $f = 30.00$ Mcps, and H_z^* will be 7047 gauss. The field will now be slowly increased. Suddenly, at the field value H_z^* the beat note in the receiver speaker will change briefly in intensity. One can repeat the experiment without manually adjusting the field. The amplified output of the saw-

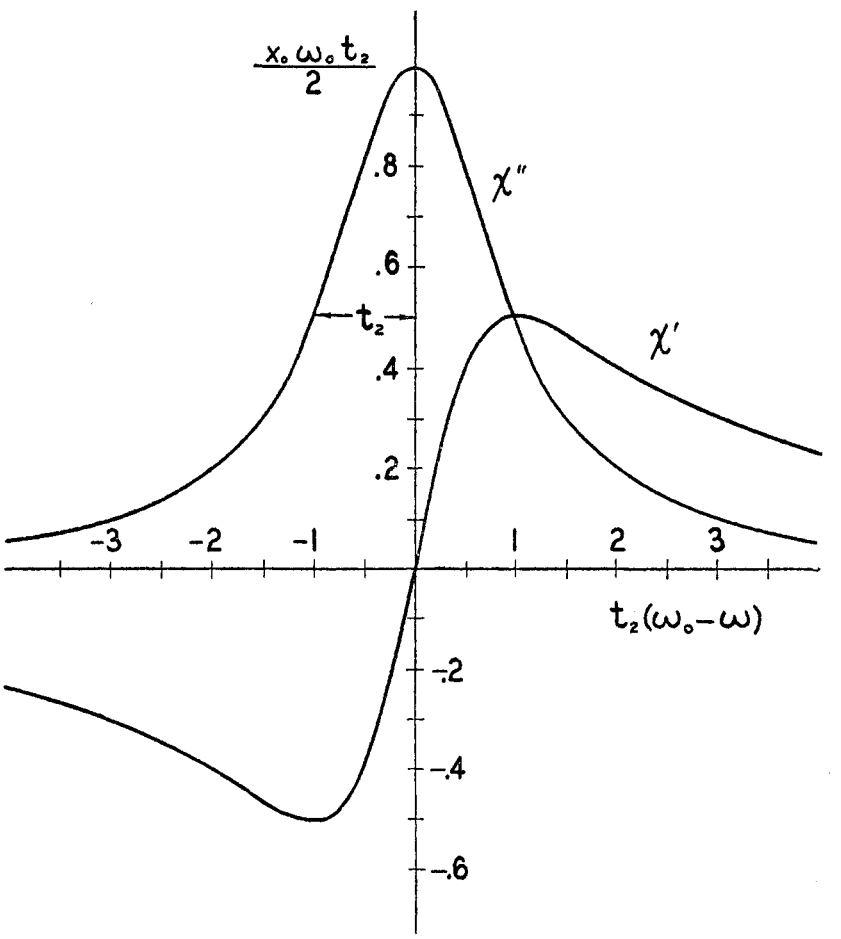

FIG. 2. Absorption (χ'') and dispersion (χ') curves of Lorentz shape represented by susceptibility components χ'' and χ' (404).

tooth generator of an oscilloscope will be connected through an impedance-matching device (cathode follower) to a third set of coils so that the field is linearly swept through H_z^* at some low frequency ($\sim$0.1 cps). To obtain a visual indication, the D.C. input terminals of the oscilloscope are connected to the detector output of the receiver. An unsymmetrical curve is traced by the electron beam on the long-persistence screen. By appropriate adjustment of the coupling of the coils, one can get either of the two simple shapes shown in figure 2.

The fact of nuclear transmission having been established, one seeks an explanation in both classical and quantum-mechanical terms. The former will help most in understanding transient phenomena and the latter in steady-state processes.

A. The classical dipole in a magnetic field

Free electrons and some nuclei are known to be spinning about their own axes. Having mass they possess angular momentum, and if the axis of rotation is free to orient in space, one has a gyroscope. Any torque applied to the latter will cause it to precess with an angular velocity ω, which is related to the torque L by the equation:

$$L = \frac{dp}{dt} = \omega p \sin(\omega, p) = \boldsymbol{\omega} \times \mathbf{p} \tag{2}$$

(ω, p) is the angle between the axis of precession and the angular momentum vector, and the result may be concisely expressed in vector notation as the vector product of $\boldsymbol{\omega}$ and $\mathbf{p}$. One needs next to consider the origin of the torque which leads to the precession.

If a magnetic dipole is not aligned in the direction of a magnetic field H_z it experiences a torque

$$L = \mu H_z \sin(\mu, H_z) = \boldsymbol{\mu} \times \mathbf{H} = -\mathbf{H} \times \boldsymbol{\mu} \tag{3}$$

Equating expressions 2 and 3,

$$\boldsymbol{\omega} \times \mathbf{p} = -\mathbf{H} \times \boldsymbol{\mu} \tag{4}$$

A rotating charge can be considered as a circulating current and will act as a magnetic dipole of moment

$$\mu = iA$$

where i is the equivalent current and A is the cross-sectional area of the enclosed loop. But the charge q making $v/2\pi r$ revolutions per second is equivalent to a current

$$i = \frac{q}{c} \frac{v}{2\pi r}$$

The ratio q/c gives the charge in electromagnetic units; hence

$$\mu = \frac{qvr}{2c}$$

The angular momentum p is $m_q vr$, where m_q is the mass of the charged particle. Hence

$$\mu = \frac{q}{2m_q c} p = \gamma p$$

μ is collinear with p, with the direction determined by the sign of the charge (in this classical picture). One would have no explanation on this basis for the magnetic moment of the neutron. The ratio of magnetic moment to angular momentum, the "magnetogyric" ratio, is represented by γ, which is a constant. Substituting into equation 4,

$$\omega \times \mathbf{p} = -\gamma \mathbf{H} \times \mathbf{p} \tag{5}$$

and hence

$$\omega_0 = | \omega | = \frac{\mu}{p} H = \gamma H \tag{6}$$

The precession frequency is then directly proportional to the field strength H. It is important to note that *the precession frequency does not depend on the angle of inclination.*

One has established that magnetic dipoles precess when placed in a magnetic field and their precessional frequency (sometimes called the Larmor frequency) is given by equation 6.

It is now necessary to explain the effect of a perpendicular radiofrequency field on the precessing dipoles. Let a small alternating voltage of magnitude $H_x = 2H_1 \cos \omega t$ be applied to a coil along the x-axis. This is equivalent to two counter-rotating fields

$$H_1 \cos \omega t + H_1 \sin \omega t$$

and

$$H_1 \cos \omega t - H_1 \sin \omega t$$

H_x will be perhaps 10^{-4} of H_z. One of these fields will be rotating in the same direction as the precessing dipole. If ω is made equal to the precession frequency ω_0, the ends of the rotating and the precessing vectors would be stationary with respect to one another. The dipole will then experience a torque tending to pull it toward the x-y plane. The motions of the dipole and field vectors are shown in figure 3. One neglects the effect of the other rotating component and is generally justified in so doing (76). For any frequency other than this resonance frequency the rotating field would exert no coherent effect on the dipole, tending first to tip it in one direction and then the opposite. By using a rotating coordinate system one may focus attention on changes of inclination of the magnetic moment vector relative to the z-axis (453, 585). This is the behavior of essential interest. When the dipole dips toward the x-y plane an E.M.F. is induced in the y-axis (receiver) coil. By leaking a little of the transmitter energy to the

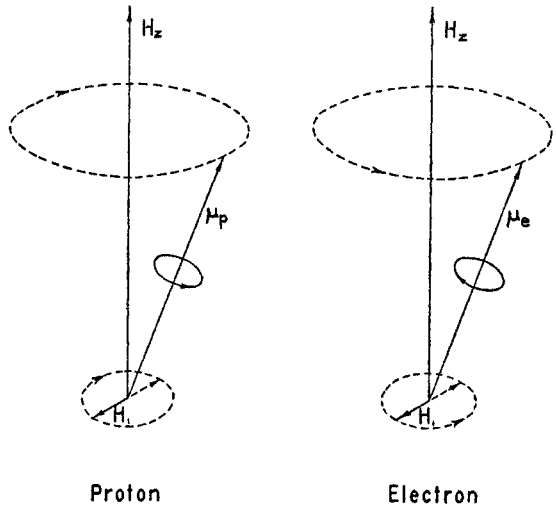

FIG. 3. Precessional motion of proton and electron spin magnetic dipoles in a magnetic field. A field H_1 perpendicular to the steady field H_z and rotating at the precession frequency in the same sense as the magnetic moment vector will tip the latter toward the plane of H_1.

receiver coil, one may use an amplifier which passes only a narrow band of frequencies around ω and hence rejects noise except that in this band.

The tipping effect of a perpendicular oscillating field on a rotating dipole may be demonstrated with a macroscopic model, using a spinning bar-magnet (574).

If the proton behaves as a classical dipole, the quantity γ of equation 6 divided by 2π should be equal to 4257 for protons, as given by equation 1. Notwithstanding this grossly classical treatment of quantized phenomena, nuclei (and free electrons) do indeed obey equation 6. No deviation from linearity of frequency and field as large as 0.01 per cent has been found for the proton from 6 (97) to over 20,000 gauss. The corresponding frequencies are 25 kcps and 85 Mcps. Recent observations (613) have been made at 2 gauss at a frequency of 8 kcps.

These phenomena require clarification to make them appear analogous to the interaction of matter with radiation in other spectral regions. The energy W of a magnet of moment $\boldsymbol{\mu}$ in a field $\mathbf{H}$ is

$$W = -\mu H \cos(\mu, H) = -\boldsymbol{\mu}\cdot\mathbf{H}$$

One notes that dipoles must absorb energy from the radiofrequency field when increasing their angle of inclination with the steady field H_z. If one chooses to conduct a radiofrequency absorption experiment, the samples should be "illuminated" in such a way that this absorption is observable. Again one supplies a steady field H_z, but the oscillating field

$$H_x = 2H_1 \cos \omega t$$

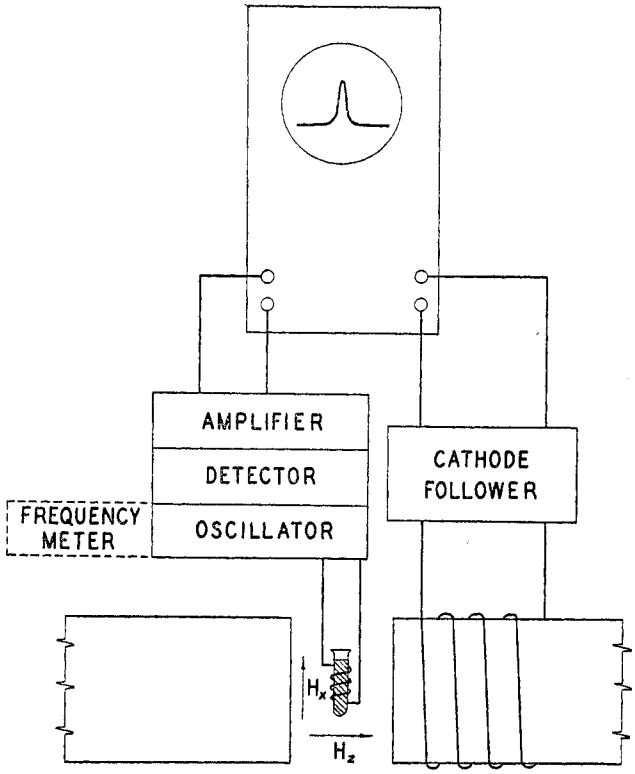

FIG. 4. Magnetic resonance absorption apparatus

is supplied by a coil which with a variable capacitor forms the frequency-determining element of a regenerative oscillator. Circuit parameters will be adjusted so that the level of oscillation is very low—in fact, the unit will barely be oscillating.

Water is again used as the sample. The arrangement shown in figure 4 is not much different from that of figure 1. In particular the sawtooth sweep circuit again provides a slow linear variation of the field H_z. For variety, let the field be fixed at 7047 gauss and the variable capacitor be tuned at a very slow rate. Observing the oscilloscope, one notes that at 30.00 Mcps a bell-shaped curve is traced out repeatedly. It strongly resembles a simple absorption curve in other respectable parts of the spectrum.

Reference to figure 5 will help to clarify the situation. The applied field H_z is shown as being slightly smaller than the value H^*; hence equations 1 and 6 are satisfied late in the sweep period. (They are also during the retrace, but on the oscilloscope the return trace is blanked out.) If H_z is increased to coincide with H^*, the peak will be centered on the trace, whereas if H_z had decreased somewhat, no signal whatever would be observed. The abscissa of the oscilloscope trace is proportional to the field variation, which can be measured by the frequency change necessary to shift the line a measured amount.

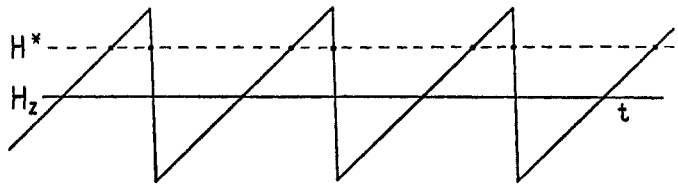

FIG. 5. Magnetic field scanning with a linear sweep. If the steady field H_z lies sufficiently close to the resonant value H^*, a recurrent signal may be displayed on an oscilloscope. While the resonant condition is satisfied during the rapid return, this occurs during the retrace and will normally be blanked out.

If the coil and sample were moved toward a pole edge, the line center would shift in position because the field would have a different value. Moreover, the line amplitude would diminish and its width would increase greatly, since various parts of the sample would see different fields.

By replacing the water with a salt solution, one may likewise reduce the level of oscillation in the absence of magnetic fields. One has increased the energy dissipated per cycle by substituting a poorer dielectric. In physical parlance, the factor of merit Q of the tuned circuit has been decreased during the period of absorption. Q is defined as 2π times the ratio of the energy stored to that dissipated per cycle. (There are alternative definitions.) The periodic decrease in level of oscillation amounts to a weak amplitude modulation of the 30 megacycle carrier. Demodulation of this low frequency may be accomplished in the same stage or in a separate detector. Under favorable conditions, no separate amplifier is needed.

If a beat-frequency meter is coupled loosely to the oscillator and adjusted to give a low-frequency beat tone, one observes that at the first appearance of the wing of the absorption line, the frequency of the tone changes. Its pitch will be above the steady tone on one half of the line and below on the other half. The behavior of the beat tone in traversing the absorption line and the appearance of the curve labelled χ' are closely related. In other spectral regions the index of refraction shows an analogous behavior in the region of an absorption line—i.e., shows anomalous dispersion. Instead of a rapid variation of the dielectric constant, one has a varying permeability of the sample. The inductance of the coil then changes in the same way. The permeability change is zero at the absorption peak but reaches a maximum on either side of the line. However, it is only the absorption which is detected by this apparatus. The dispersion leads to phase shifts which can be detected with radiofrequency bridges, as also can absorption.

Had the experiment been done on ice instead of water, the absorption would have been so weak that more complicated procedures would have to be used to detect its occurrence. With a comparable absorption coefficient, a radio wave of the resonant frequency would traverse 100 kilometers of ice before its intensity would be reduced to one-half (446).

The choice of a frequency near 30 Mcps fixes the resonant field for protons

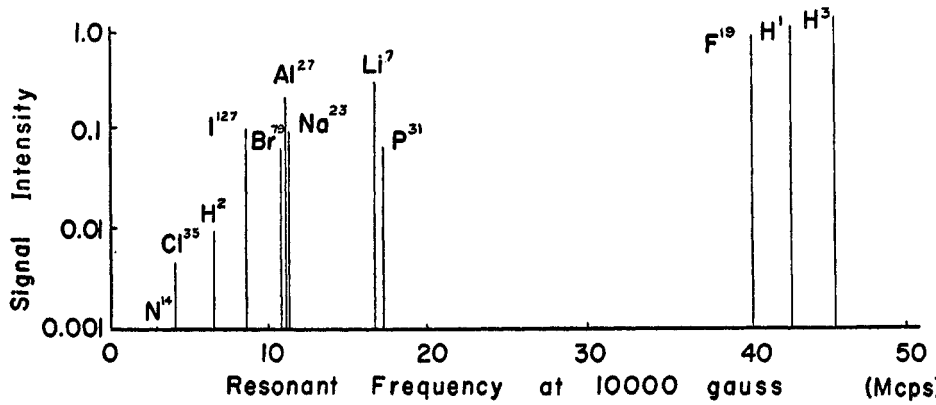

FIG. 6. Frequencies and relative intensities of resonance for nuclei in a field of 10,000 gauss.

near 7050 gauss, while for fluorine nuclei it is 7500 gauss. With most other nuclei such a frequency involves field values so high that it would be difficult to attain adequate stability and homogeneity. Relative signal intensities and resonant frequencies at 10,000 gauss are shown in figure 6 for some important nuclei. For greatest signal intensity it is desirable to work at the highest value of field at which the variation over the sample volume does not obscure the effects being studied. With solid samples of any nuclei and for liquid samples with nuclear spin $I > 1$, it is readily possible to observe natural line widths. In the most homogeneous fields yet attained (10^{-4} gauss variation over the sample), the apparent width of the proton line in liquids has progressively diminished with improved homogeneity.

The nuclear induction or absorption experiments may be done with any nucleus possessing net angular momentum and hence a magnetic moment. For many nuclei the magnetic moments are small, and their nuclear induction or absorption signals may be very difficult to detect. Regrettably, C^{12} and O^{16} have zero magnetic moment, as have other nuclei of even atomic number and even mass number, which represent about 60 per cent of the total number of stable nuclei.

By comparing the resonant frequencies for two different nuclei in the same field, one gets directly the ratio of γ_1/γ_2, their "magnetogyric" ratios. In order to determine the magnetic moments, it is necessary to know the spin. These spins may be determined, as will be shown later, by observing hyperfine structure or by measurement of relative intensities for equal numbers of nuclei. Compilations of such data have been made (458, p. 78; 580). Table 1 represents a very convenient compilation by Varian Associates (570) of often-used nuclear data. The moment of W^{183} should be revised in favor of the more recent value of 0.115 (525).

Now that one speaks in optical terms about absorption and dispersion he will be admitted—under suspicion—to the ranks of spectroscopists. They are impressed with a line of width less than 10^{-10} cm.$^{-1}$ (the narrowest yet observed).

TABLE 1

Spin resonance data for nuclei

(Reproduced by permission of Varian Associates)

Isotope*	*n-m-r* Frequency for a 10 Kilogauss Field	Natural Abundance	Relative Sensitivity for Equal Number of Nuclei		Magnetic Moment, μ, in Multiples of the Nuclear Magneton ($eh/4\pi Mc$)	Spin, I, in Multiples of $h/2\pi$	Electric Quadrupole Moment, Q, in Multiples of $e \times 10^{-24}$ cm.^{2}
			At constant field	At constant frequency			
	mc.	*per cent*					
n^{1}*	29.17	—	0.322	0.685	−1.91305	1/2	—
H^{1}	42.57	99.9844	1.000	1.000	2.79277	1/2	—
H^{2}	6.535	1.56×10^{-2}	9.64×10^{-3}	0.409	0.85741	1	2.77×10^{-3}
H^{3}*	45.41	—	1.21	1.07	2.79810	1/2	—
He^{3}	32.44	$10^{-5} - 10^{-7}$	0.443	0.762	−2.128	1/2	—
Li^{6}	6.267	7.43	8.51×10^{-3}	0.392	0.8221	1	4.6×10^{-4}
Li^{7}	16.55	92.57	0.294	1.94	3.257	3/2	-4.2×10^{-2}
Be^{9}	5.987	100.	1.39×10^{-2}	0.703	−1.178	3/2	2×10^{-2}
B^{10}	4.576	18.83	1.99×10^{-2}	1.72	1.801	3	0.111
B^{11}	13.67	81.17	0.165	1.60	2.689	3/2	3.55×10^{-2}
C^{13}	10.71	1.108	1.59×10^{-2}	0.251	0.7023	1/2	—
N^{14}	3.077	99.635	1.01×10^{-3}	0.193	0.4037	1	2×10^{-2}
N^{15}	4.316	0.365	1.04×10^{-3}	0.101	−0.2831	1/2	—
O^{17}	5.772	3.7×10^{-2}	2.91×10^{-2}	1.58	−1.893	5/2	-4×10^{-3}
F^{19}	40.07	100.	0.834	0.941	2.628	1/2	—
Ne^{21}	—	0.257	—	—	—	$\geqslant 3/2$	—
Na^{22}*	4.434	—	1.81×10^{-2}	1.67	1.745	3	—
Na^{23}	11.267	100.	9.27×10^{-2}	1.32	2.217	3/2	0.1
Na^{24}*	2.42	—	1.15×10^{-2}	2.02	1.69	4	—
Mg^{25}	2.606	10.05	2.68×10^{-2}	0.714	−0.8547	5/2	—
Al^{27}	11.10	100.	0.207	3.04	3.641	5/2	0.149
Si^{29}	8.460	4.70	7.85×10^{-2}	0.199	−0.5549	1/2	—
P^{31}	17.24	100.	6.64×10^{-2}	0.405	1.131	1/2	—
S^{33}	3.267	0.74	2.26×10^{-3}	0.384	0.6429	3/2	-6.4×10^{-2}
S^{35}*	5.081	—	8.50×10^{-3}	0.599	1.00	3/2	4.5×10^{-2}
Cl^{35}	4.173	75.4	4.71×10^{-3}	0.490	0.8210	3/2	-7.97×10^{-2}
Cl^{37}	3.474	24.6	2.72×10^{-3}	0.408	0.6835	3/2	-6.21×10^{-2}
K^{39}	1.987	93.08	5.08×10^{-4}	0.233	0.3910	3/2	—
K^{40}*	2.470	1.19×10^{-2}	5.21×10^{-3}	1.55	−1.296	4	—
K^{41}	1.090	6.91	8.43×10^{-5}	0.128	−0.2145	3/2	—

K^{42}*	4.35	—	8.5×10^{-3}	0.817	−1.14	2	—
Ca^{43}	2.864	0.13	6.39×10^{-2}	1.41	−1.315	7/2	—
Sc^{45}	10.34	100.	0.301	5.10	4.749	7/2	—
Ti^{47}	2.400	7.75	2.10×10^{-3}	0.659	−0.7871	5/2	—
Ti^{49}	2.401	5.51	3.76×10^{-3}	1.19	−1.102	7/2	—
V^{50}	4.244	0.24	5.53×10^{-2}	5.91	3.341	6	—
V^{51}	11.21	~100.	0.383	5.53	5.145	7/2	0.3
Cr^{53}	2.406	9.54	1.0×10^{-4}	0.29	−0.4735	3/2	—
Mn^{55}	10.56	100.	0.178	2.89	3.462	5/2	0.5
Fe^{57}	—	2.245	—	—	$\leqslant 0.05$	—	—
Co^{57}*	10.0	—	0.274	4.95	4.6	7/2	—
Co^{58}*	13.3	—	0.25	2.5	3.5	2	—
Co^{59}	10.11	100.	0.281	4.98	4.640	7/2	0.5
Co^{60}*	4.6	—	5×10^{-2}	4.3	3.0	5?	—
Ni^{61}	—	1.25	—	—	<0.25	—	—
Cu^{63}	11.31	69.09	9.38×10^{-2}	1.33	2.226	3/2	−0.15
Cu^{65}	12.13	30.91	0.116	1.42	2.386	3/2	−0.14
Zn^{67}	2.67	4.12	2.86×10^{-3}	0.730	0.874	5/2	—
Ga^{69}	10.23	60.2	6.93×10^{-2}	1.201	2.012	3/2	0.2318
Ga^{71}	12.99	39.8	0.142	1.525	2.556	3/2	0.1461
Ge^{73}	1.485	7.61	1.40×10^{-3}	1.15	−0.8768	9/2	−0.2
As^{75}	7.293	100.	2.51×10^{-2}	0.856	1.435	3/2	0.3
Se^{77}	8.131	7.50	6.97×10^{-3}	0.191	0.5333	1/2	—
Se^{79}*	2.210	—	2.94×10^{-3}	1.12	−1.015	7/2	0.9
Br^{79}	10.70	50.57	7.94×10^{-2}	1.26	2.106	3/2	0.30
Br^{81}	11.53	49.43	9.93×10^{-2}	1.35	2.269	3/2	0.25
Kr^{83}	1.64	11.55	1.89×10^{-3}	1.27	−0.968	9/2	0.15
Rb^{85}	4.113	72.8	1.05×10^{-2}	1.13	1.349	5/2	—
Rb^{86}*	6.48	—	2.8×10^{-2}	1.2	(−)1.7	2	—
Rb^{87}	13.97	27.2	0.177	1.64	2.749	3/2	—
Sr^{87}	1.845	7.02	2.69×10^{-3}	1.43	−1.089	9/2	—
Y^{89}	2.085	100.	1.17×10^{-4}	4.90×10^{-2}	−0.1368	1/2	—
Zr^{91}	4.0	11.23	9.4×10^{-3}	1.04	−1.3	5/2	—
Nb(Cb)^{93}	10.45	100.	0.488	8.10	6.167	9/2	~0
Mo^{95}	2.774	15.78	3.22×10^{-3}	0.761	−0.9098	5/2	—
Mo^{97}	2.832	9.60	3.42×10^{-3}	0.776	−0.9289	5/2	—
Tc^{99}*	9.62	—	0.381	7.46	5.68	9/2	0.3
Ru^{99}	—	12.81	—	—	—	5/2	—

TABLE 1—*Continued*

Isotope*	*n-m-r* Frequency for a 10 Kilogauss Field	Natural Abundance	Relative Sensitivity for Equal Number of Nuclei		Magnetic Moment, μ, in Multiples of the Nuclear Magneton ($eh/4\pi Mc$)	Spin, I, in Multiples of $h/2\pi$	Electric Quadrupole Moment, Q, in Multiples of $e \times 10^{-24}$ cm.^{2}
			At constant field	At constant frequency			
	mc.	*per cent*					
Ru^{101}	—	16.98	—	—	—	5/2	—
Rh^{103}	1.340	100.	3.12×10^{-5}	3.15×10^{-2}	−0.0879	1/2	—
Pd^{105}	1.74	22.23	7.92×10^{-4}	3.40	−0.57	5/2	—
Ag^{107}	1.722	51.35	6.69×10^{-5}	4.03×10^{-2}	−0.1130	1/2	—
Ag^{109}	1.980	48.65	1.01×10^{-4}	4.66×10^{-2}	−0.1299	1/2	—
Cd^{111}	9.030	12.86	9.54×10^{-3}	0.212	−0.5923	1/2	—
Cd^{113}	9.446	12.34	1.09×10^{-2}	0.222	−0.6196	1/2	—
In^{113}	9.311	4.16	0.345	7.22	5.497	9/2	1.144
In^{115}*	9.331	95.84	0.348	7.23	5.509	9/2	1.161
Sn^{115}	13.93	0.35	3.50×10^{-2}	0.327	−0.9134	1/2	—
Sn^{117}	15.17	7.67	4.53×10^{-2}	0.356	−0.9951	1/2	—
Sn^{119}	15.87	8.68	5.18×10^{-2}	0.373	−1.0411	1/2	—
Sb^{121}	10.19	57.25	0.160	2.79	3.343	5/2	−1.3
Sb^{123}	5.519	42.75	4.57×10^{-2}	2.72	2.534	7/2	−1.7
Te^{123}	11.2	0.89	1.80×10^{-2}	0.262	−0.732	1/2	—
Te^{125}	12.7	7.03	3.16×10^{-2}	0.316	−0.882	1/2	—
I^{127}	8.565	100.	9.50×10^{-2}	2.35	2.809	5/2	−0.59
I^{129}*	5.699	—	5.04×10^{-2}	2.81	2.617	7/2	−0.43
Xe^{129}	11.78	26.24	2.12×10^{-2}	0.277	−0.7726	1/2	—
Xe^{131}	3.490	21.24	2.77×10^{-3}	0.410	0.6868	3/2	−0.12
Cs^{131}*	10.6	—	0.181	2.91	3.48	5/2	—
Cs^{133}	5.617	100.	4.82×10^{-2}	2.77	2.579	7/2	$\leqslant 0.3$
Cs^{134}*	5.64	—	6.21×10^{-2}	2.53	2.96	4	—
Cs^{135}*	5.94	—	5.53×10^{-2}	2.94	2.727	7/2	—
Cs^{137}*	6.19	—	6.44×10^{-2}	3.05	2.84	7/2	—
Ba^{135}	4.25	6.59	4.99×10^{-3}	0.499	0.837	3/2	—
Ba^{137}	4.76	11.32	6.97×10^{-3}	0.559	0.936	3/2	—
La^{139}	6.050	99.911	6.03×10^{-2}	2.98	2.778	7/2	0.9
Pr^{141}	11.3	100.	0.234	3.18	3.8	5/2	-5.4×10^{-2}
Nd^{143}	2.2	12.20	2.81×10^{-3}	1.07	−1.0	7/2	$\leqslant 1.2$
Nd^{145}	1.4	8.30	6.70×10^{-4}	0.666	−0.62	7/2	$\leqslant 1.2$

Sm^{147}	1.47	15.07	8.8×10^{-4}	0.725	−0.68	7/2	0.72
Sm^{149}	1.19	13.84	4.7×10^{-4}	0.591	−0.55	7/2	0.72
Eu^{151}	10.	47.77	0.168	2.84	3.4	5/2	~1.2
Eu^{153}	4.6	52.23	1.45×10^{-2}	1.25	1.5	5/2	~2.5
Gd^{155}	—	14.68	—	—	~0.3	—	—
Gd^{157}	—	15.64	—	—	0.3	—	—
Tb^{159}	—	100.	—	—	—	3/2	—
Dy^{161}	—	18.73	—	—	—	7/2	—
Dy^{163}	—	24.97	—	—	—	7/2	—
Ho^{165}	—	100.	—	—	—	7/2	—
Er^{167}	—	22.82	—	—	—	—	~10
Tm^{169}	—	100.	—	—	—	1/2	—
Yb^{171}	6.9	14.27	4.19×10^{-3}	0.161	0.45	1/2	—
Yb^{173}	1.98	16.08	1.18×10^{-3}	0.543	−0.65	5/2	3.9
Lu^{175}	5.7	97.40	4.94×10^{-2}	2.79	2.6	7/2	5.9
Lu^{176}*	—	2.60	—	—	4.2	⩾7	6–8
Hf^{177}	—	18.39	—	—	—	1/2 or 3/2	—
Hf^{179}	—	13.78	—	—	—	1/2 or 3/2	—
Ta^{181}	4.6	100.	2.60×10^{-2}	2.26	2.1	7/2	6.5
W^{183}	1.2	14.28	2.4×10^{-5}	2.9×10^{-2}	0.08	1/2	—
Re^{185}	9.584	37.07	0.133	2.63	3.143	5/2	2.8
Re^{187}	9.681	62.93	0.137	2.65	3.175	5/2	2.6
Os^{189}	3.307	16.1	2.24×10^{-3}	0.385	0.6506	3/2	2.0
Ir^{191}	0.81	38.5	1.2×10^{-5}	9.5×10^{-2}	0.16	3/2	~1.2
Ir^{193}	0.86	61.5	1.3×10^{-5}	0.104	0.17	3/2	~1.0
Pt^{195}	9.155	33.7	9.94×10^{-3}	0.215	0.6005	1/2	—
Au^{197}	0.691	100.	2.14×10^{-5}	8.1×10^{-2}	0.136	3/2	0.56
Hg^{199}	7.614	16.86	5.72×10^{-3}	0.179	0.4994	1/2	—
Hg^{201}	3.08	13.24	1.90×10^{-3}	0.362	−0.607	3/2	0.5
Tl^{203}	24.56	29.52	0.192	0.577	1.611	1/2	—
Tl^{205}	24.80	70.48	0.198	0.583	1.627	1/2	—
Pb^{207}	8.899	21.11	9.13×10^{-3}	0.209	0.5837	1/2	—
Bi^{209}	6.843	100.	0.137	5.30	4.040	9/2	−0.4
U^{235}*	—	0.71	—	—	—	5/2	—
Free electron (assuming $g = 2.000$)	28003	—	2.85×10^{8}	658	−1836	1/2	—

* An asterisk indicates that the isotope is radioactive.

Their disdain is manifest however when one talks of line widths in gauss—obviously an ill-conceived designation! The practice obviously comes from the experiments at fixed frequency and variable field. But in what other region can one run a spectrum at constant wavelength? Regardless of origin, this offspring shows no sign of dying an early death.

In imitation of spectroscopists, one will desire to determine coefficients of absorption. Astonishingly, these turn out to be a function of the intensity of the incident energy, and they lead one to examine the processes involved in growth and decay of polarization. This behavior will be characterized in terms of two relaxation constants for simple cases. The magnetic polarization is described in terms of complex susceptibilities which are related to the static susceptibility.

For background it is desirable first to speak in terms of energy levels, so as to obtain more insight into resonant behavior. Following this, one considers general aspects of line multiplicity, which can be qualitatively described. Line widths and intensities then require consideration of relaxation phenomena and of susceptibilities.

B. Quantum-mechanical description

In atomic spectra the line splitting upon application of a steady magnetic field is called the Zeeman effect. In nuclear spin resonance absorption one makes direct observations of transitions involving the reorientation of a magnetic dipole in a magnetic field. These Zeeman energy levels between which transitions occur are degenerate in the absence of a magnetic field, and their separation

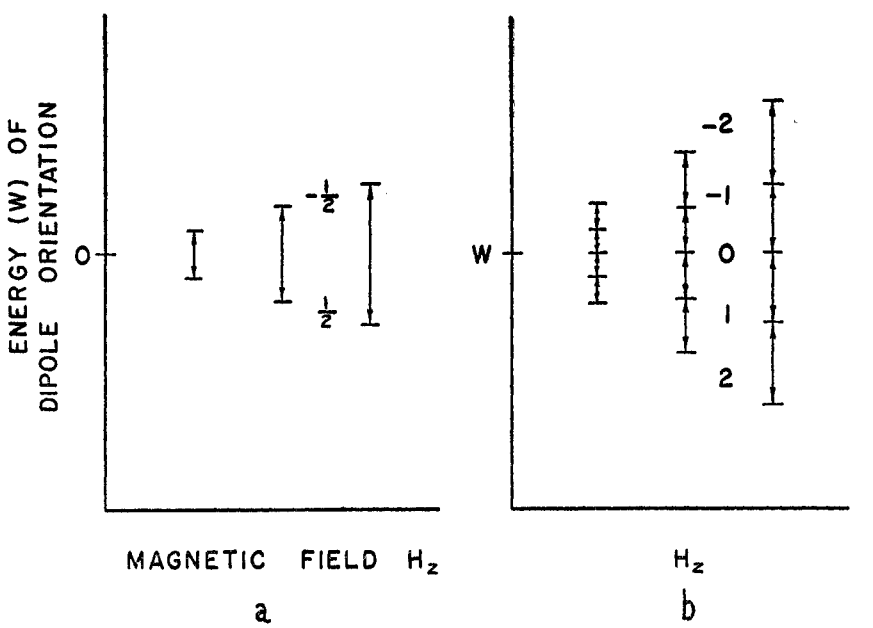

FIG. 7. The splitting of nuclear energy levels in a magnetic field: (a) $I = \frac{1}{2}$; (b) $I = 2$

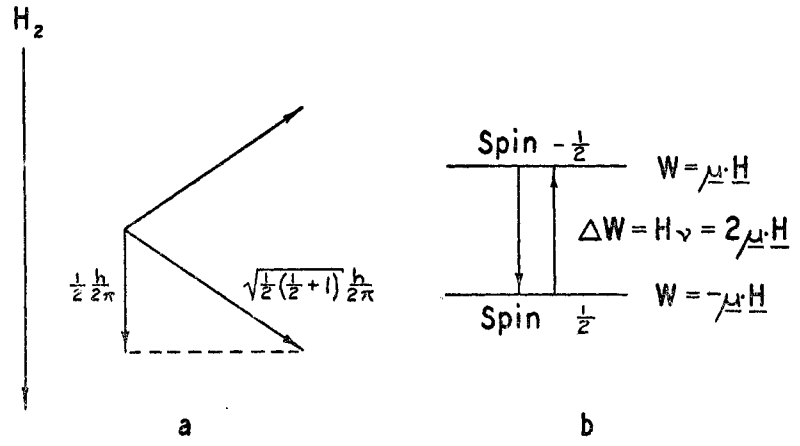

FIG. 8. Orientations and energy levels for $I = \frac{1}{2}$

increases linearly with field, as shown in figure 7. The splittings are shown for systems having two and five levels, respectively. For the two-level system the transitions are between orientations "parallel" and "antiparallel" to the field. This situation is probably unique in spectroscopy—that one should be able to vary at will the spacings of energy levels and therefore the frequency which will give rise to the transition. The magnitude of nuclear spin angular momentum is $\sqrt{I(I+1)}h/2\pi$ and its projection on an axis fixed in space (such as the field direction) will be $Mh/2\pi$. The maximum allowed value of the magnetic quantum number M will be called "the spin" and is represented by I. I will be an integer for nuclei of even atomic number and a half-integer for nuclei of odd atomic number. M will have allowed values I, $(I-1)$, $\cdots$, $(-I)$. Since a magnetic dipole lies along the angular momentum vector (though for some dipoles its direction is opposite), it cannot be parallel or antiparallel to the field. This is shown for spin $\frac{1}{2}$ in figure 8, together with the energy levels. The classical relation

$$\mu = p\frac{e}{2mc}$$

is applicable to the magnetic moment due to electronic orbital angular momentum where $p = Lh/2\pi$. For electron or nuclear spin, one must multiply by a factor g, which for free electrons is about 2 (more precisely 2.0023) and m is the electron mass m_e. For nuclei g is an irrational number such as 5.58490 for protons when m is the proton mass m_P. The magnetic moment components in the fields direction are, respectively,

$$\mu_e = g_e\frac{e}{2m_ec}\frac{Mh}{2\pi} \cong 2\left(\frac{1}{2}\right)\frac{he}{4\pi m_ec} = \mu_B \tag{7a}$$

$$\mu_P = g_P\frac{e}{2m_Pc}\frac{Mh}{2\pi} = g_P\frac{1}{2}\frac{he}{4\pi m_Pc} = g_PI\mu_n \tag{7b}$$

$$\mu_I = g_II\mu_n \tag{7c}$$

μ_B and μ_n are respectively the Bohr and nuclear magnetons, which serve as convenient measures of magnetic moment, though μ_n has no theoretical significance. The subscripts e, P, and I refer to electrons, protons, and arbitrary nuclei, respectively. The numerical values of μ_B and μ_n are 9.2712×10^{-21} and 5.0493×10^{-24} erg/gauss, respectively. "The magnetic moment" is γ times the maximum allowed component of the angular momentum vector in the field direction.

The dipole moment was defined as the energy W which a dipole possesses per unit field strength, the energy being proportional to the component of the dipole moment in the field direction:

$$W = -\boldsymbol{\mu}\cdot\mathbf{H} = -g_I\mu_n MH$$

For spin $\frac{1}{2}$, the energies of orientation "parallel" and "antiparallel" are shown in figure 8. For a transition between levels, since $\Delta M = -1$ for absorption,

$$h\nu = \Delta W = g\mu_n H = \frac{\mu}{I}H \tag{8}$$

Comparing with equations 6 and 7b, one notes that $\gamma = g_e/2m_Pc$.

Thus by considering either the resonant tipping of a dipole or the transitions between its energy levels we arrive at the same expression for the relation of frequency to field for resonance. A parallel treatment of the two aspects is given in reference 21. While this expression holds without exception for nuclei of spin $\frac{1}{2}$, it may require modification for $I > \frac{1}{2}$, if the quadrupole interaction is strong.

The interaction of a nucleus of spin I with the field H could have been written in terms of the Hamiltonian

$$\mathcal{H}_1 = -|\gamma|\frac{h}{2\pi}\mathbf{I}\cdot\mathbf{H} \tag{9}$$

which has the eigenvalues

$$W = \frac{-h}{2\pi}\gamma MH_z$$

Allowing $\Delta M = \pm 1$ transitions, one again obtains the resonance expression:

$$\omega = \gamma H$$

In a later discussion of the ethanol spectrum one will meet the similar Hamiltonian

$$\mathcal{H}_2 = -|\gamma|\frac{h}{2\pi}\mathbf{I}_a\cdot\mathbf{H}_a \tag{10}$$

where $\mathbf{H}_a$ is the magnetic field operator of an internal shielding field in atom a.

In solids where dipoles 1 and 2 separated by a distance r may interact directly one will have an interaction

$$\mathcal{H}_3 = r^{-3}[\boldsymbol{\mu}_1\cdot\boldsymbol{\mu}_2 - 3r^{-2}(\boldsymbol{\mu}_1\cdot\mathbf{r})(\boldsymbol{\mu}_2\cdot\mathbf{r})] \tag{11}$$

An indirect type of nuclear dipole–dipole interaction by way of bonding electrons is of the form

$$\mathcal{H}_4 = A\mathbf{I}_1 \cdot \mathbf{I}_2 \tag{12}$$

This will also be met in the discussion of ethanol.

III. CHEMICAL SHIELDING

At a time when physicists were busy comparing magnetogyric ratios of various nuclei and expressing these to seven or more significant figures, several disquieting papers appeared (147, 312, 443). It was reported that in compounds of phosphorus, nitrogen, and fluorine the resonant frequency for a particular nucleus depended on the compound in which it was present. This effect was called the "chemical shift," because physicists could think of no stronger term of damnation for an effect which was making insignificant several digits in their nuclear moment data. Such shifts can be established most readily for liquids and gases because their lines are relatively narrow. Early investigators had recognized the necessity of correcting their data to take into account the fact that the H of equation 6 should be the field at the nucleus instead of the applied field H_s (335). The molecular electrons undergo a precession on application of the steady field to produce a small field $-\sigma H_s$ opposing the applied one, so that

$$H = H_s - \sigma H_s \tag{13}$$

The diamagnetic effect is just what one would expect from Lenz's law, and the shielding field is proportional to the applied one. The shielding constant has been given for atoms with spherical nuclear symmetry as

$$\sigma = 31.9 \times 10^{-6} Z^{4/3}$$

where Z is the atomic number (335). The correction was calculated for and applied to the atom concerned, though usually it was present in a compound. The atomic shielding constants have been tabulated for elements 1 to 92, using a different approximation (148). While the values for heavy atoms are good, more accurate procedures (260, 455, 456) are desirable for light ones. Besides diamagnetic shielding, there may be an opposite contribution to the field at the nucleus by a temperature-independent electronic paramagnetism (456, 567). This arises from low-lying excited states and except for molecular hydrogen must be evaluated from the measured shielding field combined with the calculated diamagnetic correction. For molecular hydrogen (274, 381, 456) both terms have been calculated and σ is found to be 26.6×10^{-6}, compared with the bare proton. For hydrogen compounds, it is convenient to refer chemical shifts to water, and since the relative shift of the latter with respect to H_2 is 0.6×10^{-6} (217, 544), $\sigma = 26.0 \times 10^{-6}$ for water referred to the proton. The largest value of σ thus far reported for hydrogen compounds is 42×10^{-6} for hydrogen iodide, again referred to the proton (210). This is a relatively small displacement compared with cobalt compounds, where the percentage variation of frequency was 1.3 between $K_3Co(CN)_6$ and $K_3Co(C_2O_4)_3$, the resonance for the latter occurring at the higher frequency (444). The cobalt compounds are anomalous in another

respect. Whereas like other diamagnetic effects, shielding is not usually dependent on temperature for most nuclei, there was a 0.015 per cent increase in resonant frequency in cobalt compounds over a 60° temperature rise. This has been interpreted as meaning that there may be a low-lying molecular state which has a different shielding factor from the ground state. The same conclusion has been drawn from the large value of σ (456).

One of the easiest nuclei for which to find shielding effects is F^{19}. The moment of 2.628 μ_n gives strong signals in liquid samples, and the shielding effects are moderately large, i.e., of the order of 0.01 per cent (147). The order of increasing shielding is F_2, NF_3, CF_4, BF_3, BeF_2, and HF, with the HF resonance occurring 0.063 per cent higher in field than for F_2 (210). In a given group of the Periodic Table, the shielding generally increases with atomic weight: e.g., $CF_4 < SiF_4 < GeF_4$; $NF_3 < PF_3 < AsF_3 < SbF_3$; $ClF_3 < BrF_3$. The approximately linear relation between shift relative to F_2 and electronegativity of the fluorine is explained in terms of a large contribution of temperature-independent paramagnetism (479). Although the net orbital angular momentum of the p-electrons averages to zero, it may momentarily have large values in a diatomic or polyatomic molecule, and hence instantaneously there may be large fields at the nucleus, thus producing appreciable shielding. With spherical symmetry obtaining for s-electrons in hydrogen, the shielding effects in hydrogen compounds are much smaller than in fluorine compounds. The shielding of hydrogen fluoride relative to F_2 is calculated to be 20×10^{-4} on this basis, while the experimental value is 6.3×10^{-4}. Curiously, the fluoride ion in water has the shielding value 5.5×10^{-4}. It would be of interest to study fluoride ion in other solvents. A study of the shielding of fluorine in substituted fluorobenzenes compared to fluorobenzene showed that the shielding is proportional to the Hammett σ-value for the substituent in the meta and para positions (214). Values of Hammett's σ for substituents not previously listed were obtained in this way (214). In substituted halomethanes the shielding is not simply determined by the ionic character of the bonds (364). However, for a number of monosubstituted ethanes, the increased shift of the protons in the CH_2 group over those of the CH_3 group was found to be proportional to the Pauling electronegativity (509). The CH_3 protons in hexane served for reference.

Shielding values are tabulated in table 2. More extensive tables for H^1 (210, 365) and F^{19} (210, 214, 342) may be found in the references given.

Since differences in shielding give different values for the resonant field, it is understandable that if there are non-equivalent nuclei in the same molecule, they may under favorable conditions show individual absorption lines. The first such multiple lines were reported for the nitrogen in the ammonium and nitrate ions in aqueous ammonium nitrate (443). The separation amounted to 0.05 per cent. Only a few other shielding values for nitrogen have been reported, although work is being carried on in at least three laboratories at this time.

Multiple NSR lines in a compound do *not* arise from direct magnetic field contributions of neighbors in the liquid state. Reorientation of neighboring nuclei at a frequency of the magnitude of the separation in cycles per second will average out directly contributed fields.

TABLE 2

Chemical shielding of nuclei

$$\sigma = \frac{H_c - H_r}{H_r}$$

Sample	$\sigma \times 10^5$	Reference Compound	References
H^1			
H_2	2.66	Unshielded proton	(210)
B_2H_6	3.46	Unshielded proton	(210)
CH_4	3.03	Unshielded proton	(210)
NH_3	3.13	Unshielded proton	(210)
H_2O	2.70	Unshielded proton	(210)
HF	2.31	Unshielded proton	(210)
SiH_4	2.88	Unshielded proton	(210)
H_2S	3.06	Unshielded proton	(210)
HCl	3.11	Unshielded proton	(210)
AsH_3	3.00	Unshielded proton	(210)
H_2Se	3.38	Unshielded proton	(210)
HBr	3.44	Unshielded proton	(210)
HI	4.23	Unshielded proton	(210)
NH_3 (g)	0.15	NH_3 (l)	(391)
	$\sigma \times 10^4$		
Li^7	−2.61	$LiNO_3$ (liquid NH_3)	(218)
No shifts observed in LiCl, LiBr, CH_3COOLi, $LiNO_3$, Li_2SO_4, $Li_3C_6H_5O_7$, HCOOLi, $LiC_7H_5O_3$			(149)
Be^9	−0.1	$BeCl_2$	(314)
B^{11}			
$B(OCH_3)_3$	−0.18	$BF_3O(C_2H_5)_2$	(149)
BCl_3	−0.46	$BF_3O(C_2H_5)_2$	(149)
BBr_3	−0.44	$BF_3O(C_2H_5)_2$	(149)
N^{14}			
NH_4OH	−3.72	$NaNO_3$ (aq)	(354)
NH_4NO_3	−3.46	$NaNO_3$ (aq)	(354)
SCN^-	−1.51	$NaNO_3$ (aq)	(354)
HNO_3 (100 per cent)	−0.52	$NaNO_3$ (aq)	(354)
$(NH_2)_2CO$	−3.46	$NaNO_3$ (aq)	(354)
$N_2H_4 \cdot H_2O$	−3.46	$NaNO_3$ (aq)	(354)
CN^-	−1.12	$NaNO_3$ (aq)	(354)
$C_6H_5NO_2$	−0.17	$NaNO_3$ (aq)	(354)
CH_3NO_2	0.00	$NaNO_3$ (aq)	(354)
NH_3	−3.7	$NaNO_3$ (aq)	(443)
F^{19}			
BeF_2	0	BeF_2	(209)
BF_3 (l)	−46	BeF_2	(209)
$(SiF_6)^=$	−48	BeF_2	(209)
F^- (in saturated aqueous KF)	−58	BeF_2	(209)
CF_4 (l)	−80	BeF_2	(209)
SbF_3 (saturated aqueous)	−93	BeF_2	(209)
PF_6^- (in aqueous NH_4PF_6)	−102	BeF_2	(209)
CH_2F_2	−20	BeF_2	(209)
BF_3 etherate	−25	BeF_2	(209)
HBF_4	−30	BeF_2	(209)
1,4-Difluorobenzene	−57	BeF_2	(209)
1,3-Difluorobenzene	−62	BeF_2	(209)
1,3,5-Trifluorobenzene	−63	BeF_2	(209)
1,2,3,4-Tetrafluorobenzene	−73	BeF_2	(209)

TABLE 2—*Continued*

Sample	$\sigma \times 10^4$	Reference Compound	References
CHF_3 (l)	−88	BeF_2	(209)
CF_3COOH	−97	BeF_2	(209)
m-$NH_2C_6H_4CF_3$	−105	BeF_2	(209)
$C_6H_5CF_3$ and *m*-$ClC_6H_4CF_3$	−106	BeF_2	(209)
CH_3CF_3 and *o*-$ClC_6H_4CF_3$	−107	BeF_2	(209)
$CF_3CCl{=}CCl_2$ and *m*-$NO_2C_6H_4CF_3$	−110	BeF_2	(209)
HF (21.5 molar)	−13	BeF_2	(342)
HBF_4 in excess H_3BO_3	−30	BeF_2	(342)
SbF_3 in HF	−100	BeF_2	(342)
$CHFCl_2$ (l)	−101	BeF_2	(342)
$CFCl_3$ (l)	−185	BeF_2	(342)
UF_6	790	C_4F_8	(571)
SbF_3	−90	BeF_2	(149)
$C_2F_3Cl_3$	−96	BeF_2	(149)
BF_3 etherate	−14	BeF_2	(149)
Na^{23}	−10.4	NaCl (aq)	(149)
Na^{23}	−11.2	NaOH (aq)	(218)
$Na_2B_2O_4$	−1.01	NaBr	(506)
Al^{27}	−15.9	$AlCl_3$ (aq)	(312)
Al^{27}	−16.1	$AlCl_3$	(218)
$AlCl_3$ (s)	0.81	AlO_2^- (aq)	(205)
Al^{+3} (aq)	1.32	AlO_2^-	(205)
Si^{29}	−1.8	Na_2SiO_3 (aq)	(594)
	$\sigma \times 10^5$		
P^{31}			
P_4	45.0	H_3PO_4 (aq)	(213)
P_4 in CS_2	48.8	H_3PO_4 (aq)	(213)
PH_3	24.1	H_3PO_4 (aq)	(213)
PF_3	−9.7	H_3PO_4 (aq)	(213)
PCl_3	−21.5	H_3PO_4 (aq)	(213)
PBr_3	−22.2	H_3PO_4 (aq)	(213)
PI_3	−17.8	H_3PO_4 (aq)	(213)
P_4S_3	11.4	H_3PO_4 (aq)	(213)
CH_3OPF_2	−11.1	H_3PO_4 (aq)	(213)
$Cl(CH_2)_3PCl_2$	−18.2	H_3PO_4 (aq)	(213)
P_2I_4 (in CS_2)	−17.0	H_3PO_4 (aq)	(213)
HPF_6	11.8	H_3PO_4 (aq)	(213)
$HPO(OH)_2$	−0.45	H_3PO_4 (aq)	(213)
$POCl_2F$	0.00	H_3PO_4 (aq)	(213)
$POClF_2$	1.48	H_3PO_4 (aq)	(213)
$F_2PO(OH)$	2.01	H_3PO_4 (aq)	(213)
$H_2PO(OH)$	−1.38	H_3PO_4 (aq)	(213)
$POCl_3$	−0.54	H_3PO_4 (aq)	(213)
$C_2H_5OPOCl_2$	−0.64	H_3PO_4 (aq)	(213)
$PSCl_3$*	−3.08	H_3PO_4 (aq)	(213)
	$\sigma \times 10^4$		
Cl^{35}			
$HClO_4$ (100 per cent)	0.4	$NaClO_4$ (aq)	(355)
$NaClO_3$	−8	NaCl (aq)	(275)
$Ti^{47, 49}$			
H_2TiF_6	10	$TiCl_4$ (l)	(288)

* Data for one hundred compounds are listed in reference 417. Shifts are found to be approximately additive for phosphorus compounds (417).

TABLE 2—*Concluded*

Sample	$\sigma \times 10^5$	Reference Compound	References
V^{51}			
$VOCl_3$ (l)	−5	$NaVO_3$ (aq)	(581)
V (s)	−61	$NaVO_3$ (aq)	(581)
Na_3VO_4 (aq)	0	$NaVO_3$ (aq)	(581)
NH_4VO_3 (aq)	0	$NaVO_3$ (aq)	(581)
$VO(NO_3)_2$ (aq)	0	$NaVO_3$ (aq)	(581)
$VOSO_4$ (aq)	0	$NaVO_3$ (aq)	(581)
$K_2V_4O_9$ (aq)	0	$NaVO_3$ (aq)	(581)
V_2O_5 (s)	0	$NaVO_3$ (aq)	(581)
VCl_2 (aq)	0	$NaVO_3$ (aq)	(581)
$VOCl_3$ (aq)	0	$NaVO_3$ (aq)	(581)
$Pb(VO_3)_2$	Very broad line	$NaVO_3$ (aq)	(581)
Co^{59}			
$Co[C_2H_4(NH_2)_2]_3Cl_3$	−72.5	$K_3Co(CN)_6$	(444)
$Na_3Co(NO_2)_6$	−73.5	$K_3Co(CN)_6$	(444)
	−80.4	$K_3Co(CN)_6$	(444)
$Co(NH_3)_6Cl_3$	−82.3	$K_3Co(CN)_6$	(444)
$K_3Co(C_2O_4)_3$	−128.3	$K_3Co(CN)_6$	(444)
Cu^{63}	−22.9	Cu_2Cl_2 (s)	(312)
Cu^{65}	−23.5	Cu_2Br_2 (s)	(218)
Cu_2Cl_2	−0.6	Cu_2Br_2 (s)	(205)
$K_3Cu(CN)_4$	−80.	Cu_2Cl_2 (s)	(31)
Cu^{65}	−23.5	Cu_2Br_2 (s)	(218)
Ga^{71}	−44.9	$GaCl_3$	(218, 312)
As^{75}			
Na_2HAsO_4 (s)	1	Na_2HAsO_4 (aq)	(143)
Se^{77}			
H_2Se	15	H_2SeO_3 (aq)	(579)
Rb^{85} (s)	−65.0	RbOH (aq)	(218)
Rb^{87} (s)	−65.3	RbOH (aq)	(218)
RbF (s)	−0.6	Saturated aqueous RbCl	(220)
RbCl (s)	−0.89	Saturated aqueous RbCl	(220)
RbBr	−1.29	Saturated aqueous RbCl	(220)
RbI	−1.49	Saturated aqueous RbCl	(220)
Sn^{117}	−70.1	Saturated aqueous $SnCl_2$	(362)
Sn^{119}	−70.9	Saturated aqueous $SnCl_2$	(362)
Te^{125}	0	$TeCl_4$ (aq)	(144)
Cs^{133}	−149	CsCl (aq)	(218)
CsF (s)	−0.9	Saturated aqueous CsCl	(220)
CsCl (s)	−1.63	Saturated aqueous CsCl	(220)
CsBr (s)	−2.08	Saturated aqueous CsCl	(220)
CsI (s)	−2.52	Saturated aqueous CsCl	(220)
Tl^{203} (in TlNa alloy)	103	Tl	(85)
Tl^{205}	−154	Saturated aqueous $TlC_2H_3O_2$	(85)
$Tl(NO_3)_3$	−13.7	$TlC_2H_3O_2$	(219)
Pb^{207}	−124	$Pb(C_2H_3O_2)_2$	(85, 314)

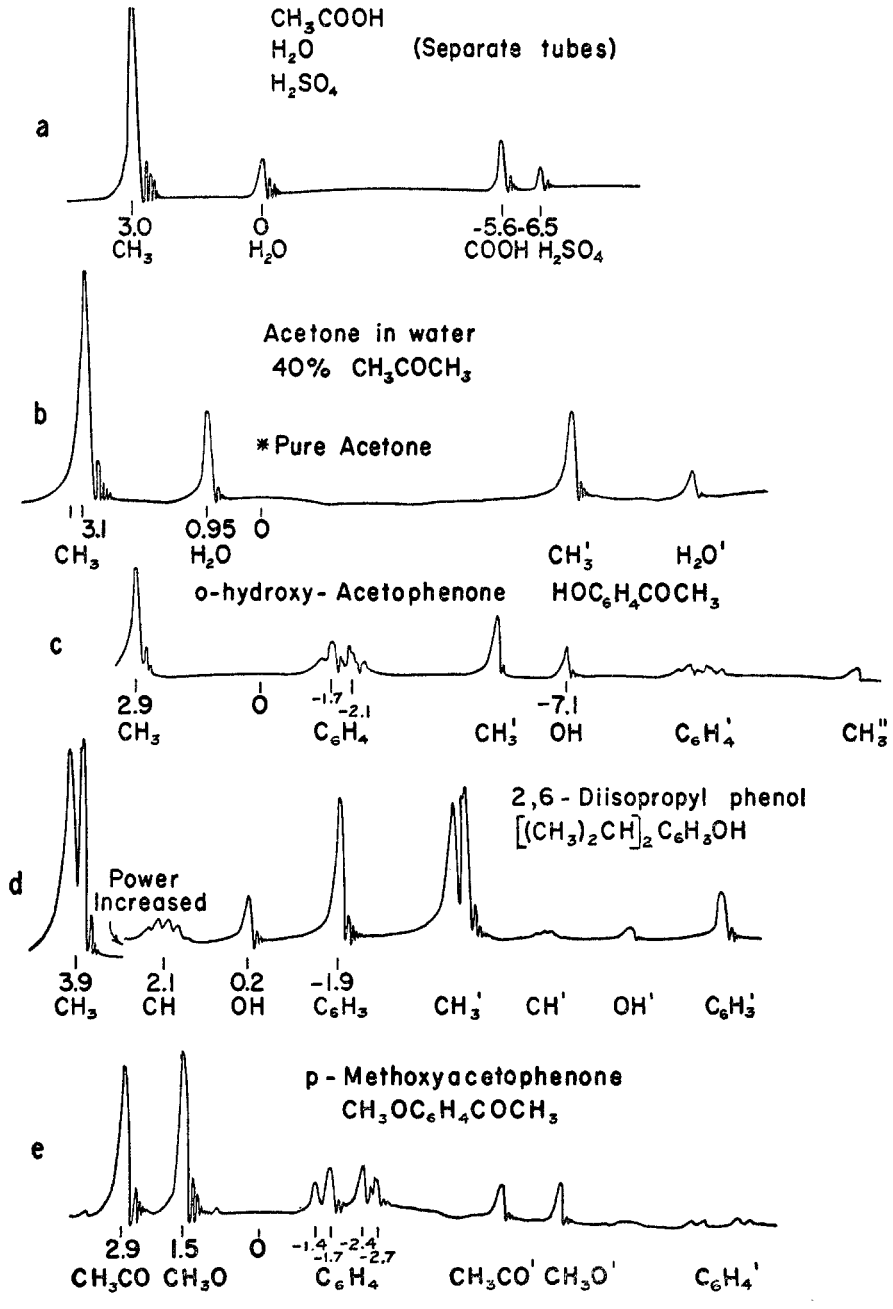

FIG. 9. Multiple resonance lines in proton-containing compounds. Numbers are displacements from the proton line in water, expressed in parts per million. (a) Resolved lines due to protons of CH_3 and COOH. Reference lines for H_2O and H_2SO_4 also appear. (b) CH_3 and H_2O lines in an acetone–water solution are both displaced from their positions in the pure compounds. The third and fourth peaks (CH_3' and H_2O') are sidebands of the CH_3 and H_2O lines displaced 250 cps from the main lines. (c, d) Extreme variations of OH proton line in phenols is shown. Note second sideband of CH_3 (labelled CH_3'') in (c). (e) CH_3 proton position is shown to be dependent on the adjacent atom.

Many hundreds of organic and inorganic compounds have been examined in the liquid phase or in solution for observation of their structure. A few traces are given in figure 9. Tables of relative shifts $\sigma = (H_c - H_r)/H_r$ for a number of proton-containing groups in a variety of compounds show a range of variation of σ for a particular group (365). H_c refers to the resonant field for the compound being observed, while H_r applies to the reference substance. Water is most frequently chosen as a reference. For the OH proton in phenols there is an extreme range of variation, with σ-values ranging from 0.2×10^{-6} in 2,6-diisopropylphenol (36) to -7.1×10^{-6} in *o*-hydroxyacetophenone. The OH range spans that of known COOH values as well as that of H_2SO_4. In many cases the σ-value will decrease as one goes to more acidic protons, thus indicating less diamagnetic shielding. Shielding values for proton groups are given in table 3.

From the multiple proton resonance peaks of diborane it was concluded that the bridge model is confirmed and the bridge protons show more hydride-like character than the other protons (392).

TABLE 3

Proton shielding in organic groups

Group	Type	$\sigma \times 10^6$ (Referred to H_2O)	Number of Compounds
OH	Alcohol	−0.7 to +0.6	17†
OH	Phenol	−7.1 to +0.2	(69)*
COOH		−7.1 to −5.6	8
SO_3H		−7.0 to −6.3	3
SH	Mercaptan	+3.3	1
SH	Thiophenol	+2.0	1
NH	Alkyl amine	+4.3, 4.5	2
NH	Aryl amine	+1.9, 2.0	2
NH_2	Alkyl amine	+3.1 to +4.2	9
NH_2	Aryl amine	(+0.4 to +2.1)	(19)*
NH_2	Amide	−2.9	1
$CH_3-C<$		+3.6 to +4.4	22
$CH_3-C=$		(+2.6 to +3.2)	(18)*
		+2.9 to +3.7	9
$CH_3-C_6H_5$		(+2.7 to +3.3)	(45)*
		+3.0 to +3.7	12
$CH_3-C\equiv$		+3.4	1
CH_3-N		+2.1 to +2.9	6
CH_3-O-		(+1.1 to +1.8)	(33)*
CH_3-X ($X \neq C$)		+1.2 to +2.3	7
CH_2 (cyclic)		+3.2 to +3.9	9
$C-CH_2-O-$		(+0.9 to +1.8)	(12)*
$C-CH_2-CO$		(+2.7 to +2.9)	(5)*
$C-CH_2-X$		+0.8 to +3.3	21
$CH_2=$		−1.0 to +0.2	7
$CH\equiv$		+2.0 to +2.6	4
$C=CH-C$		−1.6 to +0.5	9
C_6H_x		(−3.8 to −0.7)	(156)*
Other aromatic		−3.9 to −1.8	4
X—CHO		−3.7 to −2.6	5
C—CHO		−5.2 to −4.3	18*

* Values from reference 36.

† Undesignated data from reference 365.

For precise comparisons of shielding, especially in a series of solutions, it is necessary to know the volume susceptibilities of the samples and also to take account of the effect of their shape on the field within them. The field at a dipole located in a cavity inside a liquid will be

$$H = H_z - (4\pi/3 - \alpha)\chi H_z \tag{14}$$

α is the demagnetizing factor for the shape of the sample, being $4\pi/3$ for a sphere and 2π for a cylinder. χ is the volume susceptibility. The determination of susceptibilities is discussed in Section IX.

A. Concentration-dependent shielding

The shielding of a particular nucleus depends on the difference between a diamagnetic and a paramagnetic term, both of which should be temperature-independent. In verification of this, the separation of multiple resonance in several fluorine compounds was found to be independent of temperature over a range of about 200°C. (209). However, if a molecule possesses a state of energy within kT of the ground state and if this state has a different shielding constant, the shielding will be a function of temperature (341). It will likewise be an average over the two states if the lifetime of both is sufficiently short. Such states are present if association or hydrogen bonding occurs, or if there is a chemical exchange which occurs at a rapid rate. The first observation of such an effect was made in methanol and ethanol (26). While the separation of CH_3 and CH_2 lines did not change with temperature, the OH-CH_2 separation was found to decrease as the temperature was increased. Dilution of the alcohol with chloroform had the same effect as raising the temperature. Both of these effects serve to diminish the number of hydroxyl hydrogens instantaneously hydrogen-bonded, and the proton is shielded more. Dilution experiments on phenols give more complicated behavior, e.g., dilution 4:1 with cyclohexane does not change the shielding of the OH proton (36).

When chemical exchange can occur at a rapid rate, as protons between water and an acid, a given proton will have exchanged positions a number of times during an observation. A single line appears at a position which is the number average of the positions in the two compounds (226), since the proton "sees" an effective shielding field intermediate between the two fields without exchange.

$$H_aA + H_bB \rightleftarrows H_bA + H_aB$$

The lifetimes are conveniently expressed in terms of a correlation time τ. If τ is long compared with the line width, one sees separate lines; if τ is very short, one sees a single sharp line. In the intermediate case $\tau \approx 1/\Delta\omega$, one has a single broadened line. One may be able to set limits on the rate of exchange from the behavior of a line. Lifetimes from 10^{-4} sec. to 1 sec. have been estimated (24, 226). Deviations from linear variations of shielding with concentration have been interpreted as indicating incomplete dissociation for concentrated solutions of sulfuric, perchloric, and nitric acids (226, 258, 354) as well as for hydrochloric,

hydrobromic, and hydriodic acids (355). The dissociation constant for nitric acid has been calculated to be 22 (258) and that of perchloric acid as 38 (258). The apparent degree of dissociation of nitric acid has been determined both from H^1 and N^{14} resonance; the N^{14} absorption occurs at a field which is the average between that for HNO_3 (pure) and NO_3^- (354). In the later work, account was taken of the correction for the susceptibility and shape of the samples. In very dilute solutions, it appears that perchlorate ion is more effective than chloride ion or nitrate ion in reducing the degree of association of water molecules (258). At high concentrations of perchloric acid the dissociation constant curve approaches a limiting slope, which is taken as evidence that in the nearly anhydrous acid all the water is bound in the form of H_3O^+ ions. In concentrated hydrogen halide solutions the "undissociated molecules" cannot be covalently bonded HX, for interaction of the large nuclear quadrupole moment with the asymmetrical charge distribution would broaden the halogen line past detection. This effect is explained in Section VIII. The species present is probably the ion pair $H_3O^+X^-$, where such interaction is not present because of the spherical symmetry of the halide ion.

Studies with Tl^{203} and Tl^{205} show large variations of resonant field with anion concentration for $TlCl_3$, $TlNO_3$, $Tl(NO_3)_3$, and $TlC_2H_3O_2$ (219). The system ammonia plus water shows slightly increased shielding of the single proton line with increasing concentration, much the same as for ammonium salts. The line does not fall on the one predicted for a linear shift from pure NH_3 and H_2O (208). Phosphorus in carbon disulfide solutions shows a linear increase in shielding as a function of concentration (418). Other applications of shielding will be given after relaxation phenomena have been treated.

B. Shielding by paramagnetic substances

Early workers were accustomed to adding paramagnetic salts to their samples to give an enhanced signal. In the first shielding work on ammonium nitrate, it was found that the separation of the NH_4^+ and the NO_3^- nitrogen lines was increased by the addition of manganous chloride (443). Later it was shown that ferrous, cobaltous, and cupric ions will displace the resonance frequency of fluorine, lithium, hydrogen, and deuterium (81, 149, 200). The amount of the shift is dependent upon the shape of the sample. Consider a nucleus in a spherical cavity in the liquid. The field within a sample of matter is less than the applied field by an amount $\alpha\mathfrak{M}$, where α is called the demagnetizing factor and is determined by the sample shape. $\mathfrak{M}$ is the magnetic moment per unit volume. The field H' arising from the paramagnetic ions will be given by

$$H' = (4\pi/3 - \alpha)\mathfrak{M} + \beta\mathfrak{M}$$

where β is to be determined by experiment. For an isotropic medium it would be zero. If a spherical sample were used, α would be $4\pi/3$ and one would expect zero contribution from the paramagnetic ions. Experimentally it is found that β is not zero and may be positive or negative. The value depends upon both the

type of nucleus and the compound in which it is found. Anticipating later discussions, one remarks that in crystals the factor g defined by

$$g = \frac{\mu_{eff}}{\sqrt{S(S+1)}} = \left(\frac{3\chi kT}{N\mu_B^2 S(S+1)}\right)^{1/2} \tag{15}$$

may take principal values $g_{||}$ and $g_{\perp}$ when the internal electric field is parallel or perpendicular to the applied magnetic field. When the two are unequal, the resultant g is anisotropic and a net field shift should result (81, 200).

C. Shielding in metals

Reference to table 2 will disclose that the resonant fields for metals are lower than for their salts (149, 218, 312, 559, 85). The amount of the so-called "Knight shift" ranges from 0.026 per cent for Li^7 to 1.54 per cent for Tl^{205}. The direction of this shift is opposite to that of the diamagnetic shielding of molecules by electrons. This effect also shows a slight dependence upon temperature (205, 362) and an anisotropy (85).

Those electrons in the high-energy tail of the Fermi band contribute a weak paramagnetism which may be difficult to detect directly. Nevertheless their effect in reducing the resonant field value is relatively great. The value of the shift may be calculated if electronic wave functions are sufficiently well known and is given by the expression (559):

$$\frac{\Delta H}{H} = \frac{hc\Delta\nu I\chi_m m_a}{\mu_I\mu_B(2I+1)} \frac{< |\psi_F(0)|^2 >}{|\psi_a(0)|^2}$$

Here χ_m is the contribution of electron spin to mass susceptibility, m_a is the atomic mass, $< |\psi_F(0)|^2 >$ represents the average of the probability density at the nucleus of the conduction electrons at the Fermi surface, and ψ_a is the wave function of an s-electron in a free atom. It has become a favorite pastime of theoretical physicists to test electron wave functions for metals by calculating the resonance shift (291, 310, 318, 319, 320). The practical significance of the shift lies in the fact that it is a measure of the probability of finding a high-energy electron near a nucleus.

IV. ELECTRON-COUPLED SPIN INTERACTIONS

If diamagnetic shielding alone were responsible for multiple resonance in a single compound, one would expect a number of lines equal to the number of non-equivalent nuclei of a given species. In the gaseous or liquid state or in solutions of compounds of phosphorus, fluorine, nitrogen, antimony, boron, and hydrogen one has observed considerably more lines than expected on this basis (212, 215, 444).

In a rigid solid, nuclei Y in a group XY_n may contribute mutually a dipolar field which can assume a small number of values depending on the magnetic quantum number. If $I = \frac{1}{2}$ and $n = 2$, this local field will have either of two values if neighboring groups are ignored. A pair of lines may arise, symmetrically

disposed about the applied field H_z. However, in the liquid state or even in the solid near the melting point, the frequent and abrupt reorientations which the nuclei undergo cause them to see an average field value and no such multiplets may persist. When first examined in aqueous solution the antimony resonance of the SbF_6^- ion appeared to be an exception, for seven components were present (444). Although incorrectly interpreted (12), these were the first of a new type of hyperfine structure lines to be observed. For six fluorine nuclei of spin $\frac{1}{2}$ the total quantum number may be 3, 2, 1, 0, -1, -2, -3 ($2I + 1$ arrangements) with statistical weights 1:6:15:20:15:6:1 obtained from the number of ways in which six spins can give the total quantum number. The observed relative intensities conform to these weights (145), which are just the sixth binomial coefficients. The problem then is to explain how one nucleus (the antimony in this case) may acquire a small number of discrete polarizations due to nearby nuclei (fluorine) where these are moving frequently with respect to each other. If one considered only the static fields given by μ/r^3, the line would be smeared out instead of showing multiplet structure.

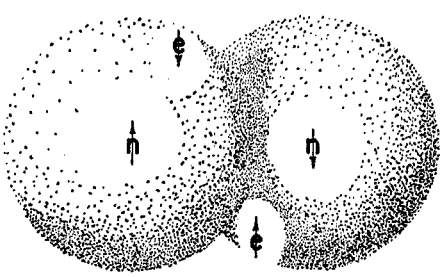

FIG. 10. Nuclear dipole coupling *via* electronic spin dipoles in a covalently bonded molecule.

The explanation for the transmission of polarization has been given in terms of polarization of the bonding electrons and is pictorially represented in figure 10 for a case of nuclei of positive magnetic moment (460). Assume that instantaneously nucleus 1 has a given orientation. This will cause its bonding electron to be oriented more than half of the time in the opposite sense, since the sign of the magnetic moment of the electron is negative. The bonding electron of the adjacent atom must have an opposite spin and will contribute to the polarization of nucleus 2. This effect may be further propagated and in organic compounds can be transmitted through four bonds. The electron spin does not enter into the explanation of shielding effects, since the field is externally applied and affects electrons equally (458, p. 118). Earlier proposed interactions proved too weak to explain the observed effects (212, 215, 233, 363).

The simplest example from a theoretical point of view is gaseous HD, where one would predict that the hydrogen should give a triplet ($2I + 1 = 3$ for D) and the deuterium a doublet. Although the absorption in gases is very weak, the predicted patterns were found. The electron-coupled spin–spin interaction for

gases and liquids is of the form $hJ_{12}\mathbf{I}_1\cdot\mathbf{I}_2$ (460). For HD the coupling constant J_{HD} is approximately given by the relation:

$$J_{HD} = (64\mu_n^2 h\gamma_H\gamma_D/9\Delta) \mid \psi \mid^2_{1H2D}$$

Here Δ represents a mean energy of excited states of HD, and the square of the wave function measures the probability of finding one electron each on hydrogen and deuterium (459). Although Δ is difficult to evaluate, the expression implies that the splittings would be the same for hydrogen and deuterium resonance expressed in cycles per second and independent of applied field. The measured separation of electron-coupled splitting components gives J_{HD} as 43 cps (101, 522, 612). In other compounds the field independence of the electron-coupled splittings has been verified down to fields of several hundred gauss (216, 444, 452). The splitting has likewise been found to be independent of temperature (216). Experimentally it has been found from examination of hundreds of compounds that electron-coupled spin–spin interaction does not give rise to observable effects for structurally equivalent nuclei, i.e., in ethane no splitting of the proton resonance would be observed. This result can be given quantum-mechanical justification (216).

In many compounds the electron-coupled splitting is smaller than that due to shielding of non-equivalent nuclei. When this is true, progressively increased resolution will allow one first to draw conclusions as to the presence of non-equivalent nuclei and then obtain patterns which may be characteristic of particular adjoining groups. However, the two types of splitting may produce comparable effects. Electron-coupled splittings less than 0.1 milligauss have been found in ethanol, while in the SbF_6^- ion the splittings are about 1.9 gauss. It is helpful to take traces at two frequencies, e.g., 30 and 40 Mcps. The chemical shielding lines will be displaced by a factor of 4/3, while the spacing of electron-coupled components is unchanged. A second procedure which is useful when non-identical nuclei A and B are involved is to irradiate simultaneously at the resonant frequencies of both. High power used at the frequency of the nucleus B eliminates the electron-coupled splitting, since B undergoes numerous transitions among its levels during a period of observation (9). The shielding pattern then persists. This technique proved useful in verifying the spin of C^{13} as $\frac{1}{2}$, since irradiation at the C^{13} frequency caused the two proton lines in $C^{13}H_3I$ to collapse to a single sharp line (473). The splitting pattern of nucleus A must necessarily change progressively from a multiplet to a singlet as the radiofrequency level is increased at the resonant frequency of nucleus B. The fluorine resonance in Na_2PO_3F would normally be a doublet, since $I = \frac{1}{2}$ for phosphorus. Simultaneous irradiation at the phosphorus resonance frequency gives a central component which grows with radiofrequency field level, while the outer components become weaker and more widely separated (88). Radiofrequency pulse experiments conducted with molecules giving rise to electron-coupled structure show slow modulation or "beats" of the transient induced signals and are due to the spin–spin interaction described above (231, 233, 234, 363). However, although the experiments are done in an easily obtainable inhomogeneous field, the results are laborious to interpret.

Ethanol has been more intensively studied for its shielding and electron-coupled splittings than any other molecule to date (24, 25). Since the CH_3, CH_2, and OH groups are progressively less shielded, they will give rise to proton lines in this order as the applied field is linearly reduced. As the overall separation of the three lines is only about 0.030 gauss in 7050 gauss (125 cps in 30 Mcps), their observation required the attainment of a field more homogeneous than any previously produced. As better homogeneity was attained, the CH_2 and CH_3 lines were found to be further split from spin–spin interaction. As is to be anticipated if the protons on adjacent groups interact *via* their bonding electrons, the CH_3 line became a triplet and the CH_2 line a quadruplet. There remained unanswered for a time the question as to why the OH proton did not participate in spin–spin interaction. On careful drying and purification to reduce the frequency of chemical exchange, the OH line was indeed found to give a triplet from interaction with the CH_2 protons, while the latter should be split into eight components, due to the OH proton. Even finer structure will be taken up shortly, after citing other examples where this simple approach gives the correct number of electron-coupled splitting lines. Figure 11 shows progressive resolution of ethanol lines.

The proton lines from substituted benzenes are usually multiple and have not yet been fully interpreted. For a large number of compounds with different groups in the 1- and 4-positions, one has two pairs of lines well separated from one another (33, 36), as in figure 9e. In many monosubstituted benzenes, e.g., fluorobenzene or toluene, the proton resonance of the ring hydrogens (33, 36) is a single line. The protons split the fluorine resonance of fluorobenzene into six components as if they were all equivalent (33).

Ammonia upon rigorous drying gives a triplet proton line structure, since the spin of N^{14} is 1 (391). Although it has not been reported, the nitrogen resonance line should be a quadruplet. The BH_4^- ion gives four electron-coupled splitting proton lines, since the spin of B^{11} is 3/2 (392). There are also present seven weak proton lines due to B^{10} of spin 3. The B^{11} pattern consists of five lines. As was pointed out in connection with HD, the electron-coupled splitting separation of adjacent lines by mutual interaction should be the same for the two nuclei. This was verified here. The electron-coupled splitting pattern on B_2H_6 is too complex for resolution at present, but it agrees in a qualitative way with expectations of the bridged proton model:

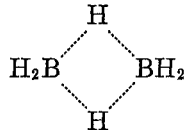

In the FHF^- ion the hydrogen shows a triple line and the fluorine a double one (592).

The P^{31} doublet in H_3PO_3 and the triplet in H_3PO_2 are taken as evidence for one proton directly bonded to phosphorus in the former, while there are two in the latter (216). Other phosphorus and fluorine compounds give electron-coupled splitting patterns which are in agreement with expectation (216). In

numerous cases electron-coupled structure is absent where one might have expected it. While explanations have been advanced for its non-appearance (216), it is only in case rapid chemical exchange occurs (such as in ethanol in the presence of acids or bases) that the cause has been definitely established for a particular molecule.

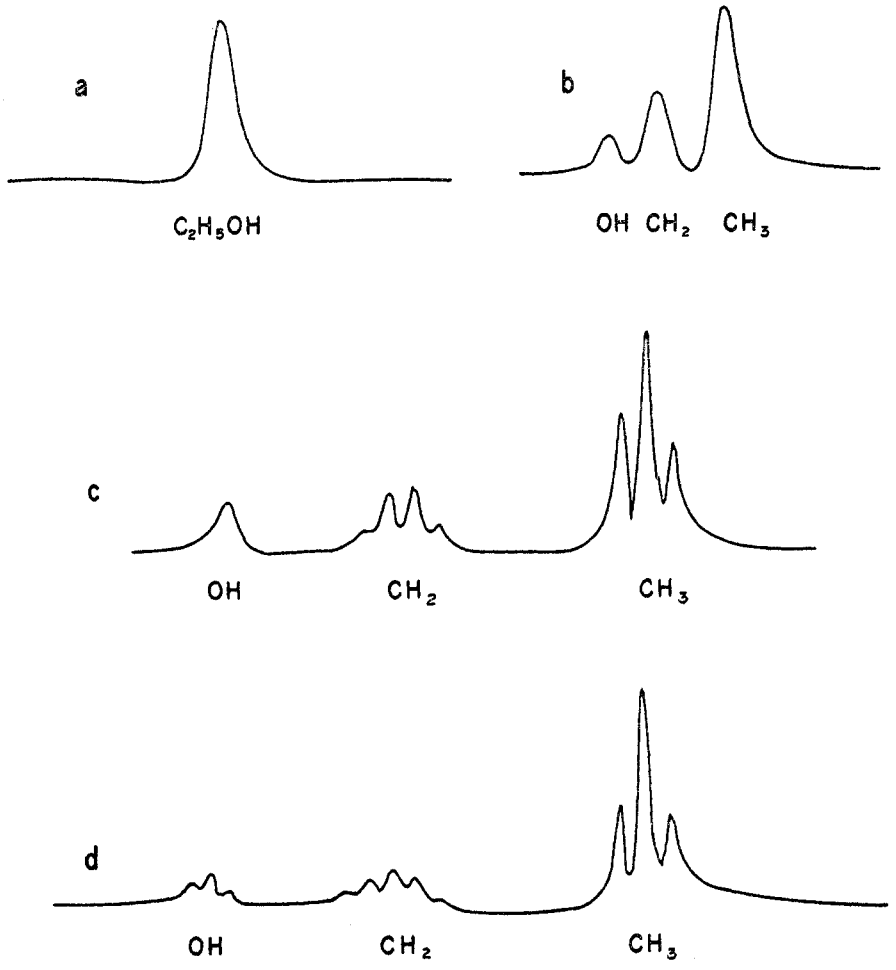

FIG. 11. Nuclear spin resonance in ethanol under progressively better resolution. (a) Unresolved line. (b) Resolved shielding components. (c) Electron-coupled dipolar splitting. Chemical exchange of the OH proton in an impure sample is responsible for the single OH line. (d) Splitting of the OH line in a purer sample. Note changed appearance of CH_2 line. Some of the CH_2 components are unresolved.

It has been suggested that indirect coupling of nuclei by conduction electrons in metallic silver would give a narrow line if only one isotope were present. Since Ag^{107} and Ag^{109} are nearly equal in abundance, the line is broad (474). Magnetic interaction of nuclei by way of bonding electrons in GaSb and InSb has been invoked to explain the invariance of line width with temperature and other

variables. The observed line is presumably the envelope of many multiplets (511).

Returning to ethanol, one finds surprisingly good correspondence between theory and experiment for a large number of lines. Here the Hamiltonian may be written as the sum of three terms

$$\mathcal{H} = \mathcal{H}' + \mathcal{H}'' + \mathcal{H}''' \tag{16}$$

corresponding to chemical shifts and first- and second-order spin–spin interaction, respectively (9, 24). The chemical shift Hamiltonian is

$$\mathcal{H}' = \frac{-h}{2\pi} \mid \gamma \mid [(\mathbf{H}_z + \mathbf{H}_1)\cdot\mathbf{I}_1 + (\mathbf{H}_z + \mathbf{H}_2)\cdot\mathbf{I}_2 + (\mathbf{H}_z + \mathbf{H}_3)\cdot\mathbf{I}_3] \tag{17}$$

with eigenvalues

$$E' = \frac{-h}{2\pi} [(\omega_0 + \omega_1)M_1 + (\omega_0 + \omega_2)M_2 + (\omega_0 + \omega_3)M_3] \tag{18}$$

where $\omega_0 = \mid \gamma \mid H_z$ and $\omega_i = \mid \gamma \mid H_i$. The subscripts 1, 2, and 3 refer to the OH, CH_2, and CH_3 groups, respectively. If there were no other interactions the allowed individual transitions with $\Delta M = 1$ would give lines with intensities 1:2:3.

Now allowing the CH_3 and CH_2 groups to interact, the Hamiltonian $\mathcal{H}''$ becomes

$$\mathcal{H}'' = \mathcal{H}' - \frac{h}{2\pi} J_{32}\, \mathbf{I}_3\cdot\mathbf{I}_2 \tag{19}$$

where J_{32} measures the interaction between $\mathbf{I}_3$ and $\mathbf{I}_2$ and is simply the electron-coupled line separation in radians per second.

A first-order approximation replaces $\mathbf{I}_3$ and $\mathbf{I}_2$ by their z components $\mathbf{I}_{3_z}$ and $\mathbf{I}_{2_z}$ with eigenvalues M_3 and M_2. Then the magnetic energy of the system E'' is given by:

$$E'' = E' - \frac{h}{2\pi} J_{32} M_3 M_2 \tag{20}$$

The sign of J_{32} is unknown. Letting $\Delta M = \pm 1$ for CH_3 transitions, the equation predicts lines of frequency $\omega_0 + \omega_3 \pm J_{32}$ and $\omega_0 + \omega_3$ when M_2 takes the values ± 1, 0. Similarly for CH_2 transitions, lines occur at $\omega_0 + \omega_2 + J_{32}M_3$, where M_3 takes the values $\pm\frac{3}{2}$, $\pm\frac{1}{2}$.

If the CH_2 and OH protons interact because the latter are exchanged very slowly equation 19 would have an extra term, $\frac{-h}{2\pi}(J_{21}\mathbf{I}_2\cdot\mathbf{I}_1)$, and equation 20 should have the added term $\frac{-h}{2\pi} J_{21}M_2M_1$. M_1 can take the values $\pm\frac{1}{2}$ so that each of the four previous lines will be split into two components of about half the original intensity and separated by J_{21}, since the latter is found to be less than J_{32}. The OH single line now becomes a triplet, just as for CH_3. Progressive stages of resolution are shown in figure 11.

When second-order effects are calculated, terms such as J_{32}^2 and M_3^2 appear. The final equation which gives energy levels for pure ethanol is a function of the I and M values of all the groups and is

$$E = \frac{-h}{2\pi}\Big\{(\omega_0 + \omega_1)M_1 + (\omega_0 + \omega_2)M_2 + (\omega_0 + \omega_3)M_3 + J_{32}M_3M_2 - \frac{J_{32}^2}{2(\omega_2 - \omega_3)}[M_3(I_2^2 + I_2 - M_2^2) - M_2(I_3^2 + I_3 - M_3^2)] + J_{21}M_2M_1 - \frac{J_{21}^2}{2(\omega_1 - \omega_2)}[M_2(I_1^2 + I_1 - M_1^2) - M_1(I_2^2 + I_2 - M_2^2)]\Big\} \quad (21)$$

The three CH_3 lines become eight, the eight CH_2 lines become twenty-five, and the three OH lines become four. Most of the predicted thirty-seven lines are observed. It is a real experimental triumph that such resolution has been achieved, and one does not worry about failing to resolve some of the lines only 0.1 cps removed from adjacent ones.

The considerations outlined above do not lead to the right number and intensity of electron-coupled components in all cases (361). Examples of such failure are $CF_2{=}CH_2$, which has eight observed lines for both hydrogen and fluorine, and $CF_3CF{=}CF_2$, for which fifty-two lines have been observed. Ten lines are predicted by a group-theoretical approach for both hydrogen and fluorine in $CF_2{=}CH_2$, and their intensities have been calculated with an accuracy probably exceeding that of direct measurement. A molecular orbital approach to calculation of coupling constants has been made (359, 360). Similar calculations are much needed, especially for aromatic compounds.

V. RELAXATION EFFECTS

A. Thermal relaxation

In optical absorption spectroscopy one may measure absorption coefficients which are independent of the intensity of illumination if photochemical reactions do not occur. One is accustomed to a rapid return from an excited state to the ground state, the energy most commonly being degraded into heat. It is unnecessary to irradiate a sample in order to cause a return from an excited state.

In NSR spectroscopy, strong irradiation may weaken or eliminate observable absorption or induction signals. The very isolation of nuclear dipoles from their surroundings in comparison with electronic interactions gives rise to this situation. Lifetimes of the excited state in liquids may be of the order of seconds, while for solids at low temperatures they may be hours. Much longer times had originally been predicted (582). Nuclear dipoles of spin $\frac{1}{2}$ are affected only by magnetic fields. Anticipating later results, one finds that fluctuating magnetic fields which have a component at the precession frequency may induce a return to the ground state. Lattice vibrations in solids are ineffective because their frequency ($\sim 10^{10}$/sec.) is much too high.

From the gamma-ray region through the visible spectrum the probability of stimulated emission (i.e., induced by the radiation) is very small, but for magnetic

resonance it is large and equal to the probability of absorption. On the other hand, the probability of spontaneous emission is negligibly small. As a consequence, a strong radiofrequency field may quickly excite dipoles to an upper level and equalize the population of the several states. Although individual dipoles still continue to absorb energy, an equal number are being returned to lower levels and no detectable continuous absorption is observed.

Let a sample containing N nuclear dipoles per cubic centimeter be rapidly thrust into a magnetic field. If their spin is $\frac{1}{2}$, they will be equally distributed between the two energy states which were originally degenerate. (The application of a field thus does not itself produce a macroscopic polarization.) Since such a distribution would correspond to an infinite temperature, some of these must find their way to the ground state. The equilibrium excess of the number $N(\frac{1}{2})$ in the ground state over the number in the excited state $N(-\frac{1}{2})$ will be equal to:

$$N(\tfrac{1}{2}) - N(-\tfrac{1}{2}) = \left[\frac{N(\frac{1}{2})}{N(-\frac{1}{2})} - 1\right] N(-\tfrac{1}{2}) = N(-\tfrac{1}{2})\left[\frac{\exp(\mu H/kT)}{\exp(-\mu H/kT)} - 1\right] \approx N(\mu H/kT) \qquad (22)$$

since $N(-\frac{1}{2})$ is very nearly $N/2$. The magnetic moment of the proton is the second largest of nuclei with spin $\frac{1}{2}$, being exceeded only by that of H^3. For this especially favorable case of nuclear polarization the fraction excess in the ground state at 7000 gauss and 300°K. is about 10^{-5}. Though this number appears small, the observable amplitude of the induction or absorption signal arises from this excess.

When a sample containing nuclear dipoles has come to equilibrium in a magnetic field, the temperature to be used in the Boltzmann factor is that of the sample, whereas when the field was first turned on, the "spin temperature" was infinite, corresponding to a perfectly random orientation. The dipoles "cool off" at a rate which is to be given below. If $I > \frac{1}{2}$, a spin temperature is meaningful only if the population of all the levels is given by a Boltzmann distribution.

One may tentatively assume that there is a characteristic relaxation time t_1 for transfer of excitation energy to the surroundings in the form of heat. Let us call the summation over instantaneous values of z-components of magnetic moment for all nuclear dipoles the macroscopic polarization $\mathfrak{M}_z$ and its equilibrium value $\mathfrak{M}_0$. $\mathfrak{M}_0$ is given by the relation:

$$\mathfrak{M}_0 = \chi H_z = \frac{N\mu^2 I(I+1)}{3kTI^2} H_z \qquad (23)$$

Assume that the attainment of equilibrium is a first-order process:

$$d\mathfrak{M}_z/dt = (\mathfrak{M}_0 - \mathfrak{M}_z)/t_1 \qquad (24)$$

Initially the polarization $\mathfrak{M}_z$ is zero, and upon solving equation 24 one gets:

$$\mathfrak{M}_z/\mathfrak{M}_0 = 1 - \exp(-t/t_1) \qquad (25)$$

Equation 25 is valid for the growth of polarization in the field H_z in the absence of the oscillating field:

$$H_x = 2H_1 \cos \omega t$$

The effect of the latter is to give (60) for the steady state the equation:

$$\mathfrak{M}_z/\mathfrak{M}_0 = 1/(1 + \gamma^2 H_1^2 t_1 t_2) \tag{26}$$

where the significance of t_2 is as explained below. One observes that instead of $\mathfrak{M}_z$ becoming in time equal to $\mathfrak{M}_0$, it is reduced by the factor of saturation in the denominator. However, for liquids the second term in this factor may often be made small compared to 1. The same term will appear later in the equations giving the shape of the absorption curve. Assuming that the saturation factor is close to 1, we may use equation 25 to determine t_1. If by means of an oscilloscopic record camera one were to photograph the amplitude of the signal as a function of time after inserting a sample and plot the log of the difference between the signal amplitude and that of the steady-state signal as a function of time, the slope would be $-t_1$. In practice one may leave the sample in position and observe the signal when the sweep amplitude is suddenly increased from several times the apparent line width to a much larger value, thus giving the dipoles a much longer time to recover between resonant periods.

Time t_1 varies from 10^{-5} to 10^4 sec. in order of magnitude, the latter being obtained for ice at low temperatures (477).

An extremely weak radiofrequency field applied over many precession periods represents one extreme of excitation. The other would be short intense pulses. Analysis indicates that if relaxation times are sufficiently long, one can get just as intense a signal from a weak as a much stronger radiofrequency field (481).

A striking illustration of the effect of a saturating radiofrequency field is the sudden large increase in signal amplitude when the liquid sample is caused to flow (44, 87, 540).

Having seen that oscillating magnetic fields at the precession frequency will cause transitions, one proceeds to inquire how these may arise when not externally applied.

In liquids and gases the molecules undergo rapid and irregular reorientations. The motion of the nuclei will have a Fourier component at the precession frequency and the intensity of this component will determine t_1. In dielectric relaxation experiments a correlation time was used by Debye as the time constant with which a group of oriented electric dipoles achieves random distribution (138). It is given by the expression

$$\tau_{\text{Debye}} = \frac{4\pi\eta a^3}{kT} \tag{27}$$

η is the viscosity and a is the radius of the spherical molecule. For water at 20°C. $\tau_{\text{Debye}} = 0.8 \times 10^{-11}$ sec. A somewhat analogous correlation time τ_c is

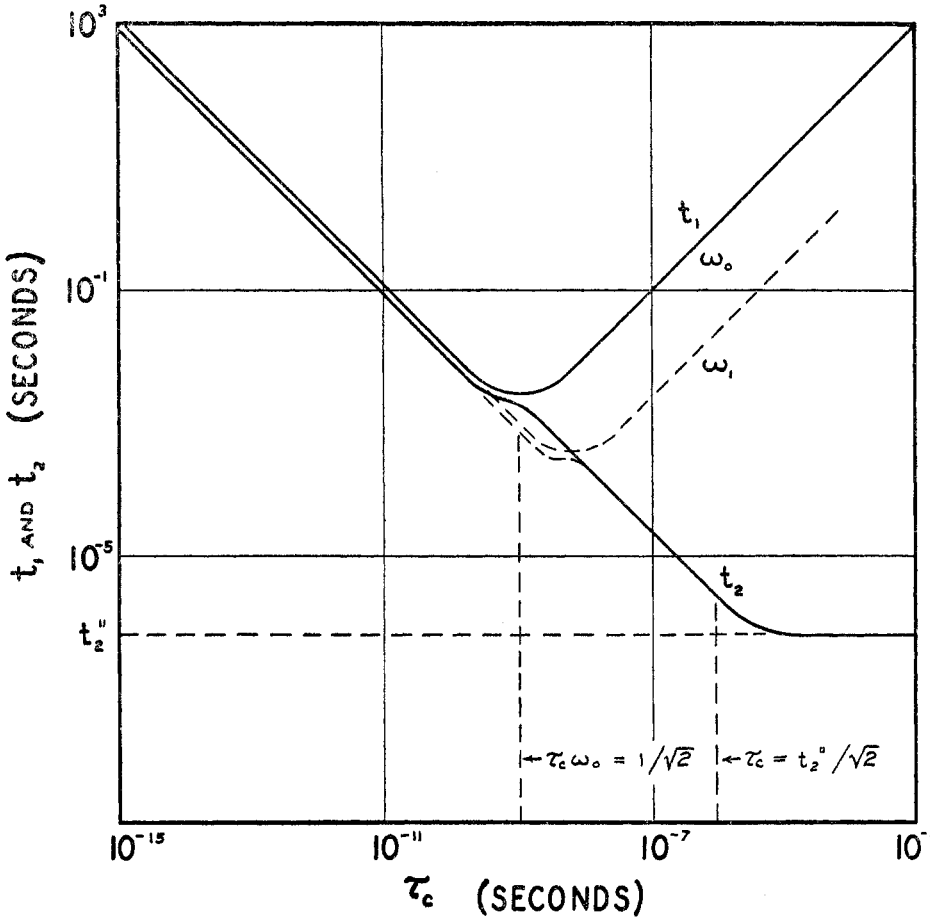

FIG. 12. Relaxation times t_1 and t_2 as a function of correlation time τ_c. t_1 is given by equation 29 (84).

defined for nuclear motions and leads to the following relation for viscous liquids (84):

$$\tau_c = \frac{4\pi\eta a^3}{3kT} \tag{28}$$

It is assumed that the correlation time is the same for rotational and translational motion. It is related to t_1 and the resonant frequency ω_0 by the equation

$$\frac{1}{t_1} = C\left[\frac{\tau_c}{1+\omega_0^2\tau_c^2} + \frac{2\tau_c}{1+4\omega_0^2\tau_c^2}\right] \tag{29}$$

which gives the contribution from nearest neighbors (84). The measurement of t_1 then allows the determination of τ_c. C can be calculated for an assumed type of motion, but it may be evaluated experimentally by noting that t_1 will have a minimum when

$$\omega_0\tau_c = \frac{1}{\sqrt{2}}$$

This shows that reorientations are most effective in relaxation when their correlation frequency is essentially equal to the precession frequency. Equation 29 is plotted in figure 12 as the upper curve.

Notwithstanding its simplicity, equation 29 has received verification for both solids and liquids over a wide range of t_1 and τ_c values. Combining equation 29 with a calculation of contributions from neighboring molecules expressed in terms of a diffusion coefficient, t_1 for water at 20°C. was calculated to be 3.4 sec. This was considered to be satisfactory agreement with the measured value of 2.3 sec. Remarkably, the theoretical value turned out to be better than the experimental ones (84, 229). When the dissolved oxygen was removed, t_1 was found to be 3.6 ± 0.2 sec. (112).

Since a diffusion coefficient gives no insight into diffusion mechanisms, a treatment of spin diffusion as a random-walk process to nearest neighbor sites has been developed for a face- and a body-centered cubic lattice (556, 557).

For non-spherical molecules such as benzene, rotation is hindered and t_1 is larger than for spherical molecules (190). Measurements of t_1 in liquids under high pressure show considerable effects of changed translational diffusion, while rotational diffusion is little altered. t_1 decreases with increase in pressure (47). For hydrogen gas and ethane t_1 was found (402, 575) to vary with pressure as predicted (84), but the opposite behavior was found in He^3 (6).

Early workers used ferric or manganous salts to lower the relaxation time t_1 of water or of dissolved salts to obtain stronger signals (75, 442). The relaxation time t_1 in terms of the number N of paramagnetic ions of effective moment μ_{eff} per cubic centimeter in a solution of viscosity η is given (84) by equation 30:

$$\frac{1}{t_1} = \frac{12\pi^2\gamma^2\eta N}{5kT}\mu_{eff}^2 \tag{30}$$

An excess will both shift the line position (149, 200) and broaden it (84, 627) (uncertainty-principle broadening), the order of broadening being $Mn^{++} > Cr^{+++} > Fe^{+++} > (Cu^{++}, Co^{++}, Ni^{++}, Er^{+++}) > Fe^{++}$ (57). Manganous chloride can give a 1-gauss-wide proton line at a concentration of 0.2 molar (57).

Diamagnetic ions in solution are reported to lower the relaxation time of the protons in water by as much as fourfold (93).

If oxygen at low pressure is added to a gaseous sample its magnetic dipoles (due to its triplet state) in random motion may produce fluctuating magnetic fields which have a component at the precession frequency, and hence both induce transitions and greatly reduce t_1. Practical use has been made of this effect (6, 70) because of the usual low density of gaseous samples. Further examples are found in Section IX.

If a liquid is observed at its freezing point and then cooled, the line becomes much broader and weaker, corresponding to a longer t_1 value. For example, ice at 80°K. has $t_1 = 2.5$ hr. (477). Equation 29 has been found to apply to a number of solids, and τ_c becomes progressively longer at low temperatures. While times of the order of 10^4 sec. appear long, they are much shorter than would be expected from relaxation by lattice vibrations. It appears that unexpectedly

short t_1 values in solids often are determined by the presence of traces of paramagnetic ions (78, 237, 305, 432) or lattice imperfections (470). For example, one obtains unusually strong signals from Cu^{63} and Cu^{65} in metallic copper. This is attributed to a shortening of t_1 by the presence of cupric-ion impurities (430). Nuclear dipoles produce fluctuating fields, but paramagnetic ions will have a moment about 10^3 times the nuclear value and be 10^6 times as effective according to equation 30. The early value of t_1 for ice at $-180°C.$ as 10 min. was probably low because of impurities (407).

The lowering of t_1 in solids by deliberate addition of paramagnetic impurities has been studied and is found to be in accord with prediction (78, 134). It is understandable that those nuclei in the immediate vicinity of a paramagnetic ion in a solid can interact directly with it to lose orientation energy. To account for the thermal relaxation of remote nuclei, the process of spin diffusion has been suggested (78). A nucleus remote from an ion may reduce its energy by making a $\Delta M = +1$ transition while its neighbor gains this energy in a $\Delta M = -1$ transition. If the process is repeated by a second nucleus with another closer to the ion (presumably located at a lattice imperfection), the energy eventually can be transferred to the ion and finally to the environment by spin–orbit interaction. The orbit of a magnetic impurity is modulated by lattice vibrations and because of spin–orbit coupling, the electronic dipole is flipped. This causes a nearby nuclear dipole to make a transition. Experiments on lithium fluoride irradiated with x-rays verify this spin diffusion mechanism. t_1 could be reduced from 5 min. to 10 sec. by irradiation (434).

Thermal relaxation in crystals has been treated as a magnetic dipolar interaction between nuclei and electrons of a filled band, the latter being coupled to the lattice vibrations (377). Although the calculated order of magnitude of t_1 can be made reasonable, it remains to be shown that this mechanism predominates over relaxation by impurities or quadrupole interaction (described later) in systems thus far observed.

The metals represent a separate class of solids as far as thermal relaxation is concerned. Together with paramagnetic solutions they possess some of the shortest t_1 values for nuclei (424). It has been mentioned that electrons near the top of the conduction band displace the resonance field of nuclei to lower values at a fixed frequency because of their paramagnetic properties. The displacement δH of the resonance field or "Knight shift" is related (323) to the relaxation time t_1 by the equation:

$$t_1 = \frac{2\mu_n^2}{hkT\gamma^2\left(\frac{\delta H}{H}\right)^2}$$

The value of t_1 may be reduced to 10^{-4} sec. or less, so that the lines may become broad (218, 388). The temperature-dependence of line width and t_1 are largely due to self-diffusion. The line width of sodium metal changes from about 2.3 gauss at low temperature to a value less than 0.05 gauss (205) in the region of the melting point. Similar narrowing occurs for the ESR line (340). Curiously,

in lithium and sodium the line width *doubles* when the solids melt (249, 387). For sodium and aluminum the value of t_1 decreases with increasing temperature, while lithium shows both a maximum and a minimum (249, 424). The one case of a nucleus being relaxed by electrons of a separate metal appears to be that of protons in palladium (386).

B. Dipole–dipole interactions

The interaction of a dipole with its surroundings has been characterized by the thermal relaxation time t_1. The interaction of dipoles with one another gives rise to both static and rotating field components.

A dipole will produce at a distance r a field of μ/r^3 gauss. If r is 1 Å., and we are considering protons, this amounts to about 14 gauss. In solid hydrogen, resonance has been obtained at 165 kc. with zero applied field, corresponding to the field of about 39 gauss of the neighboring protons (462). When one takes into account the various values of μ/r^3 for the near neighbors of a particular dipole, it is seen that such interaction has the effect of broadening the energy levels of the assembly of dipoles and hence of the absorption lines. Calling the spread in local field H_{loc}, we get from the resonance equation

$$\Delta\nu = \mu H_{\text{loc}}/Ih \tag{32}$$

This is interpreted as meaning that if two dipoles are precessing in phase at a particular instant, they will get out of phase in $1/\Delta\nu$ sec. This is one interpretation of t_2. The energy of interaction will be μ^2/r^3 and from the Heisenberg uncertainty principle, we would expect a Δt given by

$$\Delta t \approx \frac{1}{\Delta E}\frac{h}{2\pi}$$

about $(h/2\pi)(r^3/\mu^2)$, which we shall correlate with t_2. As one dipole precesses about H_z at the Larmor frequency, it is producing at a neighboring dipole of opposite spin an alternating field at just the frequency to cause a transition, so that they may simultaneously reverse their orientation in a "spin exchange," thus limiting the lifetime of each state. Only identical nuclei are capable of undergoing spin exchange, whereas unlike ones can still contribute to the local field. If the system contains nuclear species A and B, one can reduce the local field at A by causing B to make rapid reorientations (243).

The apparent value of t_2, which will be called t_2', may be obtained from the half-width of the absorption curve when dipole–dipole interaction determines the line width (28, 84). Except for solids, this may not be the true value, since the width is often a measure of the inhomogeneity of the magnetic field over the sample. The value of t_2 is related approximately to t_2' and t_1 by the expression (84):

$$\frac{1}{t_2} = \sqrt{\frac{2}{\pi}}\frac{1}{t_2'} + \frac{1}{2t_1} \tag{33}$$

It is possible to determine t_2 from the form of the signals on sinusoidal modulation even in the presence of field inhomogeneities (170, 171, 191). In solids one com-

monly finds that dipole–dipole interactions are appreciable and give rise to lines several gauss wide. Since, as will be shown later, t_2 is equal to the half-width $\omega_0 - \omega$ of the line at half-height, it will be equal to $\sim 4 \times 10^{-5}$ sec. for a line 2 gauss wide. For water $t_2 = 1.4$ sec. (555); hence the line width should be 0.2 cps or $\sim$0.05 milligauss. The narrowest line thus far observed (in ethanol) has a width of about 0.5 cps (24) or roughly 0.1 milligauss. Only a few investigations of t_2 values of related compounds have been made (89, 115).

The "loss of phase memory" may be expressed in terms of the macroscopic polarizations $\mathfrak{M}_x$ and $\mathfrak{M}_y$ by the equations:

$$-\frac{d\mathfrak{M}_x}{dt} = \frac{\mathfrak{M}_x}{t_2} \qquad -\frac{d\mathfrak{M}_y}{dt} = \frac{\mathfrak{M}_y}{t_2} \tag{34}$$

Each of these equations will later be modified to include the effect of the oscillating magnetic field. Whereas the component of magnetization in the z direction changes with a time t_1 to the steady-state value, the x- and y-components decay to zero with time constant t_2. It has therefore been called the transverse relaxation time (69).

It is highly instructive to interpret figure 12, which depicts the variation of both t_1 and t_2 with the correlation time τ_c, the characteristic time (equation 29) for molecular reorientation. At very low temperatures random jumps will occur infrequently and t_2 will have some limiting small value of the order of 10^{-6} sec. The line will have a constant width up to a temperature at which the time between jumps has decreased to the order of magnitude of t_2. Now two dipoles are neighbors for a shorter period of time and the number of spin exchanges in unit time is decreased. Therefore t_2 begins to increase and will continue to do so monotonically with decrease of τ_c. (The line width may show a sudden decrease in a small temperature interval and then remain relatively constant up to the melting point. This behavior, not predicted by the t_2–τ_c curve, will be considered later.) Returning to low temperatures, one observes t_1 to be very long (sometimes of the order of hours), decreasing as τ_c decreases until it reaches a minimum value in the region where $\omega\tau$ approaches unity. At higher temperatures, where the correlation time becomes still smaller, t_1 again increases and is now approximately equal to t_2. The very motion which results in the increase of t_2 at low temperatures is responsible for the reduction of t_1, since in a jump the internal field is rapidly varied, giving rise to Fourier components around the Larmor frequency. In the process the orientation energy is given to the environment. Although this simple interpretation requires that relaxation processes are described by a single correlation time, nevertheless such behavior is shown by a number of substances over a wide range of correlation times.

In figure 13 the resonance absorption line appears as a damped oscillation after the resonant condition has been passed. Such an effect is observed for rapid sweep or modulation rates in a field homogeneous enough to give narrow lines. The time spent at resonance will then be small compared with t_1, t_2, and $1/\gamma\Delta H$, where ΔH represents the field inhomogeneity over the sample. With the applied frequency fixed, the field passes rapidly through the resonant condition with the precession frequency of the nuclei changing continuously as the

field changes. Close to resonance this frequency will yet be close to the applied frequency and one observes the beat frequency between the two as a damped train of waves of changing frequency (84). If the observed line width were not caused by inhomogeneity of the field, the exponential decay constant would be t_2.

When these "wiggles" occur, the first peak will not coincide with the center of resonance but will occur after it (282). The experimental observations are in good accord with theory (54, 156, 169).

The resonance experiments thus far described involve observation after stationary-state conditions have been established. By observations of transient behavior when the radiofrequency field is suddenly turned on, it is possible to determine both t_1 and t_2 (554). These procedures are described in Section XII. Alternatively, one may study the signals obtained when a strong radiofrequency field is suddenly turned off. Speaking classically, there remains a net magnetic moment in the x-y plane, and this induces a signal which decays at a rate de-

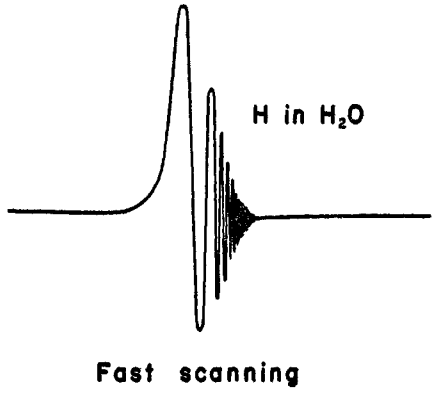

FIG. 13. Transient effects of rapid passage through proton resonance in water

pending on the field inhomogeneities and the time t_2 (69, 230). This is referred to as "free" precession in contrast with the forced precession with a steady radiofrequency field.

Yet another signal, "the spin echo," obtained in the absence of a radiofrequency field, is obtained by applying two strong pulses with intervening time t. At time $2t$ one observes a symmetrical signal similar to those under steady-state conditions (102, 137, 231). The first pulse is of sufficient magnitude and duration to rotate the macroscopic polarization vector 90 degrees from the z-axis into the x-y plane. To an observer in the coördinate system rotating about the z-axis at the precession frequency, the vector would appear to turn about the H_1 axis. Because of the spread in precession frequencies, the vectors corresponding to the nuclei of a particular frequency would fan out in the x-y plane. Now a second pulse of the same intensity and twice the duration will have the effect of reflecting each of these vectors in the x-z plane. Whereas before they spread out of phase, they now come together and at time $2t$ will again be in phase and induce an echo signal. This echo effect has been likened (232) to the result of a

foot race if, at a prearranged signal after starting, all runners were to reverse their direction. Although they had spread out after starting together because they moved with different speeds, they would cross the finish line together if they retained their original speeds. This latter qualification must be taken into account in treating the signal amplitude, for self-diffusion will take a nucleus into a region of different H (231). Both t_1 and t_2 may be determined by appropriate modifications of procedure (102, 231). Alternatively, the effect may be used to calculate the coefficient of self-diffusion in liquids (102).

VI. RELATION TO MAGNETIC SUSCEPTIBILITY

The static magnetic susceptibility, χ_0, is defined by the equation

$$\chi_0 = \frac{\mathfrak{M}}{H}$$

where $\mathfrak{M}$ is the magnetic moment per unit volume. Applied to nuclear dipoles, the equation

$$\chi_0 = \frac{N\mu^2 I(I+1)}{3kTI^2} \tag{35}$$

should and does appropriately represent the variation of the static susceptibility with temperature, since the dipole–dipole interactions are weak. It is of the order of 10^{-10} for protons, whereas diamagnetic susceptibilities are of the order of 10^{-6}. It would be a hopeless task to try to observe the effect of nuclear paramagnetism at room temperatures by susceptibility measurement, since one must lower the temperature to 2°K. before the paramagnetic contribution to the susceptibility of H_2 is 20 per cent of the total (337). It is convenient to define a complex susceptibility

$$\chi = \chi' - i\chi'' \tag{36}$$

in terms of components in-phase and out-of-phase with the applied field. (These complex susceptibilities will turn out to be measures of dispersion and absorption, respectively.) Thus

$$|\chi| = (\chi'^2 + \chi''^2)^{1/2}$$

When χ is multiplied by the complex field $2H_1 \exp(i\omega t)$, one gets the observable polarization as the real part of the product, which is

$$\mathfrak{M} = \chi'(2H_1 \cos \omega t) + \chi''(2H_1 \sin \omega t) \tag{37}$$

The quantity χ'' is seen to give rise to a component of the polarization which is out of phase with the applied field. It is related to χ' by the Kramers–Kronig relations (193, 408):

$$\chi''\nu_1 = -\frac{2}{\pi}\int_0^\infty \frac{\nu_1 \chi'(\nu)}{\nu^2 - \nu_1^2}\, d\nu \tag{38a}$$

$$\chi'\nu_1 = \frac{2}{\pi}\int_0^\infty \frac{\nu \chi''(\nu)}{\nu^2 - \nu_1^2}\, d\nu + C \tag{38b}$$

To evaluate χ' and χ'' one obtains the steady-state solutions of the Bloch equations:

$$\frac{d\mathfrak{M}_x}{dt} = \gamma(\mathfrak{M}_y H_z + \mathfrak{M}_z H_1 \sin \omega t) - \frac{\mathfrak{M}_x}{t_2} \tag{39a}$$

$$\frac{d\mathfrak{M}_y}{dt} = \gamma(\mathfrak{M}_z H_1 \cos \omega t - \mathfrak{M}_x H_z) - \frac{\mathfrak{M}_y}{t_2} \tag{39b}$$

$$\frac{d\mathfrak{M}_z}{dt} = \gamma(-\mathfrak{M}_x H_1 \sin \omega t - \mathfrak{M}_y H_1 \cos \omega t) + \frac{(\mathfrak{M}_0 - \mathfrak{M}_z)}{t_1} \tag{39c}$$

These are obtained by combining the separate algebraic equations resulting from

$$\frac{d\mathfrak{M}}{dt} = \gamma \mathfrak{M} \times \mathbf{H} \tag{40}$$

with the defining relations for t_1 and t_2 given previously. The components

$$\begin{aligned} H_x &= H_1 \cos \omega t \\ H_y &= -H_1 \sin \omega t \end{aligned} \tag{41}$$

give a field which rotates in the same sense as a precessing dipole of positive γ (see equation 5). The vector equation for time rate of change of polarization is merely equation 3 multiplied by γ so as to give $d\mu/dt$ and then rewritten in terms of the macroscopic polarization $\mathfrak{M}$. Solving for the steady-state values of $\mathfrak{M}_x$, $\mathfrak{M}_y$, and $\mathfrak{M}_z$, the quantities χ' and χ'' become (404):

$$\chi' = \frac{\chi_0 \omega_0 t_2}{2} \frac{t_2 \Delta\omega}{1 + (t_2 \Delta\omega)^2 + \gamma^2 H_1^2 t_1 t_2} \tag{42}$$

$$\chi'' = \frac{\chi_0 \omega_0 t_2}{2} \frac{1}{1 + (t_2 \Delta\omega)^2 + \gamma^2 H_1^2 t_1 t_2} \tag{43}$$

Here ω_0 represents the angular frequency at the center of resonance and $\Delta\omega$ is $\omega_0 - \omega$. Both susceptibility components are seen to be frequency-dependent with the saturation term met before. Assuming the latter to be small in comparison with 1, the value of χ_0 is multiplied by a very large factor at resonance for absorption, since ω_0 is usually of the order of 10^6 or 10^7. The plots of χ' and χ'' are of the form $Cx/(1 + x^2)$ and $C/(1 + x^2)$, respectively, as shown in figure 2, if the saturation term is neglected. χ' of figure 2 represents a dispersion curve, while χ'' is a typical absorption curve of a damped oscillator and is usually called a Lorentz curve. The fact that the dispersion curve χ' looks like the derivative of the absorption curve χ'' is understandable in view of the Kramers–Kronig relations (equations 38) given before.

One may test these relations by calculating the static susceptibility and comparing with experiment. The value of χ' at zero frequency is given by:

$$\chi'(0) = \frac{2}{\pi} \int_0^\infty \frac{\chi''}{H} dH \tag{44}$$

H may be considered constant and replaced by H^* corresponding to the peak of absorption, and therefore one integrates $\chi''\, dH$ over the narrow line. Paramagnetic salts give values generally agreeing within 5 per cent of the static susceptibilities (396). The paramagnetic susceptibility of solutions of potassium in liquid ammonia is determined in this way (269). These relations are not applicable if saturation occurs (421). Figure 14 shows χ_0, χ', and χ'' as a function of frequency (449).

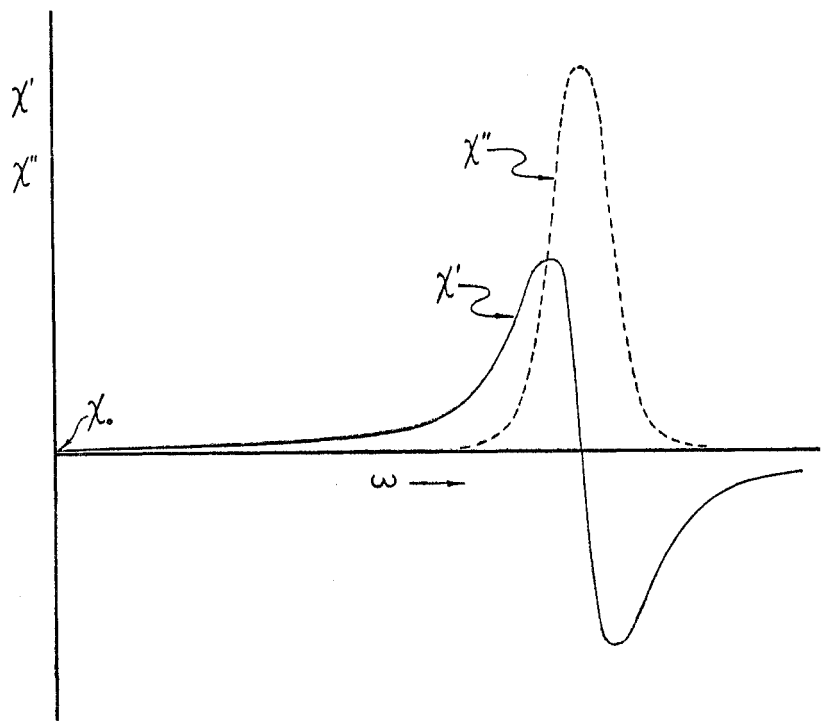

FIG. 14. Susceptibility components as a function of frequency. To show χ_0 non-zero, the vertical scale near resonance is greatly contracted and the horizontal scale is much expanded (449).

Combining equations 43 and 35, one would expect that NSR signal strength should vary inversely with absolute temperature *if line width does not change with temperature*. Such behavior is roughly in agreement with observation (56).

The Bloch equations (39a, 39b, 39c) and their consequences were obtained from macroscopic considerations. One may also arrive at more complex but essentially similar relations from a microscopic viewpoint, using statistical methods (586). This approach more clearly indicates the essential assumptions for the validity of the simpler equations. These are:

(1) If $I = \frac{1}{2}$, lines should be relatively narrow.

(2) If $I \geqq 1$ and $\mu H_z << kT$, the lines again should be narrow.

(3) If $I > 1$, and there is appreciable relaxation by coupling of nuclear

quadrupole moments with electric field gradients, the molecular surroundings should be isotropic. They should have a characteristic frequency large compared to the precession frequency, which means that $t_1 = t_2$. This restricts the samples to gases or liquids of low viscosity. Notwithstanding these restrictions, the simple equations have permitted interpretation of a very large body of diverse experimental observations. The relaxation treatment of this approach has been criticized recently (203).

Chemists are usually more interested in absorption than in dispersion, so it is natural to inquire about the relations between the out-of-phase susceptibility and the amplitude of the absorption. The energy $\mathcal{P}$ absorbed per cubic centimeter in carrying a substance through ν cycles of magnetization and demagnetization per second is

$$\mathcal{P} = \nu \int \mathbf{H} \cdot \mathrm{d}\mathfrak{M} = \nu \int \mathbf{H} \cdot \frac{\mathrm{d}\mathfrak{M}}{\mathrm{d}t}\,\mathrm{d}t$$

Taking H to be $2H_1 \cos 2\pi\nu t$ and $\mathrm{d}\mathfrak{M}/\mathrm{d}t$ from equation 37 and integrating between times 0 and $1/\nu$,

$$\mathcal{P} = 2H_1\,\omega\chi'' \tag{45}$$

The out-of-phase susceptibility χ'' may then be interpreted as an absorption coefficient. $\mathcal{P}$ will be exceedingly small except in the immediate neighborhood of ω_0, where χ'' is appreciable. When $t_2\Delta\omega = 1$, the absorption is half the maximum and $t_2 = 1/\Delta\omega_{1/2}$ or the reciprocal of the half-width at half-height of the line, as mentioned before. One observes that if $\gamma^2 H_1^2 t_1 t_2 << 1$,

$$\chi''_{\max} = \frac{1}{4}\chi_0 \frac{\omega_0}{\Delta\omega_{1/2}}$$

showing that at the center of resonance the static value χ_0 is multiplied by the ratio of frequency to line width. This is reminiscent of the definition of the selectivity of a tuned circuit (an alternative definition of Q). The apparent square-law dependence of absorption upon the radiofrequency field is deceptive, for when H_1 is moderately large, it will make an appreciable contribution to the saturation term and will make absorption a maximum for a value of H_1 equal to $1/\gamma\sqrt{t_1 t_2}$. M_z under these conditions is then $M_0/2$. One may say that at high radiofrequency power levels the spin temperature rises, thus reducing χ''.

Recent work on copper and aluminum appears to indicate that χ' shows saturation at considerably higher radiofrequency levels than χ'', contrary to the prediction of the Bloch equations (461, 554).

One may apply equation 43 with equation 35 to the determination of nuclear spin I. Using a fixed small value of H_1, one may determine the derivative of signal amplitude first for a nucleus a of known spin and then for a nucleus b of interest. Only the applied field H_z will be changed. The ratio of these amplitudes will be (441):

$$\frac{N_a I_a(I_a + 1)\gamma_a^3 t_{2a}^2}{N_b I_b(I_b + 1)\gamma_b^3 t_{2b}^2}$$

N_a and N_b will be the number of nuclei a and b. An absolute method is given in reference 110.

Equation 43 would indicate that at a frequency zero the absorption would be zero, when rather it should reduce to the Debye equation:

$$\chi'' = \frac{\chi_0 \omega\tau}{1 + \tau^2\omega^2} \tag{46}$$

If one assumes that during collisions occurring with the mean time τ the x and y components of polarization attain their Boltzmann distribution values, one may derive an equation which reduces to the Debye form at $\omega \simeq 0$ (46, 183).

Besides the steady-state solution of the Bloch equations, there have been numerous solutions for a variety of transient conditions (28, 169, 231, 235, 282, 536, 554). Extensions have been made to take into account such factors as effects of modulation.

These equations have thus occupied a central position in the theoretical framework of nuclear spin resonance. Other formulations have been proposed (227, 228, 331), but none has yet been extensively developed.

VII. NUCLEAR SPIN RESONANCE IN SOLIDS

In the liquid and gaseous states one deals with narrow lines which are generally resolved and capable of giving detailed structural information about individual molecules. For solids near their melting points the lines are generally broader and weaker. If there were multiple lines in the liquid, these would have coalesced. The shapes of NSR signals are not in general given by Lorentz curves, as might be implied by the expression for χ''. This account has ignored the static contribution of neighboring dipoles. If one considers only the static contribution of a large number of neighbors, the excess number possessing a given orientation might be expected to be distributed randomly and given by a Gauss curve. Examples of both extremes are found, but intermediate shapes are most common (408). If there are groups of equivalent nuclei AX_2, AX_3, AX_4, etc., and these groups are not too close to one another, the line may still show multiplicity in the solid state. Internuclear distances may then be inferred from the separation of the spin–spin components. As the temperature of the solid is progressively reduced, the line becomes broader until it reaches a limiting width. At one or more narrow regions of temperature, the line may suddenly become much wider. Such rapid changes imply a marked change in rate of molecular reorientation. If the line lacks structure, one may yet be able to draw conclusions about nuclear arrangement if calculations of mean-square frequency deviation for the proposed model agree with experiment. If t_1 and t_2 are measured for a single crystal, the nature of molecular reorientations may be elucidated.

At temperatures so low that internal motions may be neglected, the line width in a solid is governed by the following considerations:

1. Dipole interactions lead to a short value of t_2, both because of a static local field contribution and because a precessing component may limit lifetimes of a spin state. The shorter the value of t_2, the broader is the line.

2. Quadrupole moments may exist if the spin of the nucleus is 1 or more, and these interact with electric field gradients to shift and split energy levels. Where the splitting is large, it leads to discrete components. More commonly it broadens a line which is already wide.
3. Paramagnetic ions may markedly reduce relaxation times because of their tremendous local fields. Having magnetic moments 10^3 or 10^4 times as large as those for nuclei, they may exert an effect down to concentrations of the order of 10^{-6}. In inorganic samples such contaminations are difficult to avoid.

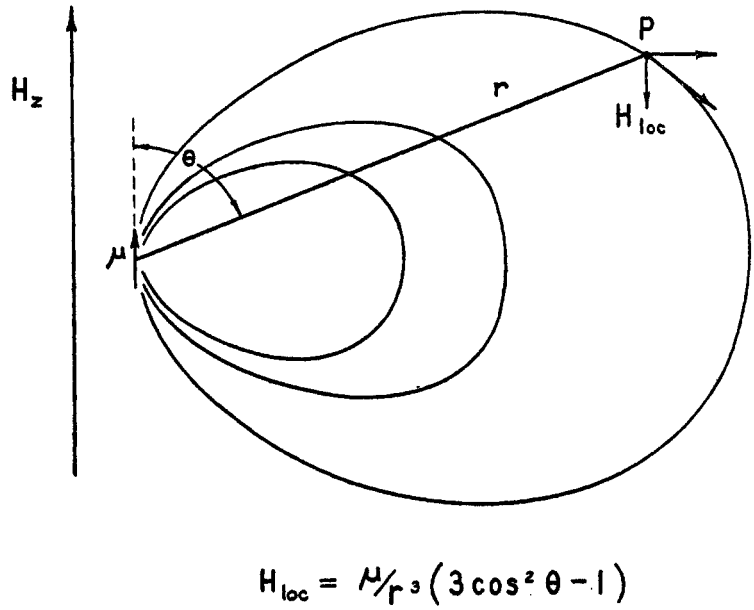

FIG. 15. The local field contribution of a dipole at a point P

4. In metals the thermal relaxation time t_1 may become very small because of spin relaxation by the conduction electrons. It may therefore be said that the resulting indeterminacy broadening is due to the shortness of t_1, recalling equation 33 and noting that t_1 cannot be less than t_2.

One may begin by considering nuclei of spin $\frac{1}{2}$ in pure solids; hence the width should be governed solely by dipole–dipole interactions. If such nuclei are located in pairs remote from one another, each nucleus will experience a local field due to the other and the sense of this field will be determined by the spin $\pm \frac{1}{2}$ of its neighbor. The effective field will then be

$$H_{\text{eff}} = H_z \pm \frac{\mu}{r^3}(3\cos^2\theta - 1)$$

where r is a vector connecting the two nuclei and θ is the angle between this vector and the field direction H_z as in figure 15. The field magnitudes $\pm \mu/r^3$

from this classical picture turn out to be wrong, for the coefficient should be 3/2 instead of 1. This result is obtained by considering the interaction energy in its quantum-mechanical form:

$$\mathcal{H} = r^{-3}[\boldsymbol{\mu}_1 \cdot \boldsymbol{\mu}_2 - 3(\boldsymbol{\mu}_1 \cdot \mathbf{r})(\boldsymbol{\mu}_2 \cdot \mathbf{r})r^{-2}] \tag{11}$$

where $\boldsymbol{\mu}_1$ and $\boldsymbol{\mu}_2$ are the magnetic moment operators for the nuclei (403). The solution of this equation for z components shows that the original energy levels have been shifted so that the allowed transitions obey the equation

$$h\nu = 2\mu H_z \pm 3\mu^2 r^{-3}(3\cos^2\theta - 1)$$

The factor 3/2 arises only for identical nuclei which, precessing at the same frequency, do not undergo transitions independently but always together in a "spin-exchange" process. The first such system studied was $CaSO_4 \cdot 2H_2O$, where it was known from crystal structure data that the lines connecting the protons of hydrate water molecules have two permitted directions. For an arbitrary value of θ one would expect two pairs of lines, which may coincide at special values of θ. From the separation of a pair of lines the value of r is computed to be 1.58 Å., μ being known. One virtue of this method is that the cube of the interproton distance is determined directly; hence the error in r is only a third that in r^3. Other hydrates studied in this way have the interproton distances given in table 4.

In $CaSO_4 \cdot 2H_2O$ and $Li_2SO_4 \cdot 2H_2O$ the directions of the interproton lines in a single crystal were found from the variation of line separation with angle of orientation in the field. Interproton distances only may be found for powdered hydrates when allowance is made for the broadening due to neighboring water molecules. All of the work done on powders will doubtless be repeated with single crystals to specify the proton locations completely.

Solid hydrogen in the ortho form gives rise to a sharp resonance line just below its freezing point. It becomes broader and shows first two and then four outer components when the temperature is reduced to 1.4°K. (237, 462). The temperatures at which the lines appear depend on the concentration of the ortho form (537). The unusual behavior is attributed to molecular rotation of the randomly distributed ortho molecules (462, 553).

TABLE 4

Interproton distances in hydrates

Hydrate	Interproton Distance	Reference	Hydrate	Interproton Distance	Reference
	Å.			Å.	
$CaSO_4 \cdot 2H_2O$	1.58	(403)	$(NH_4)_2CuCl_4 \cdot 2H_2O$	1.59	(279)
$Li_2SO_4 \cdot 2H_2O$	1.55	(529, 530)	$CuCl_2 \cdot 2H_2O$	1.60	(279, 427)
$KH_4B_8O_{10} \cdot 2H_2O$	1.55	(524)	$HClO_4 \cdot H_2O$	1.58	(295, 296)
$K_2SnCl_4 \cdot H_2O$	1.62	(280, 281)	$H_2PtCl_6 \cdot 2H_2O$	1.58	(524)
$K_2HgCl_4 \cdot H_2O$	1.607	(280, 281, 278)	$(COOH)_2 \cdot 2H_2O$	1.65	(276)
$K_2CuCl_4 \cdot 2H_2O$	1.62	(279)			

Predictions of line shape have been made for X nuclei in AX_3 and AX_4 groups arranged in triangular and tetrahedral configurations, respectively. For a rigid isolated triangle nine lines should appear. The contributions of neighbors will smear these into three lines (15), as in figure 16. Perhaps the most interesting chemical application of line structure of an AX_3 type system has been the study of acid hydrates. Calculations of expected line shapes for H_2O molecules and H_3O^+ support the latter as the form in which the water occurs in the solid state for those compounds in table 5. For oxalic acid dihydrate it was found that water is present as H_2O molecules and not as hydronium ions (276, 440).

The pyramidal groups CH_3, CCl_3, and CF_3 at sufficiently low temperatures show the expected line structure for a symmetrical triangular array (211, 436).

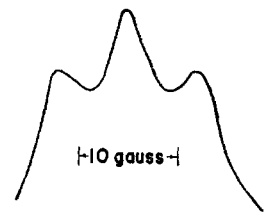

FIG. 16. Proton lines in solid $HNO_3 \cdot H_2O$ due to H_3O^+ ion (464)

TABLE 5

Structure of hydrates

Hydrate	Structure	Reference	Hydrate	Structure	Reference
$HNO_3 \cdot H_2O$.....	$H_3O^+NO_3^-$	(464)	$H_2PtCl_6 \cdot 2H_2O$..	$(H_3O^+)_2PtCl_6^=$	(524)
$HClO_4 \cdot H_2O$.....	$H_3O^+ClO_4^-$	(294, 295, 296, 464)	$H_2SO_4 \cdot 2H_2O$....	$(H_3O^+)_2SO_4^=$ or $H_3O^+HSO_4^- \cdot H_2O$	(524)
$H_2SO_4 \cdot H_2O$.....	$H_3O^+HSO_4^-$	(464)	$H_2SeO_4 \cdot H_2O$....	$H_3O^+HSeO_4^-$	(524)

The ion FHF^- is of interest as a linear X_3 group with dissimilar nuclei, in which infrared and neutron diffraction experiments had indicated a symmetrical arrangement (304, 419). Line-shape studies on a powder indicate that the hydrogen atom is within ± 0.06 Å. of the center of the ion (592).

For an X_4 group in a tetrahedral array the difficult calculation of line shape has been carried out. It would predict seven lines if the field were along the two-fold axis and twenty if along one edge of the tetrahedron (52, 552). Owing to the broadening of neighboring groups, there is little discernible structure even for a single crystal.

A calculation of line shape for a particular model then implies assumption of knowledge of all X positions. Even if a calculated line shape appears to agree with the experimental one, it would be desirable to have some quantitative measure of correspondence. It has been shown that for a rigid lattice the second moment is such a measure, regardless of line shape or molecular complexity

(445, 569). This quantity may be expressed either as the mean square field or as frequency deviation. These are defined as

$$\overline{\Delta H^2} = \int_{-\infty}^{\infty} f(H)(H - H^*)^2 \, dH; \quad \int_{-\infty}^{\infty} f(H) \, dH = 1$$

$$\overline{\Delta H^2} = \left(\frac{h}{g\mu_n}\right)^2 \overline{\Delta\nu^2}$$

where $f(H)$ represents the amplitude of the absorption curve at the field H when the line maximum occurs at H^*. $(H - H^*)^2$ is the square of the deviation from the line center. This may be cast into a convenient form for direct application to the absorption derivative curves which are obtained experimentally (408). Perhaps the most significant single contribution to the study of line shapes has been the derivation of expressions for both second and fourth moments of line shape, given the separations of atoms and relative orientations (445, 569). The second moment may be written as

$$\overline{\Delta H^2} = \frac{3}{2} \frac{I(I+1)}{N} g^2\mu_n^2 \sum_{j \neq k} (3\cos^2\theta_{jk} - 1) r_{jk}^{-6} + \mu_n^2 \sum_j \sum_f \frac{I_f(I_f+1)}{3N} g_f^2 (3\cos^2\theta_{jf} - 1) r_{jf}^{-6} \quad (47)$$

where N is the number of nuclei in resonance in a subgroup for which the broadening is being calculated and I, g, and r_{jk} refer to their spin, g-factor, and interatomic distances, respectively. The quantities with subscript f refer to nuclei of spin $\neq 0$ of a different type. If paramagnetic substances were present one would add a term similar to the second, with I replaced by S and μ_n by μ_B.

With few exceptions (52, 276, 280, 403, 528, 529, 530) investigators have chosen to eliminate the $(3\cos^2\theta - 1)$ term by use of a powder sample which would allow them to replace the factor by its spatial average of 4/5. Knowing the second moment from experiment they were able only to ascertain Σr^{-6}. By trial and error inter- and intragroup contributions to the second moment were tried until the model gave agreement with the known moment. Fortunately, the intragroup contributions are nearly always predominant, though occasionally one member of a neighboring group makes a large contribution, as is true of the protons in oxalic acid dihydrate (276). In the case of benzene the inter- and intragroup contributions were separated by the use of two deuterium-substituted samples (16, 18) as well as benzene itself. The same technique should prove useful for other carefully chosen substances of high symmetry. Table 6 summarizes internuclear distances not cited before.

When one has large concentrations of paramagnetic ions present, as in an alum crystal, the proton lines of the water molecules may be broadened to a width of several hundred gauss by the large local fields of the ions and may be difficult to detect. If one selects a crystal in which there are strong exchange interactions (569), such as $CuSO_4 \cdot 5H_2O$ (79, 425) or $CuCl_2 \cdot 2H_2O$ (425, 426), a single line 10–15 gauss wide is observed at room temperatures. In the liquid helium region a

TABLE 6

Structural information from powders

Powders	Distances	References
	Å.	
NH_4F	(N—H) = 1.024	(211)
C_6H_6	(H—H) = 2.495 ± 0.018	(16,18)
$ClCH_2CH_2Cl$	(H—H on one carbon) = 1.71 ± 0.02	(211)
$N_2H_4 \cdot H_2SO_4$ (=$N_2H_6SO_4$) $N_2H_4 \cdot 2HNO_3$ (=$N_2H_6(NO_3)_2$)	(H—H) = 1.71 ± 0.015	(438)
$N_2H_4 \cdot 2HF$ (=$N_2H_6F_2$)	(N—H) = 1.075 ± 0.02	(139)
PH_4Br PH_4I	(P—H) = 1.42 ± 0.02	(439)

large number of lines is observed over a region of up to 600 gauss, their width being 10 gauss or less. For $CuCl_2 \cdot 2H_2O$ the data appear to be satisfactorily explained, and the positions of the protons have been located. Thus while the local fields do not unduly broaden the individual lines, the separation of the line components is very great. Further, the ions tend greatly to lower t_1 for the protons. No fluorine resonance was observed in manganous fluoride at low temperatures, and this is taken as evidence that t_1 is 10^{-6} sec. or less (82). The theory of second moments (445, 569) has been elaborated to deal with interactions at low temperatures between paramagnetic ions and nuclei (297). It has been suggested that a careful study of resonance lines for solids might reveal variations of interproton distances (405).

Some structural inferences have been drawn on the basis of second-moment calculations on proton-containing compounds where there was a question as to the number of nuclei in a group or of their arrangement in space. These include (besides the hydronium compounds) support for the ionic structure of glycine (505), for the ions $N_2H_5^+$ and $HC_2O_4^-$ in hydrazine oxalate (438), for the structure $NH_2 \cdot HgCl$ for "infusible white precipitate" (140), and for the planar structure of urea (19).

In metals the resonance lines are commonly found to be unsymmetrical, owing to variations in depth of penetration of the radiofrequency field. The magnitude of this effect has been calculated for planar and spherical samples (80).

In fairness, the drawbacks of the NSR method of structure determination in solids should be enumerated. First, the crystal structure must be known to the point that only interatomic distances for one type of nucleus are uncertain. These nuclei should preferably be attached to an atom of known position. Second, high-temperature modifications cannot be studied, since these almost

invariably would be narrowed by internal motions. The limitation to nuclei of spin $\frac{1}{2}$ is a third disadvantage. Accurate x-ray investigations are now locating hydrogen positions, and neutron diffraction will probably come into more general use. The NSR method will probably remain of limited applicability.

Reference to figure 12 will indicate that at low temperatures t_2 attains a limiting value, and (barring quadrupole broadening) the line width will be determined by this value. Lattice vibrations are indeed occurring, but their frequencies ($\sim 10^{10}$ cps) are too large and the amplitudes too small to seriously affect relaxation times. Far more effective are sudden jumps—translations or partial rotations. These have the effect both of altering static field contributions and of providing rapidly varying magnetic fields which will have a component at the Larmor frequency. Mention has been made of t_2 as a time in which two nuclei originally precessing in phase would get out of phase. If one of two nuclei makes a sudden jump so that it has a new neighbor in a time short compared with t_2, the interaction time will be lengthened. The sudden motion which lengthens t_2 also provides a fluctuating field which leads to thermal relaxation. In order to be able to calculate the second moment, one would need the time average of equation 47. If the internuclear vector r assumes a large number of different orientations during a precession period, the average value of the $3\cos^2\theta - 1$ term would become small and finally essentially zero as the reorientation frequency increased. Although equation 47 will no longer be useful after line narrowing has begun, one may glean some information about molecular motion from the narrowing. In the simplest case one finds that when the reorientation requires some well-defined activation energy, the correlation time τ_c will show an exponential dependence on the temperature. For example, for ammonium chloride the correlation time was found (447) to be given by the expression:

$$\tau_c = 2.6 \times 10^{14} \exp(2370/T)$$

The correlation times were found from measurements of t_1 (131, 477) over a temperature range of about 200°, in conjunction with equation 29.

$$\frac{1}{t_1} = C\left(\frac{\tau_c}{1 + 4\pi^2\nu_0^2\tau_c^2} + \frac{2\tau_c}{1 + 16\pi^2\nu_0^2\tau_c^2}\right) \tag{29}$$

The τ_c values ranged from 10^{-10} to more than 10^{-4} sec. As implied above, the plot of $\log \tau_c$ vs. $1/T$ was linear over the entire range. This interval encompasses both the region around 130°K., in which the line width drops nearly fivefold in a 20-degree interval, and the specific heat discontinuity around 240°K. The failure to observe any discontinuity in τ_c indicates that there was no sudden "onset of rotation," but rather that the same type of motion was going on at all of the temperatures. This motion necessarily involves the whole NH_4 group, for the contributions of neighbors are a small fraction of the total line width. It should be noted that the nitrogen and chlorine nuclei make line-width contributions. The NH_4 tetrahedron may execute a jump which is equivalent to a 120° rotation about one of its threefold axes. This leaves the structure unchanged, and the contributions of neighbors are largely unaffected. However, when these partial rotations occur

frequently enough, the contribution of the ions themselves is negligible. The midpoint of the line-width transition corresponds to a value of τ_c between 10^{-5} and 10^{-6}. As the temperature is increased, the frequency of the jumps is increased to such an extent that the tetrahedra spend an appreciable time in the intermediate positions and loss of orderly arrangement occurs at the λ-point. The frequency of the jumps at the line-width transition is too small to allow it to be distinguished on specific heat curves (225), though its effect on dielectric relaxation might be observable in polar compounds. Zero-point torsional oscillations have been shown to reduce the line width from its rigid-lattice value in the ammonium halides (52). A similar study has been made for benzene (18).

Inferences as to molecular motions in other types of compounds have been based largely on line-width measurements and cannot be said to be as fully documented cases as those of the ammonium halides and benzene. These include studies on NH_4IO_3, NH_4CNS, NH_4NO_3, and $(NH_4)_2SO_4$ (223); $ClCH_2CH_2Cl$ (211); Cl_3CCH_3, CH_3COCH_3, CH_3NH_2, CH_3I, C_2H_5Cl, C_2H_5Br, C_2H_5I, CH_3OH, CH_3CN, C_2H_5OH, and C_2F_6 (224); cyclohexane (17); cyclopentane, n-C_5H_{12}, n-C_6H_{14} (476); CH_3CCl_3, $CH_3C(NO_2)_2CH_3$, $CH_3CCl(NO_2)CH_3$, $(CH_3)_3CBr$, $(CH_3)_3CCl$, and $(CH_3)_4C$ (436); KH_2AsO_4, $NH_4H_2PO_4$, and $NH_4H_2AsO_4$ (382); n-$C_{18}H_{38}$, n-$C_{23}H_{58}$, n-$C_{32}H_{66}$, n-$C_{12}H_{25}OH$, C_6H_6, o- m-, and p-$(CH_3)_2C_6H_4$, 1,3,5-$(CH_3)_3C_6H_3$, $C_6(CH_3)_6$, $C_{10}H_8$, and $C_{14}H_{10}$ (8, 11, 475); $(CH_2OH)_2$ (475); aluminum (500); n-$C_{16}H_{33}OH$ (321); HCl, HBr, HI, H_2S, H_2Se (3, 4); rubber (35, 117, 221, 254, 255); various polymers (34, 221, 254, 257, 383, 515); CH_3SiCl_3, $(CH_3)_2SiCl_2$, $(CH_3)_3SiCl$, $(CH_3)OSiCl_3$, $(CH_3)_2SiOSi(CH_3)_2$, $[(CH_3)_2SiO]_3$, $[(CH_3)_2SiO]_5$, and $[(CH_3)_2SiO]_x$ (a silicone rubber) (467). These chlorosilanes and methyl siloxanes do not attain a rigid-lattice line width at 77°K. and some of these not even at 4°K. Narrowing is ascribed principally to motion about the carbon–silicon bond, with additional motion of larger units.

The liquid-crystalline phase of p-azoxyanisole shows an unusual degree of rigidity. A three-component line is observed, with the outer two components presumably due to the proton pairs on the sides of the benzene rings and the central narrow one to the methoxyl protons (532, 533). Normal motion of the benzene ring would eliminate such static field contributions. Other liquid crystals show more complex behavior (155).

An unusual line-width behavior is shown by supercooled 2,3-dimethylbutane on warming above 64°K. The line first narrows and then suddenly becomes broad again. Rotation at lattice defects is presumed to occur in the transition region (496).

Methane appears to show three minima in its t_1–temperature curve, one for each of two crystal modifications and one just above the melting point (549). These have been ascribed to differing types of motion in the three regions (552).

The interesting question of mobility of hydrogen in metals has been studied by observing proton line widths as a function of temperature. For titanium at room temperature the line is broad (12 gauss), showing both rigidity of protons and close spacing. For tantalum the proton line is less than 1 gauss wide at room temperature, but becomes much broader around 215°K., indicating loss of mo-

bility (180, 181). Observations of t_1 and t_2 for hydrogen in palladium indicate rapid self-diffusion and that such motion is primarily responsible for relaxation (386).

VIII. QUADRUPOLE INTERACTIONS

Nuclei of spin greater than $\frac{1}{2}$ may possess non-spherically symmetrical nuclear charge distributions and are said to have quadrupole moments Q. Positive and negative signs imply the symmetry of a prolate and oblate spheroid, respectively. When there exists an electric field gradient, the quadrupoles undergo a precession, which is responsible for displacing nuclear spin levels. For a spherical or purely cubic electric field no displacement would occur. Quadrupole energies range from negligible small values to those far in excess of nuclear magnetic interactions. For an isolated nucleus of spin greater than $\frac{1}{2}$ the energy levels are given by the following equation in strong magnetic fields (431):

$$W = \frac{-M\mu H_z}{I} + \frac{eQ[3M^2 - I(I+1)]}{4I(2I-1)} \frac{\partial^2 V}{\partial z^2} \tag{48}$$

M takes on values from $-I$ to $+I$ and V is the electrostatic potential at the nucleus due to all charges outside it. The gradients may arise both within a molecule and from its crystalline environment. It is implied that the magnetic interactions are stronger than the electric and therefore the latter may be expressed as a perturbation on the former. In liquids or gases the Brownian motion tends to reduce intermolecular electric field gradients to zero, though this may not be true for intramolecular gradients, as in covalently bonded groups. The time-averaged interaction is generally larger than the magnetic interactions and provides a powerful relaxation mechanism because of the fluctuating gradients (29, 77). Thus, while in solids relaxation times t_1 may be of the order of hours if quadrupolar effects are absent or small, they may be tenths of a second if the interaction is large (431), the fluctuating gradients arising from lattice vibrations. In solution the chloride ion (figure 17) shows a line width of several tenths of a gauss (355), as compared with proton line widths more than a thousandfold smaller, and demonstrates the shortness of both t_1 and t_2. For the symmetrical groups ClO_4^- (355), $TiF_6^=$ and $TiCl_4$ (288), $AsO_4^{\equiv}$ (143), and SbF_6^- (444) resonance lines are relatively easy to obtain, while lines of lower symmetry are difficult or impossible to observe, owing to quadrupole broadening.

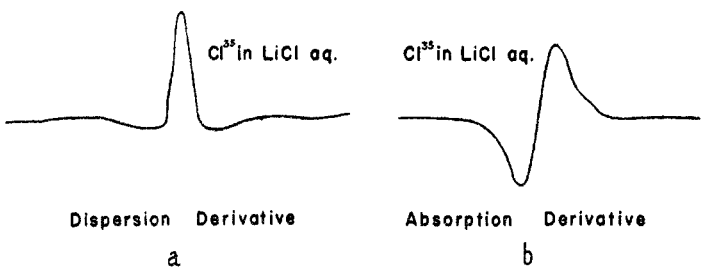

FIG. 17. (a) Derivative of Cl^{35} dispersion curve in lithium chloride; (b) derivative of Cl^{35} absorption curve in lithium chloride.

If one deals with a single crystal, $\partial^2 V/\partial z^2$ will in the simplest case of axial symmetry have a value which varies as $3\cos^2\theta - 1$, where θ is the angle between the magnetic field and an axis of symmetry (51, 100). More generally there will be nuclei in non-equivalent positions and the field gradients will be complicated. The predicted number of lines ($2I$) are observed in favorable cases (figure 18), and some spins have been determined or confirmed in this way (96, 238, 492). For powdered samples the lines may be so smeared out that it is difficult to observe them if the quadrupole interaction is even moderately large. With nuclei of half-integral spin, the second term of equation 48 becomes zero and the central line arising from the transition $M = \frac{1}{2}$ to $M = -\frac{1}{2}$ is unchanged by the quadrupole interaction. In many cases it will the the only one observed.

Even in apparently cubic crystals there may be large field gradients arising from lattice imperfections. Thus in lithium fluoride crystals the line of expected intensity was found, while for potassium iodide and potassium bromide the halogen lines were, respectively, 0.3 and 0.4 of that expected. These ratios are close to those expected for the intensity of the $\frac{1}{2}$ to $-\frac{1}{2}$ transition with quadrupole splitting. The intensities of the lines were further reduced by stressing the

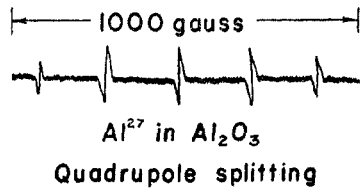

FIG. 18. Al^{27} resonance in Al_2O_3, showing splitting due to the quadrupole moment of the nucleus (542).

crystals. Estimates have been made of the number of dislocations (434). A similar study has been made on sodium chloride crystals (298). This technique has been applied to metals and alloys, where in some cases the quadrupole interactions were so large that absorption could only be observed at low temperatures (85). One per cent of silver in copper appreciably weakened the central transition. It is possible that quadrupole effects may prove to be good quantitative measures of disorder in crystals. In $KNbO_3$ the quadrupole splitting was found to be strongly structure- and temperature-sensitive, and a number of phase transitions were located (132). (Further observations and theoretical developments are to be found in references 37, 277, 313, 414, 415, 416, 497, 576, 577, and 578.)

IX. MISCELLANEOUS APPLICATIONS OF NUCLEAR SPIN RESONANCE

One of the earliest NSR applications was the precise measurement of magnetic fields in terms of the proton magnetic moment. From being a quantity difficult to measure with precision (to say nothing of accuracy) magnetic fields of high degree of homogeneity may now be measured relatively to nearly the limit of frequency comparisons. The accuracy is limited to that of the proton gyromagnetic ratio (544, 547; 458, p. 71).

$$\gamma_p = 26753.0 \pm 0.6 \text{ sec.}^{-1} \text{ gauss}^{-1}$$

For measurements of low fields (150 gauss or less) one obtains stronger signals from free radicals or solutions of potassium in ammonia. For the latter, $g = 2.0012 \pm 0.0002$ (269). Field gradients have been explored (45, 146).

Proteins, starches, and other materials containing water in varying degrees of binding may show a sharp line superimposed on a much broader one if the water content exceeds several per cent (283, 394, 502, 503, 504). Estimations of the amount of free water and of the degree of orientation of the bound water have been made.

The effective magnetic moment, $\mu_{eff} = (3\chi kT/N\mu_B^2)^{1/2}$, where χ is the susceptibility of a paramagnetic ion or molecule, may be measured by its effect on the thermal relaxation time t_1 in NSR absorption (84, 112, 384, 626, 627). In many cases the values are close to those obtained from susceptibility measurements. Recent work tends to indicate that μ_{eff} is less than the static value of μ (327). Ions such as Fe^{+++}, Mn^{++}, Gd^{+++}, Cr^{+++}, and Cu^{++} are roughly ten times as effective in equivalent concentrations as Co^{++}, Nd^{+++}, and Dy^{+++}, which have strong spin–orbit interactions (128). In others, deviations have been attributed to covalent bonding (112, 126, 626, 627). The relaxation times of protons in the presence of paramagnetic ions in solution have been used as a measure of the concentrations of such ions, using equation 30 (244). Surface concentrations of paramagnetic ions on catalysts have been determined by suspending them in water and determining the proton relaxation times (468, 499, 535).

Electron-coupled structure in liquids has been used in at least two cases to establish the spin of a nucleus. Both C^{13} and Si^{29} were shown to have $I = \frac{1}{2}$ (393, 473) by giving rise to a doublet proton resonance.

Keto–enol equilibria increase the number of distinguishable protons. After identifying each line and getting relative areas under them, the fraction in each form may be determined if serious overlapping does not occur (286).

One of the first quantitative NSR analysis procedures for hydrogen in hydrocarbons involves measuring the amplitude of a dispersion signal at high radio-frequency power. A sinusoidal modulation of 80 cps is used and the sample is scanned as rapidly as the recorder can follow. Although relaxation times of samples varied by 10^2, the amplitude of the signal varied no more than 5 per cent per unit hydrogen concentration (610).

Two unusually simple methods of determining magnetic susceptibilities have been devised for high-resolution spectrometers. In the first the sample is divided into two sections having demagnetizing factors 0 and 4π, respectively (311). Two lines appear, separated by ΔH, and are related to the volume susceptibility χ by the equation:

$$\frac{\Delta H}{H_z} = 4\pi\chi$$

In the second method the sample is annular, with a capillary containing a reference liquid centered in the outer tube (463). Two lines again appear and one has

$$\frac{\Delta H}{H_z} = 4\pi\left[(\chi_1 - \chi_2)\frac{a^2}{r^2} + (\chi_2 - \chi_3)\frac{b^2}{r^2}\right]$$

Here χ_1, χ_2, and χ_3 refer, respectively, to the susceptibility of the inner reference liquid, of the glass capillary, and of the annular liquid. r refers to the mean radius of the annular liquid, while a and b are the inner and outer radii of the inner glass tube. The above expression would drop the first term if one were to use a solid glass rod in place of the capillary.

Yet another procedure observes displacement of proton resonance in water capillaries serving as cavities inside a paramagnetic sample (159). Some refinements appear to be necessary to obtain accurate results.

Isotope abundance ratios may be obtained by comparing areas of NSR lines when $\gamma^2 H_1^2 t_1 t_2 = 1$ for each (condition of incipient saturation) (253).

The degree of crystallinity in Teflon and polyethylene has been estimated at 72 and 64 per cent from studies over the range $-180°$ to $+200°$C. The crystalline and amorphous regions appear to have their own t_1 and t_2 values with narrow lines for the amorphous forms (611).

The signs of nuclear moments may be determined by feeding a pair of crossed transmitter coils of a nuclear induction probe from a common source with one 90° out of phase with the other. A rotating field is produced and if its sense is appropriate, an induction signal will appear (469). The sign may also be found from the phase of the derivative curve (32, 441). It has been proposed to use two samples placed beside one another in a solenoid supplied only with an alternating field. Two signals each will be present on each half-cycle, and their phase will be inverted with respect to each other. If the signs of the nuclear spins are identical, their signals will show the same sequence (351).

The measurement of flow rates by amplitude of a NSR signal has been suggested (87, 540), making use of such high radiofrequency levels that partial saturation would occur if the liquids were at rest.

Some inferences as to ordering of solid structures may be obtained from NSR absorption. For example, antiferromagnetic arrangement of metal atoms in a body-centered cubic lattice has been suggested (623). For niobium and vanadium this arrangement is apparently excluded, because it would lead to a zero-field splitting, which was not observed (315).

Electronic distribution in alloys has been studied by investigating the shift of resonance frequency relative to the pure metal. Some anisotropy of the shift has been found in white tin. Thallium alloys gave a shift which varied continuously with composition (85).

A demonstration of the non-equivalence of nuclear absorption and nuclear induction involves use of polarizing and detection coils some distance from one another along a flowing liquid. Precessing nuclei induce an E.M.F. in the detector coil but do not absorb energy from it (507). Another experiment which can only be described in terms of nuclear induction involves polarization of nuclei with a coil at right angles to the earth's field. This field is cut off very suddenly and the nuclei then turn in the direction of the earth's field, inducing an E.M.F. in a receiver coil at right angles to both. The value of the earth's field is found from the curve of decay of the polarization. The precession frequency is only 2185 cps! (401).

Partial covalent character is attributed to solid rubidium and cesium halides,

since if the binding were purely ionic, the cation resonance line should show no variation in position in the several halides. The observed differences in shielding indicate that the extent of covalent character increases in going from fluoride to iodide (220).

This heterogeneous list only foreshadows extremely varied applications of NSR techniques by chemists who will apply them to areas not yet foreseen.

X. SOURCES OF ERROR

A partial listing of sources of errors follows:

1. In using a phase detector to plot weak lines, one gets the derivative of the absorption or dispersion curve only if the amplitude of the modulating field H_x is small compared to the line widths. The apparent second moment $\overline{\Delta H^2}$ is related to the true second moment $\overline{\Delta H^2}'$ by the relation (14, 413):

$$\overline{\Delta H^2}' = \overline{\Delta H^2} + H_x^2/4$$

This is experimentally verified for ammonium chloride (225). Even with very small modulation fields, serious line distortions may arise with improper adjustment of the phase detector (235).

2. When the modulation frequency is of the same order of magnitude as the line width expressed in frequency units, phase-detector plots will not give the true line shape. Dispersion curves will be distorted more severely than absorption curves. The effect arises from resonances occurring at $\nu_0 \pm n\nu_m$, where ν_0 is the frequency corresponding to the center of resonance, ν_m is the modulation frequency, and n is an integer. These sidebands are predicted by the Bloch equations (99, 301, 517). This effect is helpful in providing calibration markers at intervals ν_m where signal amplitudes are large enough to permit direct observation of the signal instead of its derivative. Such calibration sidebands appear on traces in figure 9.

3. The separation of maximum and minimum of the phase-detector trace of an absorption curve has very frequently been used as a measure of width of broad lines. However, it has been found questionable, since the apparent width increases as the amplitude of the radiofrequency field decreases (131).

4. In pulse experiments the tuned coils of a nuclear induction apparatus may produce a damping of resonance which may be greater than the effects of either thermal or dipole–dipole relaxation (83). Such a damping effect had been suggested earlier (538).

5. Line asymmetry may cause an apparent shift of position of the maximum of the absorption line (282).

The novelty of NSR and ESR measurements and the assumed insensitivity to the presence of impurities gives misleading results such as the following:

1. More lines may be present than can be accounted for.
2. The position of lines may be appreciably shifted. In impure cresols the OH line is not visible, because it is shifted under the C_6H_4 group.
3. Failure to observe the expected number of components because of catalysis of chemical exchange.

4. Relaxation times may be appreciably in error, owing to the presence of paramagnetic impurities. The early values of t_1 for both water and ice were too low on this account.

XI. UNEXPLAINED EFFECTS

1. The line width in copper decreases markedly with increasing saturation, whereas broadening is usually expected (1). A similar effect has been noted in solid hydrogen (462).

2. Reduction in radiofrequency level increases the separation of maximum and minimum in the derivative curve for absorption when using a phase detector (131). This effect is opposite to that which would be expected if any saturation occurred.

3. The electron-coupled spin–spin splitting in $F_2PO(OH)$ drops to zero between 550 and 237 gauss (452), though it was independent of field to 550 gauss.

4. The broad triplet titanium line in $TiCl_4$ or $TiBr_4$ is unexplained. Ti^{47} and Ti^{49} have resonant frequencies separated by only 1 part in 2400 (289). The isotopes have $I = 5/2$ and $I = 7/2$, respectively.

XII. OBSERVATION TECHNIQUES

The resonant cavity method used (451) in the first NSR absorption experiments is only of historical interest, because in the radiofrequency range such cavities are large and require large samples. However, it is just such cavities that are useful in the microwave range. A radiofrequency bridge technique was much used in early work (84). Since only a minute fraction of the radiofrequency energy supplied to a coil is absorbed by the sample in it, one cannot hope to see the energy loss directly. By placing this coil (in parallel with a condenser) in a bridge with a similar tuned unit (dummy), one can reduce the output of the bridge to a point where a receiver used as an amplifier and detector is not blocked. No special care is taken to make the dummy unit identical with the sample unit. For arbitrary conditions the bridge is unbalanced both as to phase and as to amplitude, and it is highly desirable to have non-interacting controls. After balancing both, the amplitude control is slightly displaced, and enough of the applied signal appears at the output terminals to serve as a carrier for the absorption signal. A similar slight phase unbalance gives the dispersion component. Although this method is not in general use now, it serves nicely to illustrate how one may obtain either an absorption or a dispersion curve.

This homodyning procedure is a very effective means of rejecting noise, for the sharply tuned circuits of the receiver will pass only a narrow band of frequencies centered on the generator frequency f_0. With this in the range of tens of megacycles, it would be a hopeless task to find even the strongest signal in the presence of the noise spectrum containing frequencies from zero up to f_0. The noise band width is still of the order of 10^5 cps or more and one seeks additional ways of decreasing it. By modulating the field at a frequency of 30 to 300 cps and using a narrow band amplifier, the signal-to-noise ratio is much improved. Additionally the modulation serves to carry the absorbing nuclei into and out of resonance

periodically, so that orientation energy can be transferred to the surroundings. The modulation amplitude is usually several times the line width. Sinusoidal sweep will cause the appearance of a double trace on the screen, since the sample passes through resonance twice each cycle. However, with a sawtooth sweep, one of the passages occurs during the retrace, which is blanked out. With a split sample coil, lines from two compounds may be presented simultaneously (222). For high resolution, sample diameters may be as small as 2 mm., using several layers of wire to get the necessary inductance. The half-wavelength cable used to provide a phase shift of 180° in one of the halves of the bridge (84) is very inconvenient and may be eliminated by use of transformer coupling (554) or a T-section (6). For observation of absorption only, the amplitude bridge eliminates the need for phase balance (548). The twin-T bridge is of more simple construction (202, 562, 588) than the radiofrequency bridge and is easier to operate. A parallel-resonant circuit coupled to a signal generator and receiver by very small capacitors has been used (168).

The oscillating detector (259, 429, 466) is remarkable for its ease of operation and its sensitivity. For strong signals it requires only a simple audiofrequency amplifier ahead of an oscilloscope. In its original form its regeneration control exerted a detuning action, but this difficulty has been corrected in some of the numerous adaptations (120, 166, 167, 172, 174, 299, 321, 508). Some of these control automatically the level of oscillation (188) or minimize the effects of connections to the sample coil (174, 465). The essential feature of all of these units is that an oscillator is adjusted to a condition of very weak oscillation in which it is sensitive to small changes in the tuned circuit. The absorption of energy at resonance is equivalent to adding resistance to the coil, thus lowering the Q value. When the field is modulated at an audio rate, the recurrent absorption is effectively an amplitude modulation. Detection may occur in the same stage or in a separate one. Using a radio receiver, one may demonstrate absorption with AM detection or dispersion using FM detection (466). Super-regenerative detectors have high sensitivity but give a complex signal (176, 322, 466, 609). A non-linear regeneration scheme has been proposed but not tried (485).

For strong signals one can apply the output of a regenerative detector directly to an oscilloscope such as the DuMont 304A, though more commonly one uses an amplifier with a gain of 10^1 to 10^6. For slow sweep (10 cycles per second or less) a D.C. amplifier should be used to reproduce the signal faithfully. An analysis of oscillating detectors shows that they may have the same ultimate sensitivity as a radiofrequency bridge (120).

With a simple oscillating detector followed by a phase detector, one is easily able to observe a Cu^{63} resonance from the wire in the sample coil. Frequency instead of field modulation has been suggested (316).

In the more elaborate spectrometers (433, 435, 590) provision is made for slow drive of the tuning capacitor so that weak resonance lines may be sought automatically, their output feeding a phase detector and then a recorder.

When searching for unknown resonances or examining very wide lines one must decide whether it is more expedient to vary the field at fixed frequency or

vice versa. When using bridges or fixed-frequency induction probes one requires some linear sweep unit. For high-resistance magnet coils the problem is not difficult, for one can devise linear-sweep circuits in which a motor-driven helical potentiometer uniformly varies the bias on a power amplifier (222, 593). If the range of the sweep unit is insufficient, one can set the steady field at a value above the desired starting point and oppose the field by a maximum amount at the beginning, reducing the opposing current linearly to a low value. Then by aiding the field, twice the range may be covered. For low-resistance magnet coils this is much more of a problem, since rheostats of high current capacity and essentially stepless construction must be specially made and these give contact problems. Rapid field changes of thousands of gauss may be obtained by short-circuiting a series resistor (542). The trace of figure 18 was obtained in this way. In permanent magnets the sweep coils may be the ones which were used to energize the magnet, though generally it would be better to have more turns and a smaller wire size than would normally be used for such a purpose.

It is highly desirable to have Helmholtz sweep coils an integral part of a resonance probe to minimize pickup effects. Where field-controlled generators are used, large sweeps are no problem (527). Frequency sweep requires that the oscillator be capable of operating at low levels over a wide frequency range and that the amplifier be of the broad band type or that tracking be provided for. There must be an automatic gain control so that the level of oscillation can be kept proper. These considerations apply whether variable-frequency nuclear induction or a radiofrequency absorption spectrometer is used.

A. Modes of presentation

Oscilloscopic presentation of resonance signals is used wherever possible because of its convenience. For slow sawtooth sweep it is essential that the oscilloscope possess a direct-coupled amplifier. The DuMont 304A instrument serves very well not only for this reason, but also because a sawtooth output may be taken from it and used to provide field sweep through a balanced cathode follower. Such a balanced arrangement has the virtue that the average value of the field is the same with and without sweep. The sweeps on scope and field are automatically synchronized and no phase shifter is needed, as when a sinusoidal signal is obtained from a separate generator. When a line is centered on the scope trace, it is known that resonance occurs at the steady value of the field and sweep calibration data are not needed. Using external capacitors, the DuMont 304A sweep time may be increased to 10 sec. For still longer times, up to several minutes, a phantastron circuit (109) is useful. A check of sweep linearity should be made.

Recording of rapid presentations is readily done photographically, but where sweep times are several seconds or longer, a linear-recording strip chart recorder such as the Sanborn Model 127 serves admirably. Generally a direct-coupled amplifier must precede this recorder, in addition to its own amplifier. The Furst Model 220 amplifier does reasonably well for sweeps up to 10 sec. duration, but occasionally one must check to be sure whether variations of the base line are really caused by fine structure or by drift. A Kay-Lab Model 103 amplifier with chopper stabilization of the D.C. level is very satisfactory.

Repeated mention has been made of discrimination against noise. This is a very real problem, for some of the absorptions are so weak that their signal voltages are of the magnitude of noise voltage or smaller. One must then take advantage of the fact that noise is random, whereas the phase of a detected signal will be coherent. The detection device must allow the positive and negative noise pulses to cancel each other and present the average background level upon which the signal is superimposed. Numerous methods have been suggested (73, 127, 199, 400, 472, 539), but the phase detector is probably one of the most suitable devices (84, 490). It essentially reduces the frequency of a signal to a very low value so that one may make observations over a long time, thus averaging out noise. The same modulation voltage which sinusoidally varies the field is fed to the phase detector, which is sensitive to signals at the modulation frequency. For modulation amplitudes small compared to the line width, the output of the phase detector is nearly the first derivative of the signal, whether it be dispersion or absorption, though the latter is of more general interest. It is profitable to precede the phase detector with an amplifier which passes only a narrow band centered on the modulation frequency. This is generally accomplished with a twin-T filter between stages, and the filter degenerates strongly all components except the narrow range for which it was tuned. It has been shown (625) that the noise from a phase detector is determined by its output R-C time constant, which can be made of the order of minutes or even hours with polystyrene film capacitors. Phase-detector plots for absorption and dispersion in Cl^{35} are shown in figure 17. The derivative curve for absorption looks like a dispersion curve, a result which is to be expected from the Kramers–Kronig relations, equations 38.

For zero-field observations (591) it is desirable to use square-wave modulation, and under these circumstances the output of the phase detector is the absorption curve directly instead of its first derivative. The same square-wave may also be used generally in place of sinusoidal modulation. The field is swept slowly and the period of the square-wave is long in comparison with the relaxation time (253). The square pulses may require special shaping to compensate for inductance of the coils to which they are fed. Pickup effects at the modulation frequency are minimized by using antisymmetrical square-waves (462).

It is a laborious procedure to integrate a phase-detector record where fine structure is present. Electronic integration of the phase-detector output has been used (584, 591). It is desirable in some cases to follow this stage with a second integrator which, instead of feeding a recorder, operates a counter to give an indication proportional to the area under the absorption curve and thus measure the number of absorbing centers (604).

There is an alternative to the use of long scanning periods and phase detectors when looking for weak resonances. This consists in a rapid sweep over a range encompassing hundreds of gauss per second and observing the dispersion mode (542). Here there is no diminution of signal with large radiofrequency fields. Instead, the dispersion signal rises to a final value for $H_x >> 1/|\gamma|(t_1t_2)^{1/2}$. Observations have been made with direct oscilloscopic display for Na^{23}, Br^{79}, and Br^{81}. The trace of figure 18, taken in 1 sec., is comparable to phase-detector records taken over a 12-hr. period.

For absolute calibration of absorption intensity one may provide an artificial "signal" by means of a calibrator which electronically adds a calculable resistance to the tuned circuit containing the sample (591).

B. Nuclear induction

Nuclear induction was the term applied by Bloch to describe the appearance of a voltage at the terminals of a receiver coil at right angles both to the transmitter coil fed from a signal generator and to the magnetic field (69, 75). In any detection apparatus there is a voltage induced at resonance, though except for nuclear induction it is in the exciting coil. The crossed coils have been regarded by some as a geometrical analog of a bridge for balancing out nearly all of the applied voltage. However, the second coil also serves to detect magnetization components perpendicular to both H_z and H_x. For some experiments this y-axis coil is essential. The two sets of coils may be used to produce a rotating circular (469) or elliptical field (350). The early probes had coils wound on forms fitting rigidly at right angles (75). Later versions neatly avoid the inconvenience of such an arrangement, which is disturbed when a sample is changed, since a slight misalignment markedly affects the line appearance (189).

In these probes (24, 570) the coil forms have the same axis, but the ingenious arrangement of bending two rectangular coils about the length of the outer cylinder avoids congesting the vicinity of the receiver coil. This is shown in figure 1. By using plug-in receiver coils one may use samples of the maximum size allowable on comparison of line width with field inhomogeneity over the sample. Simultaneous irradiation at two frequencies may be used (88, 400). It is possible to use nuclear induction at either fixed or variable frequency. One major disadvantage of present nuclear induction probes is their lack of adaptability for varying the sample temperature. This obstacle will surely be overcome in the future.

A versatile arrangement of nuclear resonance equipment is shown in figure 19.

C. High-resolution techniques

In high-resolution work, in addition to taking great care with the electronic portions of the apparatus, it is of great importance to examine minutely every detail of the probe used. A speck of iron from a machining operation is quite enough to destroy resolution. First of all, the probe should be very rigid, with a heavy shell, and all components should be securely fastened to prevent vibration. The Helmholtz sweep coils should be accurately located with respect to the sample. The immediate environment of the sample should have cylindrical symmetry. The magnetic susceptibility of the probe materials may have an effect on the homogeneity of the field at the sample. The material of the sample tubes also affects the homogeneity, and the latter may be seriously disturbed by a curved bottom of a sample tube. It helps greatly to keep the sample coil short and to use a sample tube of as small diameter as is possible in terms of noise considerations. Spherical samples have been used with a two-piece container (24). Resolution to better than 2 cycles in 30 megacycles has been obtained with

samples 4 mm. in diameter, but 2-mm. samples are generally preferred for pure compounds where the number of absorbing nuclei is of the order of 10^{20}.

For high resolution it is essential to scan the field at a rate which is slow compared with the width of the individual lines, and this may require 10 sec. or more (40). The "wiggles" are very persistent in fields sufficiently homogeneous to show high resolution. These may obscure details of structure or make difficult an evaluation of area under a line.

Improvement of homogeneity may be achieved with a set of spiral coils on the pole faces with the current variable in each (24). However, this is tedious and the

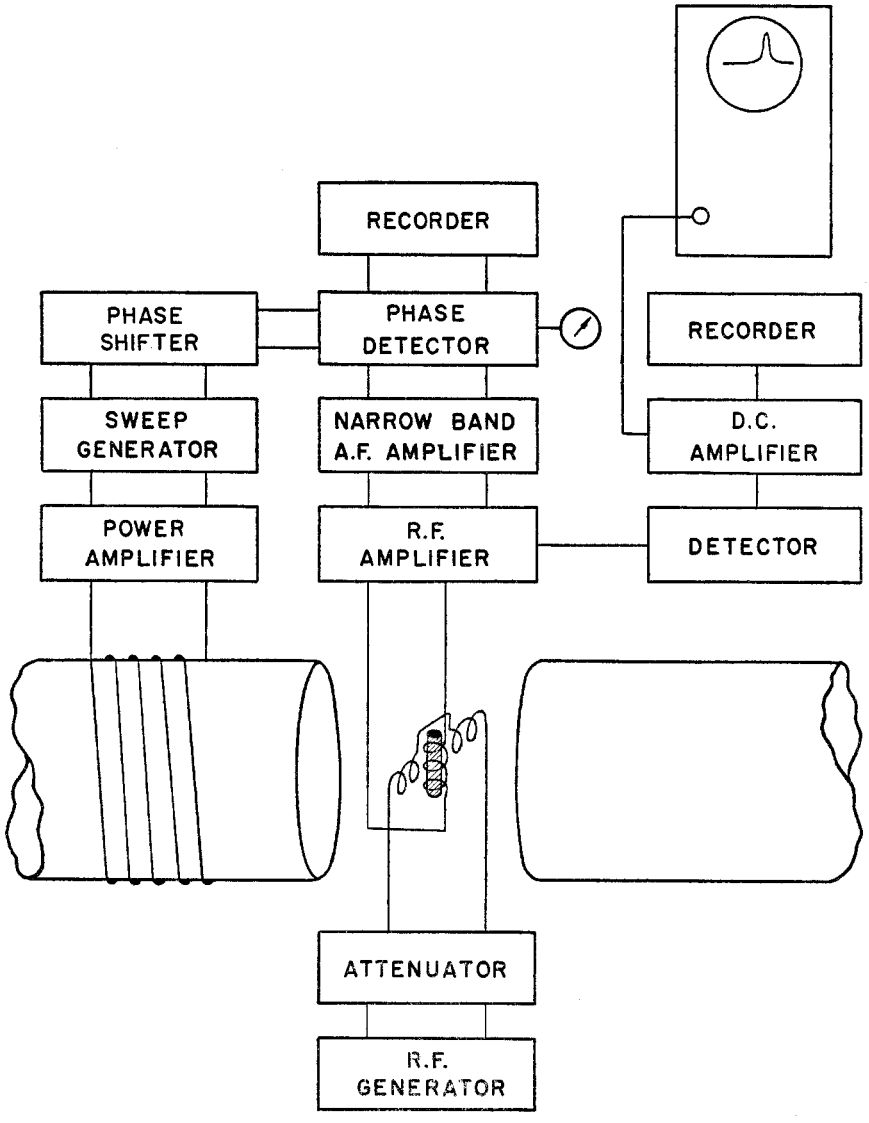

FIG. 19. Nuclear induction spectrometer

effective homogeneity may often be greatly improved by spinning the sample (72). If nuclei are moved about rapidly, it is the average field which they see that determines the resonance frequency. The effect is striking, for when a sample begins to rotate at a thousand R.P.M., the lines greatly narrow and hyperfine structure lines may appear where none were seen previously. At the same time the line amplitude may increase several fold (10). Another very useful development is a procedure for direct calibration of a fine-structure trace. Suppose that one superimposes an audiofrequency of, let us say, 250 cycles per second upon a linear sweep of period 20 sec. There will appear sidebands or images 250 cycles on each side of each resonance line (99, 301, 536, 616). These appear in the traces of figures 9b, 9c, 9d, and 9e. It is unnecessary to make the sweep amplitude large enough to include both of the sidebands of the lines. However, it is well to make it sufficiently large to include a sideband for more than one line, for then one has an independent check on the stability of all of the variables that go to determine the linearity of a particular trace. One very convenient source of a calibrated audiofrequency is the General Radio 1107A Interpolation Oscillator, which is specified to be accurate to 2 cycles by direct reading. However, if a set of accurate 10-kc. markers is available from either a 100-kc. or a 1-Mcps source, the audiofrequency may be established to less than one-tenth of a cycle. Some provision must be made for providing a point of reference on each trace so that shielding values may be established. One procedure is to have a reference liquid separated by a septum from the other liquid (258) or to use two immiscible liquids (177). Another is to use a reference capillary inside the sample (36). Spinning eliminates the line splitting mentioned under magnetic susceptibility determinations.

The radiofrequency source must be stable to about 1 part in 10^8 during the period of observation if finest details of structure are not to be obscured. Ordinary crystal-controlled oscillators are not stable enough. A BC-221 frequency meter has been used for moderate resolution (222). More satisfactory as a commercial unit is the General Radio 1106 frequency meter.

A minimal-noise preamplifier circuit of the grounded cathode-grounded grid type is a necessity for weak signals (583, 594). It may be followed by a tuned amplifier of gain $\sim 10^6$ with a diode detector. Paddles on the probe are adjusted to leak a very small amount of the homodyning component, with the phase adjusted to give an absorption or dispersion type signal. Alternatively, a heterodyne receiver may be used with a phase-sensitive detector to give the desired mode (24, 32).

There is probably no compelling advantage of one method of resonance detection over another at fixed frequency. For variable frequency one will find that a tunable nuclear induction probe, an oscillating detector, or more elaborate versions of it are the most convenient to use. This also holds for variable-temperature work, where bridge unbalance effects are annoying.

D. Relaxation time measurements

1. Thermal relaxation time

The most direct procedures involve observation of the oscilloscope trace of an absorption line as it grows or decays due to a change of radiofrequency power

under conditions of saturation (84). The change will be exponential with time constant t_1. Depending on the manner of excitation, the time constant of growth or decay of a signal with different radiofrequency power levels may not equal t_1 (531). If t_1 is of the order of minutes, the signal amplitude may be examined periodically with a weak field after a saturating field has been used (84). t_1 can be obtained from signal peak height as a function of H_1 according to equation 43 (84). (It has been customary to measure H_1 with coils of known geometry.) t_1 may also be measured by observing the peak amplitude under different modulation frequencies, for then one varies the amount of time allowed for recovery after the last period in resonance (150, 189, 352). Alternatively one may compare signals for increasing and decreasing fields (128). In metals the line width may be determined by t_1, and hence is a measure of it (218). If strong radiofrequency pulses are applied at intervals t, the initial value of M_z/M_0 is given by

$$\frac{M_z}{M_0} = 1 - \exp\left(-\frac{t}{t_1}\right)$$

Thus t_1 can be measured from the initial amplitude of a signal as a function of spacing between pulses (229, 554). Spin echo techniques are also very useful (231).

Values of t_1 from 0.01 to 10 sec. may be measured by a technique of simultaneous irradiation at two frequencies ν_1 and ν_2, where these correspond to resonant frequencies at H and $H + \delta H$ (584). δH is the amplitude of square-wave modulation on H_z. H_1 is much less than the saturation radiofrequency field and H_2 is large enough to cause rapid saturation. The value of t_1 is obtained from a curve of power absorption *vs.* frequency of the square-wave modulation.

In a purely alternating field a stationary signal is observed if the period $t > t_1$. If $t_1 > t$ no signal is visible, but if $t_1 = 2t$ the signal reappears (352).

2. Spin–spin relaxation time

For lines of width exceeding the field variation over the sample, t_2 is obtained from the line width ΔH by the expression:

$$t_2 = 2/\gamma\Delta H$$

In a sufficiently homogeneous field, the damping time of the "wiggles" would be t_2. For very narrow lines, such as those of protons in liquids, the required homogeneity is greater than has yet been attained, and the damping constant is modified. If the time between successive scannings of a line exceeds t_2, the traces show no dependence on past history. However, when the sweep period becomes equal to t_2, beats will occur because of interference between successive sweeps (481). This is true whether one uses linear (169, 170, 171, 173) or sinusoidal modulation (41, 42, 43, 191). Depending on the conditions of the experiment, one may determine t_2 from the damping constant or from signal amplitudes.

Other procedures involve pulse techniques (90, 102, 231, 536, 554).

E. Sensitivity

Equation 45 indicates that for radiofrequency fields small enough to avoid saturation effects, the absorption per cm.^{3} sec. is proportional to the complex

susceptibility χ''. This fixes the area under the absorption curve, but for observation one inquires about the amplitude of the signal above the background noise. If either t_1 or t_2 is small enough so that uncertainty broadening occurs, the peak intensity may be so small that one cannot observe it directly on an oscilloscope. One therefore will expect that for liquids, where the lines are usually narrow, the conditions will be optimum for detecting small concentrations of nuclei. The lowest thus far reported is the 0.02 per cent deuterium and the 0.04 per cent O^{17} in ordinary water (594). Since signal-to-noise ratio is proportional to $\gamma^{11/4}$ (84), one can naturally detect easily those nuclei of large ratio of magnetic moment to spin angular momentum. For stable nuclei, the order of decreasing sensitivity at a given field strength is H^1, F^{19}, Nb^{93}, V^{51}, In^{113}, Sc^{45}, Li^7, Co^{59}, Pr^{141}, Al^{27} for the ten nuclei of largest μ/I values. It will be profitable to go to the highest field strength consistent with field homogeneity over the sample, as was discussed before. Roughly speaking, the limits of detection for the most favorable cases are 10^{16} nuclei, while 10^{20} can be observed for nuclei of spin $\frac{1}{2}$ and small magnetic moment (510). The smallest detected amount reported for a solid is 0.03 mg. of fluorine in 100 mg. of aluminum oxide (167).

F. Magnetic field considerations

There is probably no parallel in spectroscopy to the arbitrarily adjustable levels in magnetic resonance. In principle, having chosen a field strength of any magnitude, one need only use the frequency $g\mu_n H/h$ (or $g\mu_B H/h$ for electron resonance in the simplest case) to achieve resonant absorption. However, since signal-to-noise (s/n) ratio varies as $H^{7/4}$ for a given dipole type (84, p. 712), it is evident that high fields are advantageous. Poor s/n ratios make operation at less than 1000 gauss difficult, though signals have been detected at a field of 2 gauss (613). Judging by the 7/4-power relation alone, one would strive for the highest attainable field. However, as field strength increases, so also does field gradient near the pole edges. Unless the pole diameter is large enough so that this effect does not alter much the field at the center, the inhomogeneity over the sample may increase enough to more than offset the gain in s/n ratio due to field increase. Resonance has been observed in fields as high as 20 kilogauss. Above about 7000 gauss the cost of a permanent magnet of sufficient gap and pole size rises sharply. The power and cooling problems may become serious above 10,000 gauss in an electromagnet. In some cases selection of field values is made on the basis of availability of certain standard electronic equipment. For example, when using an electromagnet one may work at 7050 gauss for hydrogen and 7500 gauss for fluorine nuclei, because 30-megacycle intermediate frequency amplifiers of high gain are readily available. Other than the availability of particular equipment, there is little electronic reason to choose one frequency as compared to another, since techniques are straightforward in the range of 1 to 100 Mcps.

For fields up to several hundred gauss, long solenoids with end-compensating coils are a cheap source of a homogeneous field. Helmholtz coils (water-cooled) have been used at 1000 gauss.

The choice of a permanent magnet or an electromagnet is largely governed by

the need for flexibility of operation and by considerations of stability of field. Since electron-coupled NSR absorption lines may be differentiated from shielding lines by observation at two different field values, it is helpful to have this degree of freedom. The approximate constancy of the field of a permanent magnet is a very attractive feature. "Approximate constancy" does not refer to the long-term stability of the field, for with proper initial precautions the field change per year should be negligible. The major difficulty arises from the -0.02 per cent variation in field strength per degree change of temperature (484). This change is reversible. Unless room temperature is constant, the field drift may be troublesome even in observations lasting less than a minute. Some owners of permanent magnets in temperate climates have learned how to adjust the opening of a laboratory window to compensate drift tendencies. A further disadvantage when dealing with very broad lines is the inability to sweep over a large field range without permanently altering the field. One may safely decrease or increase the field by 20 gauss in 7000 and remain on a minor hysteresis loop. A coil which was used in the original magnetization may be used for this purpose. Notwithstanding these difficulties, the freedom from considerations of power supply may be the deciding factor, especially in a small laboratory.

Two permanent magnets are sufficiently unusual to merit special mention here. The first is a yokeless design and is shown in figure 20 (58). It consists principally of two very long cylinders of Alnico V, so long that there is little leakage between the outer ends. The return path is entirely in air, and the halves are separated by spacers. Since the only machining required is grinding of one of the ends of each cylinder and the pole caps, the total cost of such a unit should be far less than that of a conventional type, though at first sight it appears extravagant of an expensive alloy. It should be clearly understood that machining costs are the major fraction of the total cost of a magnet.

The second magnet has square poles, and pole pieces (24). A pole is assembled from nine Alnico V bars, each about 10-cm. square and held at the ends in recesses in pole plates. These must be well made to retain the bars against the large repulsive forces. The yoke is made of 1-in. plate interleaved at the corners to form a U shape. The end of the U is closed with a built-up section which moves on rollers affixed to the sides. The motion is controlled by a pair of hydraulic jacks inside the yoke. The usual permanent magnet is magnetized with a large number of iron bars between the poles, and their removal requires considerable effort. Here the magnet is energized with the poles in contact and then separated to the operating distance, where it is locked with adjustable jacks. The pole faces were not lapped, but inhomogeneities are compensated by a set of flat spiral coils on each face. The current in each is separately controlled. With such a large number of variables one can produce an untold number of types of inhomogeneities to counteract existing ones, but of course the optimum setting may be difficult to find. Alternatively, one can use two sets of Helmholtz coils at right angles to produce gradients compensating those of the main field.

Turning to the disadvantages of electromagnets, one may dwell on the difficulty of regulating their supply to a sufficiently high degree. Without special

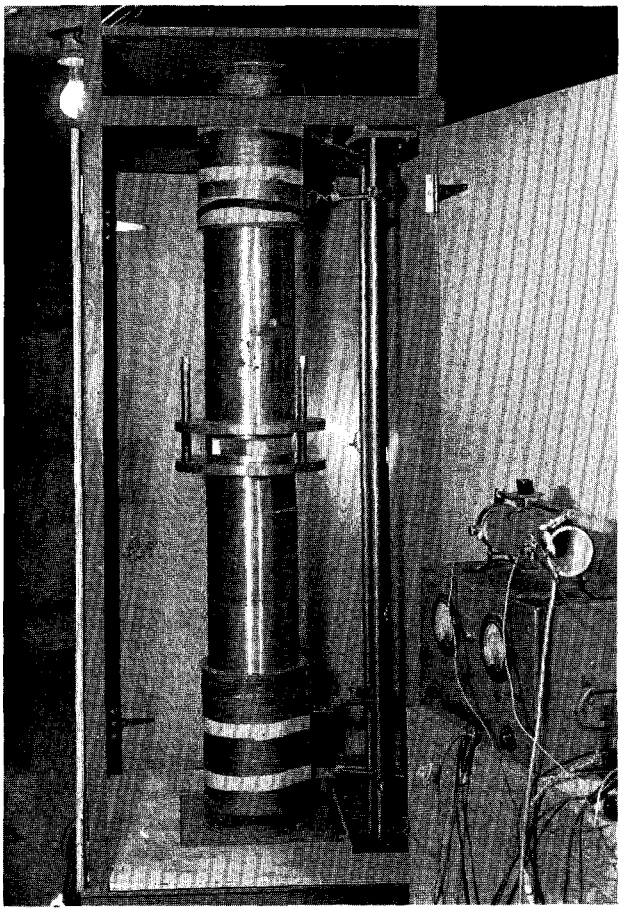

FIG. 20. Yokeless permanent magnet. The original photograph was kindly supplied by Prof. F. Bitter of Massachusetts Institute of Technology.

field control, little serious work can be done with an unregulated generator because of voltage variations and audiofrequency noise. Amplidyne control may be satisfactory for work on solids. Noteworthy achievements in generator control have been made (527, 546), the generator in one case (527) controlling currents as high as 150 amp. Outstanding success has been achieved with an electronic regulator which maintains a current up to 1 amp. constant to one part in ten million (570). Still better regulation will probably be achieved with electronic supplies. Numerous workers have used a resonance signal for field control, since the derivative of the absorption curve can furnish an error signal of appropriate sign to correct for variations (342, 399, 545, 546). Commercial versions are available (Varian Associates). Generators have the virtue that a magnet may safely be turned off with the generator motor switch, while other types of supplies may require protective devices such as gas-filled tubes or spark gaps. In-

terruption of the magnet current may cause breakdown of insulation resistance when high-resistance coils are cut by lines of force of a collapsing field.

The choice of a high- or low-resistance magnet depends on the available power supply. Low-resistance units are desirable for battery supply.

For work on solids one may find heavy-duty batteries sufficiently stable, but for high resolution one needs extraordinarily large ampere-hour capacities so that current drift is low. Submarine-type cells with ratings of the order of 10,000 amp. hr. are highly satisfactory, though expensive to install and maintain. Floating operation (charging while the magnet is operative) is permissible for broad lines, but cannot be tolerated for high resolution.

Magnet gaps should be kept as large as other circumstances will permit. A gap of 3 cm. should be considered a minimum, even if no temperature control is contemplated. It is desirable to mount small Helmholtz coils directly on the probe so that pickup from vibration in the field of fixed modulation coils is avoided. Also, the factor of merit, Q, of the probe coil or coils suffers when a metal shield is brought in close proximity. In rough work one can do without a probe shield, but at the expense of noise and excessive detuning by nearby objects. A gap of 4 or 5 cm. is more desirable, especially when dewars are to be used. For direct oscilloscopic display of the signal, it is unprofitable to use a pole radius less than the gap width or to seek signals less than one gap width from the edge of a large pole unless raised pole shims are used. The latter were first suggested by Rose (471), to prevent the normal falling-off of field from pole center to edge. Similar calculations for tapered pole caps have been made (20). On pole faces up to 20 cm., shims are definitely profitable to use, although the proportions given are not the best. Table 7, calculated by Collins (121), seems to work out better at low fields. Here the axial and radial thicknesses of the shims are given in terms of the half-width of gap for various fractional increments of the field near the shim over that at the center. In the interest of preserving a large gap, shims of low axial thicknesses are usually selected. Adjustable shims may be desirable on electromagnets used over wide field ranges. With appropriate shims the field will fall off slightly, rise slightly, and then fall off steeply as the

TABLE 7

Magnetic shim dimensions (121)

$\delta = 0.0000$		$\delta = 0.0001$	
Radial width	Thickness	Radial width	Thickness
0.5597	0.0408	0.5713	0.0431
0.3412	0.0761	0.3479	0.0794
0.2240	0.1064	0.2282	0.1101
0.1506	0.1318	0.1534	0.1363
0.0680	0.1703	0.0693	0.1758
0.0107	0.2101	0.0109	0.2165
0.0006	0.2212	0.0006	0.2276
0.0000	0.2220	0.0000	0.2288

Lengths are expressed in terms of the half-width of the gap between the shims taken as unity. δ represents the fractional amount by which the field rises over that in the center.

pole edge is approached from the center. When pole faces are 25 cm. or more in diameter, pole shims are unnecessary, even for high-resolution work. Their elimination makes easier the task of achieving a flat pole surface. It is profitable with homogeneous pole faces to lap them to optical flatness when high resolution is desired. There is considerable gain in grinding pole faces after they have been turned, provided the grinding is done in an accurate heavy-duty machine such as the Blanchard rotary grinder. Stresses in the pole faces should be relieved before grinding by annealing in a non-oxidizing atmosphere. Lapping can be done by hand with abrasive paper (320 grit or finer), using an optical flat as a guide. However, if it is done before assembly, it may be accomplished quickly and reasonably by a commercial lapping firm. If lapping has not been done, one may make plots of the field in the vicinity of each of the pole faces and then judiciously use a small piece of abrasive paper on the tips of the fingers to reduce high areas (222). Nickel plating on brass pole caps can similarly be adjusted in thickness. On one magnet it was found that field plots and optical-flat patterns indicated generally the same contours, down to the point where only a few fringes were visible in the central region.

Chrome plating of pole pieces has been found to prevent corrosion and retain homogeneity (570).

Presupposing homogeneous, stress-free, and flat pole pieces, one next requires that they be accurately coaxial and parallel. Accurate machining can take care of the coaxial requirement, but one should provide for tilting of the poles with respect to each other after the magnet has been fully assembled and tested. Lack of parallelism of the faces is shown by contour lines which crowd together where the poles are too close. This adjustment is best made by inserting a brass ring about 0.5-mm. thick between the back of the pole and the yoke. The diameter should be small enough to fit inside the ring of bolts generally used. Even though the bolts have been tightened firmly during construction, it is possible to tilt the poles by selective tightening, and this should be done until the highest field reading coincides with the center of the poles.

All evidence indicates that for good field homogeneity and stability the magnet should have a closed-yoke design, whether it is an electromagnet or a permanent magnet. Open yokes show an easily observable variation of gap with field strength. One may use non-ferromagnetic pins to separate the poles by a fixed amount, but these limit accessibility and are inconvenient to adjust. It is true that the closed yoke limits accessibility to a certain degree, but the gain in rigidity is worth much. Various workers find it convenient to have the plane of the magnet horizontal, while others have it vertical so that probes may be inserted from the side. The horizontal mount is the most convenient where dewars are used. A reasonable compromise is to use an inclined table or trunnions for varying the angle of tilt. The Bitter–Reed design allows for separation of the poles, but access is restricted in the closed position (60).

Except where unusually large fields are to be used, the material of yoke construction, as long as it is magnetically soft, is not critical. The cross-section of the yoke should be sufficiently greater than that of the poles so that the leakage

flux may be carried without saturating. Hot-rolled bars are commonly used, for these show less distortion on milling than the same material when cold-rolled. The pole face material is all-important. One desires a material of high saturation value, but even more important is the uniformity of density and freedom from inclusions. Armco magnetic iron has been most commonly used, but some steels have shown more uniform density. Stresses should have been relieved. The faces should be thick enough (about 5 cm.) to maintain rigidity of themselves. Where possible, the pole faces should be fastened to the poles by a collar or a ring of screws in preference to a single axial bolt. In the case of permanent magnets, a collar with studs should be affixed to the yoke.

Alnico V is nearly always used for permanent magnets, either in the form of a cylinder or as sectors of a cylinder held together in a strong tube. One of the most important considerations for a permanent magnet is that it should initially have been magnetized to saturation. Since it requires about 6000 amp. turns per inch to saturate, a high current source is needed, though the current needs to flow for only a few seconds. Numerous workers have suffered with very inhomogeneous fields because not all domains were aligned. A small reverse current sufficient to drop the field several per cent from its saturation value makes the field more stable to demagnetization.

It is common to find that the most homogeneous portion of a magnetic field shifts from day to day, in both permanent magnets and electromagnets. In the latter, one can do a good deal to maintain homogeneity by a proper cycling procedure. For example, in turning on a field it may be helpful to carry the field above its desired value by 30 per cent and then drop to the desired value.

On changing the operating point it will usually be found that the homogeneity at the original field has suffered, but with a proper cycling procedure determined by experience, the original state should be restored. Although a field appears homogeneous midway between the poles, it may not be so near them, for many details of surface magnetic contours are lost. Saddle points are not at all uncommon. Sometimes, in order to compensate for axial inhomogeneity one may omit connecting one of a set of magnet coils on one side. z-axis inhomogeneity is necessarily accompanied by x- and y-axis inhomogeneity, because Laplace's equation must be satisfied at every point.

The construction of a magnet with a highly homogeneous field is not to be undertaken lightly. Unless unusually good shop facilities are available and one's time is not highly valued, it would be worthwhile to consider purchase of a complete unit.

Part II. Electron Spin Resonance of Nearly Free Dipoles

XIII. INTRODUCTION

Studies of paramagnetic resonance of ions in crystalline solids have given much accurate information about crystalline electric fields. The field has been reviewed admirably (66) and has as well been the subject of brief treatments (62, 63, 136, 192, 195, 326, 565). Of at least equal general interest to chemists

are such topics as the electron spin resonance absorption of stable and unstable free radicals, free and trapped atoms and electrons, conduction electrons in metals, color centers, and triplet states in excited molecules. They are the principal topics of Part II of this review.

A radiofrequency absorption maximum in a magnetic field was first reported in 1945 in $CuCl_2 \cdot 2H_2O$ and was interpreted as a spin resonance (619). Since

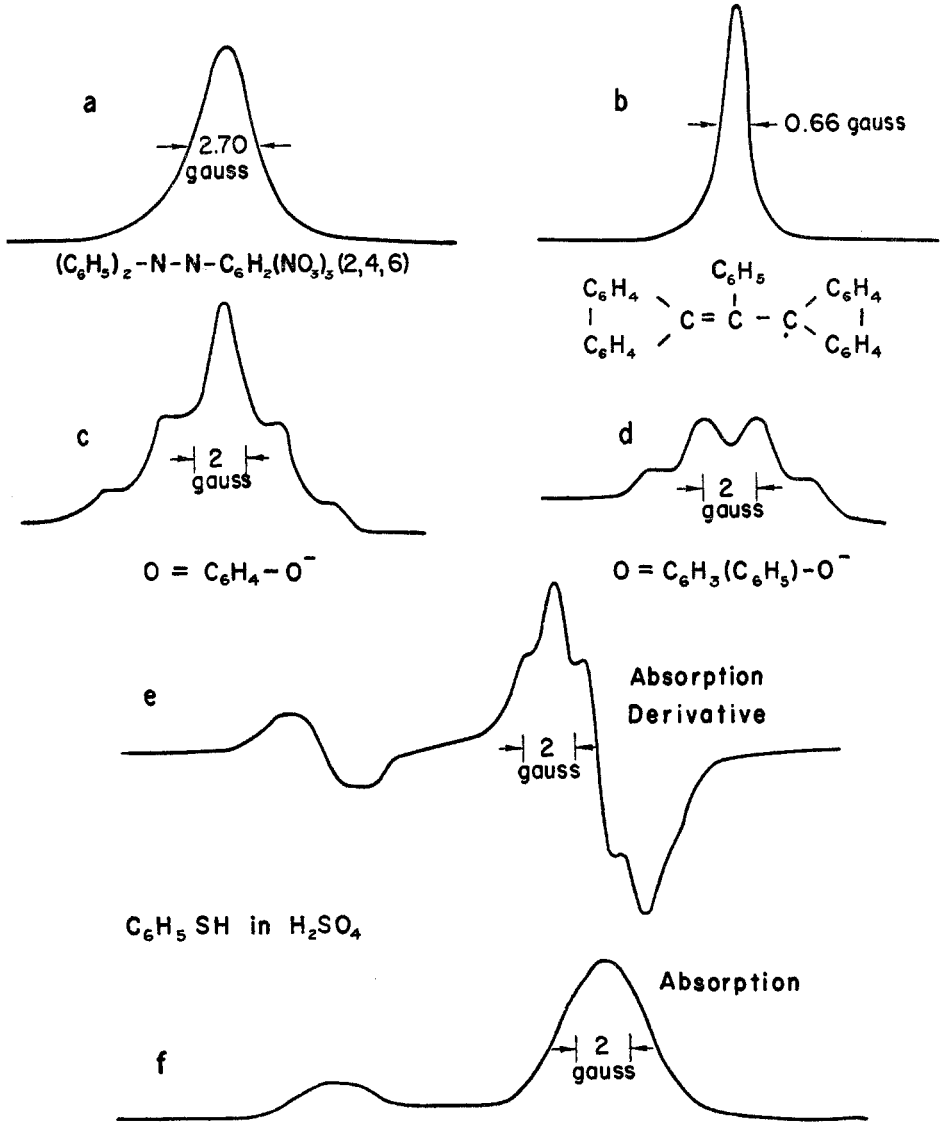

FIG. 21. Electron spin resonance absorption lines of free radicals at 9000 Mcps: (a) 1,1-diphenyl-2-picrylhydrazyl; (b) α,γ-bisdiphenylene-β-phenylallyl; (c, d) semiquinone ion-radicals from hydroquinone and phenylhydroquinone; (e) absorption derivative for two radicals from C_6H_5SH in H_2SO_4; (f) absorption curve for the same radicals.

then a large number of other salts have been investigated in detail. Such paramagnetic salts are far from being the nearly ideally simple systems which are represented by nuclei; hence one begins by seeking a system which would behave as nearly free magnetic dipoles.

As a sample which approximately fulfills the condition of having only spin magnetic moment, one may use a free radical. One of the easiest to make and use is 1,1-diphenyl-2-picrylhydrazyl (DPPH), $(C_6H_5)_2N\dot{N}C_6H_2(NO_2)_3$-2,4,6. To demonstrate experimentally its spin resonance, one may use the apparatus of figure 1 or figure 4. Using 30 Mcps as in the proton experiment of Part I, one will scan the region around 10.7 gauss. With sufficiently large sweep amplitude and proper adjustment, one may obtain the curve shown in figure 21a. The width at half-height is about 2.7 gauss, being of the same order of magnitude as that of a proton line in a solid at room temperature. However, the proton line at 10.7 gauss would have been too weak to observe directly on the oscilloscope. For many radicals the line widths are around 10 gauss, while for undiluted paramagnetic salts they may be hundreds or thousands of gauss wide. Observations of wide lines then will require fields in the kilogauss range. One chooses a frequency range in which microwave sources and components are readily available. From about 3000 Mcps upward, one generally propagates energy in a rectangular wave guide, which provides automatic polarization. If the sample is located within the guide, the arrangement is analogous to that used in optical spectroscopy. If one chooses 9000 Mcps, the resonant field will be near 3200 gauss for a free radical. Now let a section of wave guide containing a cavity electrically resonant at 9000 Mcps be placed in a magnetic field, as shown in figure 22. The resonant cavity may be considered as the microwave equivalent of an absorption cell which has a number Q of multiple reflections, where Q may be several thousand. The sample is placed at the position of the maximum of the (now enhanced) microwave magnetic field, and even a small magnet can provide a

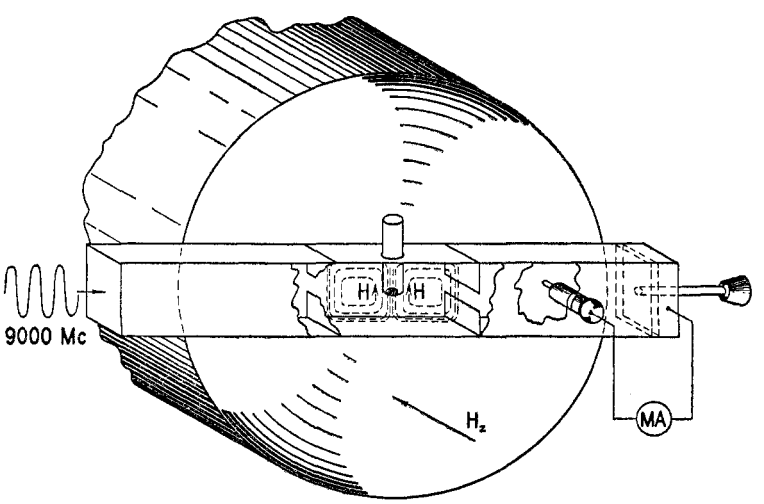

FIG. 22. Simplified representation of microwave ESR apparatus

sufficiently homogeneous field over this restricted region. The microwave field loops shown are perpendicular to the applied field H_z. With several tenths of a gram of 1,1-diphenyl-2-picrylhydrazyl centered in the cavity, the incident frequency is adjusted to give maximum detector current, so that the system is properly tuned. The field will slowly be increased beyond 3200 gauss. At 3208 gauss there will be a sharp dip in the indication of the milliammeter monitoring the transmitted power, indicating resonant absorption. Plotting current against field increment, one again gets a curve similar to χ'' of figure 2. This experiment sounds simple to perform and it is, but only because of wartime development of microwave techniques. When concentrations of absorbing centers become small or line widths large, one requires much more elaborate equipment.

If the spin magnetic moment in this sample had been entirely free to precess about the field, g would have been 2.0023. From a careful determination of the ratio of resonant frequency to field, one finds that $g = 2.0036$ for polycrystalline 1,1-diphenyl-2-picrylhydrazyl. Judging from this figure alone, one would say that the unpaired electron is nearly free, and that the orbital moment is negligible. However, if one takes a single crystal, g will show a variation (anisotropy) as the crystal is rotated (270, 306). (Rather than being a constant, g is a tensor of rank 2.) Moreover, in solution in benzene, the line broadens to an eventual width of about 50 gauss in very dilute solutions and shows a fine structure. Even in this relatively favorable case one observes more complicated behavior than for nuclear dipoles. Although the separation of multiple proton lines in solids depends on the angle between a crystalline axis and the field, the center of the pattern is not shifted. It is therefore desirable to inquire into the factors complicating electron spin resonance. Although the systems described here do not show some of these complications prominently, vestigial remnants may complicate even the simplest systems.

XIV. ELECTRON SPIN INTERACTIONS

The observable tendency of a paramagnetic substance to move into a stronger part of an inhomogeneous magnetic field is measured by the ratio of macroscopic polarization $\mathfrak{M}$ to the field H:

$$\chi = \mathfrak{M}/H$$

The susceptibility χ is given for a nucleus by the Langevin–Debye equation:

$$\chi = \frac{N\mu^2}{3kT} = \frac{Ng^2\mu_n^2}{3kT} I(I+1)$$

The g-factor and the nuclear magneton μ_n were met in Part I. The molar nuclear susceptibility being of the order of 10^{-9} C.G.S. units, it can be wholly neglected in comparison with the electronic molar susceptibilities of the order of 10^{-3}. Paramagnetic substances may be grouped in the following categories: (*1*) atoms or ions possessing an unfilled inner electron level, (*2*) atoms or molecules with an odd number of electrons, (*3*) metals, and (*4*) molecules with independent unpaired electrons (biradicals) or with coupled electrons of spin 1 (triplets). In

some of these, the paramagnetism may be very weak, and the material appears diamagnetic. Many paramagnetic substances will have orbital as well as spin angular momentum. Diluted as in molecular beams, the orbital dipoles would be free to make their contribution, the orbital vector being added to the spin vector and the resultant precessing about the field (if the latter is not strong enough to uncouple them). The net angular momentum $\sqrt{J\,(J+1)}h/2\pi$ will give rise to a magnetic moment of magnitude $g\mu_B\sqrt{J\,(J+1)}$. For a collection of non-interacting atoms, one may then write

$$\chi = \frac{Ng^2\mu_B^2}{3kT}J(J+1) = \frac{N\mu_B^2}{3kT}\mu_{\text{eff}}^2 \tag{49}$$

where μ_B is the Bohr magneton. For a free atom, g is given (607) by equation 50:

$$g = \frac{3}{2} + \frac{S(S+1) - L(L+1)}{2J(J+1)} \tag{50}$$

L and S are orbital and spin quantum numbers. One notes that $g = 2$ when $L = 0$. For this special case the electronic dipole should be the analog of the nuclear dipole and precess about the magnetic field, as shown in figure 3. The angular precessional frequency will again be given by equation 6:

$$\omega_0 = \gamma H$$

A perpendicular magnetic field which rotates about the applied field H_z at the same frequency ω_0 may tip the dipole, thus exchanging energy with it in a resonant process.

Alternatively, one may speak in terms of energy levels, which for $L = 0$ will be given by $g\mu_B MH$, where the magnetic quantum number M has the values $\pm\frac{1}{2}$. With $\Delta M = \pm 1$, the energy of the radiation which will produce a transition between the levels is

$$h\nu = g\mu_B H_z \tag{51}$$

The value of g obtained from this equation by measuring frequency and field at resonance is called the "spectroscopic splitting factor." Because μ_B is 658 times larger than μ_n, the resonant frequency for fields in the kilogauss range will be in the microwave (kilomegacycle) region. If g is given its free-electron value of 2.0023, the equation becomes

$$\nu = 2.8026H \tag{52}$$

if ν is in megacycles per second and H in gauss.

The value 2 of the factor g for a free electron was considered anomalous until Dirac was able to derive it theoretically. However, the assumption that it is exactly 2 led to a serious discrepancy between the results of two molecular beam experiments (379). In the first, the proton magnetic moment was determined in terms of the electronic moment without a knowledge of field strength. The second experiment involved a calibration of field strength assuming the electronic moment to be 1 Bohr magneton. The explanation proposed to resolve

the discrepancy (91, 494) was that the electron moment μ_e is greater than 1 Bohr magneton, μ_B. The value obtained by combining results of several experiments (179, 317) is $\mu_e = 1.001146\ \mu_B \pm 0.000012$, as compared with a theoretical value of 1.0011454 (302). A recent value of g_e/g_P is 658.2277 ± 0.0002, where g_P refers to the proton in the hydrogen atom (50).

On examination of most paramagnetic solids, one observes that g may be far from 2, its components taking such extreme values as 0.2 and 8.85 in the ethyl sulfates of cerium and erbium, respectively (65, 130). In case there is axial symmetry and the applied field is in this direction, g will have the values $g_{||}$ and $g_{\perp}$, respectively parallel and perpendicular to the field. For an arbitrary angle θ between the axis of symmetry and the applied field,

$$g^2 = g_{||}^2 \cos^2 \theta + g_{\perp}^2 \sin^2 \theta$$

On the other hand, in free radicals, metals, alkali metals in liquid ammonia and in ions in S states ($L = 0$) such as Fe^{+++} and Mn^{++}, g is nearly equal to the free-electron value 2.0023. Even for ions not in S states, one commonly finds g-values which are closer to 2 than the value predicted by equation 50. This is especially true of members of the first transition group. Such behavior is largely due to the tremendous electrostatic fields existing in ionic solids. Since the electron possesses charge, its orbital motion is then dictated (except for rare earth elements) by the crystalline fields and is little influenced by attainable magnetic fields.

In the absence of fields, an ion with orbital quantum number L would have $2L + 1$ coincident levels. The crystalline field interaction produces a separation (Stark splitting) of the orbital levels which is usually far greater than magnetic energies. The orbital magnetic moment is then said to be "quenched" and states will no longer be described by the quantum number J. The value of g will not be exactly 2, for there may still be a relatively large interaction of spin and orbital moments. In some salts (e.g., rare earths) this interaction is larger than crystalline field splittings.

It is instructive to list the several interactions of an ion. These can be summarized in the form (2):

$$W = W_F + V + W_{LS} + W_{SS} + \mu_B \mathbf{H}\cdot(\mathbf{L} + 2\mathbf{S}) + W_N - g_I \mu_n \mathbf{I}\cdot\mathbf{H}$$

The various symbols have the following meaning and approximate magnitudes:

W_F is that portion of the energy of a free ion not dependent on spin (10^5 cm.$^{-1}$).

V is the electrostatic energy due to the crystalline field (10^4 cm.$^{-1}$).

W_{LS} is the interaction due to coupling of the spin and orbital motion, usually referred to as spin–orbit coupling (10^2 cm.$^{-1}$) (156a).

W_{SS} is the spin–spin interaction (1 cm.$^{-1}$).

$\mu_B \mathbf{H}\cdot(\mathbf{L} + 2\mathbf{S})$ refers to the interaction with the applied field (1 cm.$^{-1}$).

If the ion possesses a nuclear magnetic moment, W_N represents (*1*) the interaction of the nuclear moment with the orbital and spin magnetic

moments (10^{-2} cm.$^{-1}$), and (*2*) the interaction of the nuclear quadrupole moment Q with the gradient of the electrostatic field if $I \geqq 1$ (10^{-3} cm.$^{-1}$). The final term, $g_I\mu_n\mathbf{I}\cdot\mathbf{H}$, is just the energy of a nucleus in a magnetic field (10^{-3} cm.$^{-1}$).

For crystalline fields of high symmetry, the manner of splitting of the orbital levels may be predicted by group theory (53). The fields are often predominantly cubic, with small components of lower symmetry. If an orbital singlet state lies lowest and the next state is 200 cm.$^{-1}$ or more above it, only the lower state will be occupied at room temperature. The spin degeneracy of the lowest state will then remain, and transitions between these may be studied when these degenerate levels have been split by a magnetic field. However, the crystalline field may also be responsible for further splitting. Although it cannot affect spin levels directly, it may do so indirectly through the spin–orbit coupling. If the spin quantum number is 1 or more, the spin levels may be split even in the absence of a magnetic field. This is referred to as "zero-field splitting." However, if a molecule possesses an odd number of electrons, a quantum-mechanical theorem (329) states that the spin–orbit coupling must always leave at least a twofold degeneracy in each orbital level. Hence the application of a magnetic field will still produce a separation of spin levels. However, the situation is complicated by the fact that there may be crossing of spin levels from the separate components of zero-field splitting. Multiple resonance lines will arise, and although one may get a g-value for the center of the pattern, this will not usually be equal to 2. Using a fixed frequency and increasing the field from zero, the allowed transitions with $\Delta M = \pm 1$ are necessarily coincident in energy. The absorption lines will appear in succession when the field has separated the levels by exactly this energy $h\nu$.

Even in the absence of crystalline fields, there is a mechanism for removing orbital degeneracy of the lowest level. A highly symmetrical molecule may possess such degeneracy, but if it is non-linear, the molecule will be deformed in such a way as to remove the orbital degeneracy, since by so doing its energy will be lowered (284). Thus one will not expect to find orbital magnetic moment contributions in free radicals. In metals, there is no orbital motion of conduction electrons, nor is there for trapped electrons in solids or for solvated electrons in solutions of metals in liquid ammonia.

It is convenient to define a "spin Hamiltonian" as follows for a magnetic field applied along the axis of symmetry of a crystal (2):

$$\mathcal{H} = \mu_B[g_{||}H_zS_z + g_\perp(H_xS_x + H_yS_y)] + D(S_z^2 - S(S+1)/3) + AI_zS_z + B(I_xS_x + I_yS_y) + Q'(I_z^2 - I(I+1)/3) - g_I\mu_n\mathbf{H}\cdot\mathbf{I} \quad (53)$$

$2S + 1$ is the multiplicity of the level under consideration; hence if the spin quantum number is not $\frac{1}{2}$, the S of this equation will be a fictitious "effective spin."

One may interpret the bracketed term as meaning that the "free" spin precesses about the field ($g_\perp H_x$, $g_\perp H_y$, $g_{||}H_z$). The D terms give the splitting in the

absence of a field, resulting in fine structure. The $\mathbf{I}\cdot\mathbf{S}$ terms give the interaction between nuclear and electronic moments and lead to hyperfine structure. The Q' term represents quadrupole interactions and the last the interaction between the nuclear moment and the field. A, B, and D are interaction constants and Q' denotes

$$\frac{3eQ}{4I(2I-1)}\frac{\partial^2 V}{\partial z^2}$$

By the use of this Hamiltonian, one may solve for the frequencies of resonance absorption lines (61, 62). The expression, which will not be reproduced here, has for its first term the quantity $g\mu_B H/h$.

XV. EXCHANGE INTERACTIONS

In the quantum-mechanical treatment of a system of two electrons, the wave functions must explicitly take into account the impossibility of identifying them with particular atoms. This is accomplished by the use of linear combinations

$$\psi_S = \frac{1}{\sqrt{2}}(\psi_{\mathrm{I}} + \psi_{\mathrm{II}})$$

and

$$\psi_A = \frac{1}{\sqrt{2}}(\psi_{\mathrm{I}} - \psi_{\mathrm{II}})$$

The Pauli principle requires the use of antisymmetrical wave functions which are the product of the orbital and spin functions. One will use the symmetrical combination ψ_S if the orbital function is antisymmetrical and *vice versa*. Actually, it is the symmetry of the spin function that determines the orbital function symmetry.

If E_s and E_a represent the energies of the symmetrical and antisymmetrical states respectively, $(E_s - E_a)/h$ is called the exchange frequency. If one chooses a solution to the time-dependent wave equation which reduces to ψ_{I} at $t = 0$, the function will oscillate between ψ_{I} and ψ_{II} at the exchange frequency (624).

If V_{12} is the interaction energy between two electrons, it can be shown (568) that

$$V_{12} = K_{12} - \tfrac{1}{2}J_{12} - 2J_{12}\mathbf{S}_1\cdot\mathbf{S}_2 \qquad (54)$$

Here $\mathbf{S}_1$ and $\mathbf{S}_2$ are the spin momentum vectors for the electrons, and K_{12} and J_{12} are respectively given by:

$$K_{12} = \int \psi_{\mathrm{I}}^* V_{12}\psi_{\mathrm{I}}\,d\tau$$

and

$$J_{12} = \int \psi_{\mathrm{I}}^* V_{12}\psi_{\mathrm{II}}\,d\tau$$

J_{12} is usually called the exchange integral. The last term of equation 54 is of the form $\mu \cdot \mu_2$ found for dipole interactions, and usually has a large value. This does *not* mean that there is a large magnetic interaction, for the latter is indeed very small. Rather, the $S_1 \cdot S_2$ product which for $S = 0$ and $S = 1$ gives the values $-\frac{3}{4}$ and $\frac{1}{4}$ merely determines the magnitude and sign of the electron interaction, depending on the spin alignment. Exchange is then basically an electrical rather than a magnetic interaction. The coupling between spin and orbital magnetic moments has been neglected in this "isotropic" exchange description. If crystalline electric fields are present, the form of the exchange term is altered. Six types of exchange interaction have been described (624).

It is to be recalled that random motion in liquids modulates the dipolar interactions to narrow a NSR line. Here dipolar interaction is modulated by the exchange interaction, but it is the spin orientation which is modulated instead of the spatial coördinates (196).

The importance of isotropic exchange lies in its effect on line shape and width. In the general case, exchange leads to line broadening, but for the special case of identical dipoles precessing about the same axis, a narrowing will result (68). Exchange here does not alter the second moment of the line shape (described in Section VII) but appreciably increases the fourth moment (569). The center of the line becomes sharply peaked, and to keep the area constant, the wings are much broadened. For a Gaussian line shape the deviation of the root-mean-square frequency from the center of the line is just equal to half the line width (in frequency units) measured between points of maximum slope. It is likewise equal to 0.426 times the line width at half-height. Exchange decreases both the separation of points of maximum slope and the width at half-height. Such narrowing makes it easy to observe absorption of free radicals, since the absorption peak intensity may be very large. Dipole–dipole interaction would usually be expected to give ESR lines in free radicals a width of the order of 100 gauss. Very commonly the line width is less (sometimes much less) than 10 gauss. Since the wings of an exchange-narrowed line may be difficult to distinguish from background noise, it is hazardous to attempt an experimental determination of the second moment. Fortunately it has been shown that the observable portion of such a line should have a Lorentz shape (8). This has been shown for a number of radicals (116, 597) and is true of figure 21b. For broader lines the presence of exchange narrowing may be assessed from line shape only if care has been taken that the line has not been distorted because of dispersion (596).

XVI. HYPERFINE SPLITTING

If one were seeking experimental verification for delocalization of electrons in free radicals, there is probably no more convincing area than ESR absorption. The narrowing of absorption lines as one goes from exceedingly dilute to concentrated (liquid or solid) solutions because of increasing exchange interaction is striking evidence for overlap of wave function. Additionally, the splitting of the absorption line at low concentrations into tens of components can only occur because the odd-electron function extends over many nuclei. The simplets case involves the interaction of an unpaired electron with a single nucleus of spin $\frac{1}{2}$.

Since the magnetic quantum number of the nucleus may be $+\frac{1}{2}$ or $-\frac{1}{2}$, two lines $(2I + 1)$ appear. Just such a doublet is seen for hydrogen and for phosphorus atoms, to be considered in Section XX. For deuterium atoms $(I = 1)$, a triplet occurs.

Historically, hyperfine splitting by a nuclear moment was first observed in $MnSO_4 \cdot 3H_2O$ in 1947 (621). Later and independently it was observed in a diluted copper Tutton salt (412). Hyperfine splitting was found later in the peroxylamine disulfonate ion $(SO_3)_2NO^-$ (410) and in 1,1-diphenyl-2-picrylhydrazyl (270). Subsequently it has been observed in many other radicals.

In strong fields (H_z large compared with the field contributed by the nucleus at the unpaired electron) the first-order solution of the Hamiltonian of a free radical becomes (61):

$$h\nu = g\mu_B H + J_{IS} M_I \tag{55}$$

M_I is the nuclear magnetic quantum number, and J_{IS} is the interaction constant. It has been indicated that g may be anisotropic in rigid media. For most free radicals this anisotropy is small, because of the very small spin–orbit coupling. J_{IS} likewise may be anisotropic, as has been shown for solid solutions of the ion $(SO_3)_2NO^-$ in potassium hydroxylamine disulfonate. Rapid reorientation in liquids eliminates the contributions of non-spherically symmetric wave function components (such as $2p$) so as to give an averaged value of g and J_{IS} (601). $2I + 1$ lines with equal spacing J_{IS} are then expected in the simplest case. Energy levels for the system $S = \frac{1}{2}$, $I = 1$, are drawn in figure 23a. Owing to the practice of working at constant frequency and varying the magnetic field,

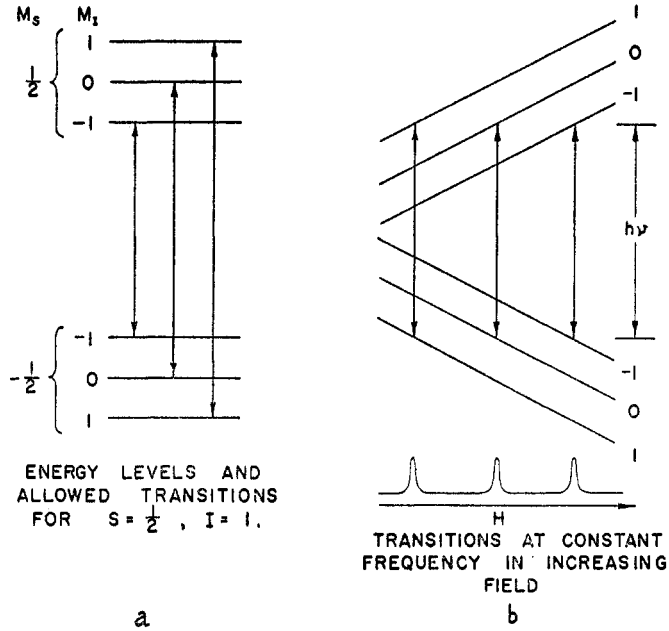

FIG. 23. (a) Energy levels and allowed transitions for hyperfine splitting, with $S = \frac{1}{2}$, $I = 1$. (b) Transitions at constant frequency in increasing field.

one observes the expected number of lines in succession as the separation of two levels becomes equal to $h\nu$. This is illustrated in figure 23b.

Where a small number of "equivalent" nuclei are present, one uses their total magnetic quantum number. In the section on semiquinones, mention is made of phenylbenzosemiquinone ion. Since this ion has three ring protons on the principal ring, the allowable quantum numbers are $-\frac{3}{2}$, $-\frac{1}{2}$, $\frac{1}{2}$, and $\frac{3}{2}$. Four lines appear with the intensity ratio of 1:3:3:1, as shown in figure 21d (605). One concludes that the wave function of the unpaired electron certainly extends over the principal ring, but not appreciably to the substituting phenyl group.

Four conditions must be satisfied for the observation of hyperfine structure (411). These are:

1. The system must be sufficiently dilute so that the hyperfine interaction is larger than either the exchange interaction or the dipole–dipole interaction.

2. If $\Delta\omega$ represents the splitting interval in frequency units, then the radical lifetime and the thermal relaxation time t_1 must be greater than $1/\Delta\omega$.

3. The radiofrequency or microwave field amplitude must be small compared to the splitting interval, both expressed in gauss.

4. The field inhomogeneity over the sample should be smaller than the splitting interval. Splitting intervals less than 0.1 gauss have been observed in compounds containing many protons, while for free hydrogen atoms the splitting is about 500 gauss. Since a phase detector will generally be used for observation of the absorption derivative, the field modulation amplitude must be much less than the splitting interval.

The ESR line for the triphenylmethyl radical appears single under low resolution when it is in a dilute solution, since the splitting interval for the hydrogen is small and the carbon does not contribute since its nuclear spin is zero. However, when the methyl carbon is C^{13}, a new doublet appears with a 22-gauss separation, since its nuclear spin is $\frac{1}{2}$ (602). Under higher resolution, the absorption curve for $(C_6H_5)_3C^{12}$ shows eighteen groups of multiple lines, with the exact number uncertain. While the pattern has not been interpreted, it clearly indicates delocalization of the unpaired electron. If one assumes (*1*) that all ring positions are equivalent, (*2*) that a significant unpaired-electron density appears on each carbon atom, and (*3*) that a hydrogen atom adjacent to such carbons contributes to the splitting, there should be a maximum of 196 lines. Assumption 1 is perhaps open to question. Dimesitylmethyl showed lines arranged in two groups, far too many to be accounted for by the ring hydrogens alone. Owing to hyperconjugation, the ring hydrogens participate in some measure (287). In the much simpler tolusemiquinone radical, the spectrum has been interpreted in terms of three interaction constants (573), one for the methyl protons and two for the ring protons. One of these is not equivalent to the others, though which is the unique one is not settled. Two xyloquinones also examined required only two interaction constants (573). Elucidation of the hyperfine structure of ring protons in more complicated molecules may be simplified by deuterium substitution. Some progress has been made in the interpretation of the hyperfine splitting of the methylamino and dimethylamino protons of substituted *p*-phenylenediamines (598).

Curiously, no fine structure has been observed for $(C_6H_5)_3N^+$, which is isoelectronic with triphenylmethyl, and the conclusion has been drawn that the unpaired electron spends little time at the nitrogen (411).

Group-theoretical calculations have been made relating the hyperfine structure of radicals with their electronic structure (599). Interpretations have been made regarding the amount of s- and p-character of atoms responsible for hyperfine splitting (601). In liquids hyperfine splitting arises from s-components, while in solids the non-s-components lead to anisotropy. The radical $(C_6H_5)_3C^{13}$ is believed to be bent appreciably toward a tetrahedral configuration because of the $2p$ contribution of the methyl carbon atom (589).

1,1-Diphenyl-2-picrylhydrazyl and related compounds in solutions about 0.001 M show an apparent structure of five lines over an interval of about 50 gauss (270). If the unpaired electron were to spend equal times on the adjacent nitrogen atoms ($I = 1$), one would expect five lines. For an arbitrary ratio of times spent on the two, there should be nine lines. When the electron interaction with one nitrogen nucleus is twice that of the other, the number reduces to seven (285, 306). The experimental curves can be fitted for 1,1-diphenyl-2-picrylhydrazyl on the basis of equal interaction with the two nitrogens. For N-picryl-9-aminocarbazyl, agreement was obtained for one interaction twice the other, without establishing which nitrogen was the more effective. The combination of seven Gaussian lines 10.9 gauss wide gives rise to five observed peaks. The compound obtained by replacing one of the o-nitro groups in 1,1-diphenyl-2-picrylhydrazyl with SO_3Na represents an intermediate case.

Equation 55, implying linear variation of frequency with field and $2I + 1$ splitting components, applies to atoms and free radicals in high fields. At low or intermediate fields, such linearity need not apply, and the number of components need not be the same as at high fields. To understand the dependence of hyperfine splitting upon H_z, one must study the variation of energy levels with field and consider the difference between the precession of nuclear spin and total angular momentum vectors at low and high fields. In weak fields **J** and **I** couple to form the resultant **F**, which then precesses about H_z, whereas in strong fields J and I are wholly or partially uncoupled (Paschen–Back effect) and precess independently. The "weak" and "strong" field quantum numbers will be different. For hyperfine structure in free-radical spectra of $(SO_3)_2NO^=$ it has been found that the equations of Breit and Rabi (92, 378) may be applied successfully (520, 561). These had been developed for hydrogen and deuterium to indicate all possible transitions in molecular beam magnetic resonance experiments in which the radiofrequency field was parallel or perpendicular to the steady field H_z. One may draw a complete energy-level diagram including low, intermediate, and high fields in terms of only one parameter, the energy-level separation in zero field (92, 378). This value may be obtained from a single high-field measurement, but it is well to verify the diagram with low-field measurements. The energy levels are given by:

$$W = -\frac{h\Delta\nu}{2(2I+1)} + g_I\mu_B MH_z \pm \frac{h\Delta\nu}{2}\left(1 + \frac{4Mx}{2I+1} + x^2\right)^{1/2} \qquad (56)$$

Here $h\Delta\nu$ is the separation of levels at zero field and g_I is the g-factor of the nucleus, responsible for the hyperfine splitting. x is $(g - g_I)\mu_B H_z/h\Delta\nu$. In zero field the vector sum of **J** and **I** is **F**, which for $I = 1$ is $\frac{1}{2}$ or $\frac{3}{2}$. Upon applying the field each of these levels is split into $2F + 1$ levels, as plotted in figure 24 (378). For the radical ion $(SO_3)_2NO^-$ in solution the value of $h\Delta\nu$ is found to be 54.7 Mcps, and excellent agreement is found at low fields between observed and calculated line positions (520, 561). The nucleus responsible for the splitting is N^{14}, with $I = 1$. The agreement between the calculated interaction of an electron with a nucleus having $I = 1$ using a model based on the deuterium atom is gratifying. In figure 25 the curves are the calculated ones, and the points are experimental observations (561). Hydrogen and deuterium atoms in irradiated

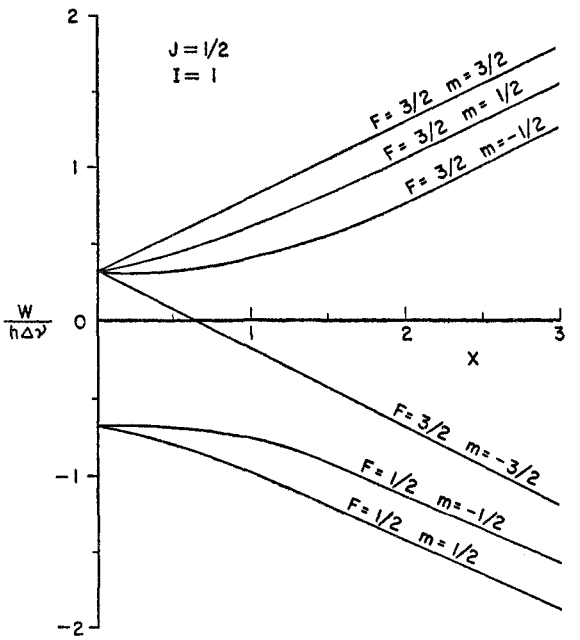

FIG. 24. Energy levels at low fields for hyperfine splitting with $S = \frac{1}{2}$, $I = 1$ (378)

acids show just the hyperfine splitting found for the free atoms, while in irradiated ice the splitting is much less (see Section XX). Further applications and interpretations of hyperfine structure are found under numerous headings.

XVII. RELAXATION TIMES

The relatively narrow free-radical ESR lines necessarily imply spin lifetimes which are long compared with the inverse line widths expressed in frequency units. While thermal relaxation times of 10^{-4} sec. are considered short for nuclei, such values would be very long for ESR absorption, t_1 in some cases being 10^{-11} sec. or less. Such short values lead to lines many times broader than typical NSR lines. Spin–spin relaxation times are correspondingly shorter. To ascertain the true lifetime and to decide what process determines line width for 1,1-di-

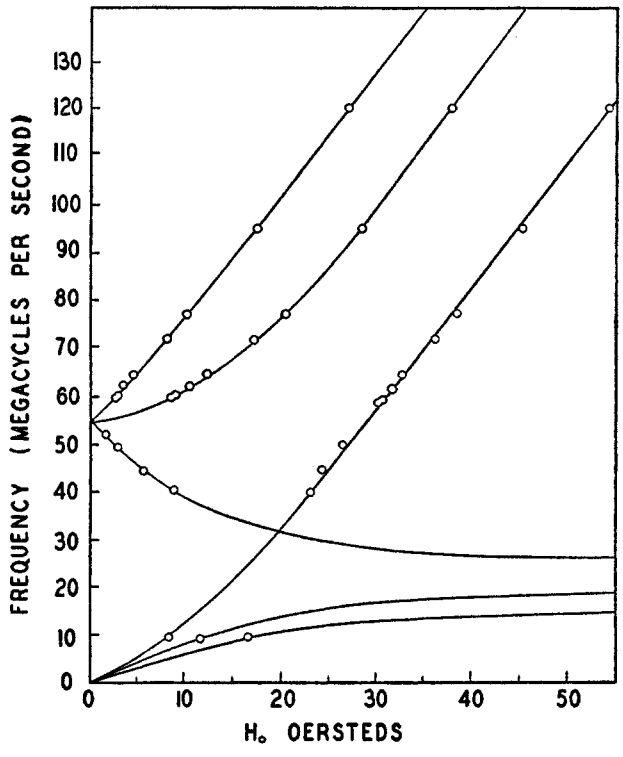

FIG. 25. Transitions of the $(SO_3)_2NO^-$ ion at low fields (561)

phenyl-2-picrylhydrazyl (DPPH) and other radicals, direct measurements of t_1 and t_2 have been made. t_1 is found to be 6.3×10^{-8} sec. for DPPH (86, 175, 346) and 1.6×10^{-7} sec. for tris(*p*-nitrophenyl)methyl (TpNPM). $1/\gamma t_1$ and $\Delta\omega_{1/2}/\gamma$ are, respectively, 0.35 gauss and 0.36 gauss for TpNPM, where $\Delta\omega_{1/2}$ represents the line half-width at half-height. For DPPH, $1/\gamma t_1 = 0.90$ gauss, while $\Delta\omega_{1/2}/\gamma = 0.97$ gauss, thus showing that $t_1 \simeq t_2$. These magnitudes indicate that the line width of both radicals is largely determined by the lifetime-limiting process of thermal relaxation. The longer lifetime of TpNPM is in qualitative accord with its narrower ESR line.

When exchange effects are prominent, the relaxation mechanism requires separate exposition. In liquids the dipolar interaction is modulated by Brownian motion. The line is narrowed and the magnetic energy is converted to the thermal energy of such motion. Exchange interaction can similarly modulate dipolar interaction and the magnetic energy becomes exchange energy (86, 196), with a characteristic time t_1. The exchange interaction modulates the orientations of the dipoles rather than their positions in space. The dipolar interaction serves to transfer exchange to thermal energy in a time far shorter than t_1. One example of this relaxation mechanism is DPPH, which has $t_1 \simeq t_2 \simeq 6.3 \times 10^{-8}$ sec., independent of temperature. The energy transfer is really a dipole–dipole relaxation mechanism, but it has the same effect as the usual thermal relaxation process in that the magnetic energy is not conserved.

The relaxation times t_1 and t_2 are related to ease of saturation of a spin system through the saturation parameter $\gamma^2 H_1^2 t_1 t_2$. Applying a microwave field $H_x = 2H_1 \exp(i\omega t)$, one gets from the Bloch equations:

$$\frac{\chi''}{\chi_0''} = \frac{1}{1 + \gamma^2 H_1^2 t_1 t_2} \tag{57}$$

where χ_0'' represents the imaginary component of the susceptibility for very low values of H_1. Experimental measurements of χ''/χ_0'' show agreement with equation 57 over more than four orders of magnitude.

Measurements of line amplitude as a function of radiofrequency power allow t_1 to be determined if t_2 is known or if $t_1 = t_2$. For 1,1-diphenyl-2-picrylhydrazyl it is found that saturation is 50 per cent when $H_1 = 1.8$ gauss and complete for $H_1 = 10$ gauss (86).

For systems in which the spin is greater than $\frac{1}{2}$ there is no uniquely defined relaxation time. It is preferable to define a relaxation probability (347), because the attainment of statistical equilibrium among unequally spaced spin levels is not given by the simple exponential-approach equation. Such a probability reduces to $1/2t_1$ for a system of two energy levels. From measured relaxation probabilities for $(SO_3)_2NO^-$ it was inferred that spin–orbit coupling is important as a relaxation mechanism.

A spin–orbit coupling model gives reasonable estimates of t_1 for alkali metals (153). The line width in sodium increases abruptly by 25 per cent when the solid melts (340).

XVIII. FREE RADICALS

The electronic paramagnetic resonance (ESR) absorption of a free radical was first observed in 1947 (328), using pentaphenylcyclopentadienyl $(C_6H_5)_5C_5$, which was known from susceptibility measurements to be completely monomeric in the solid state (374). Since the ratio of resonant frequency to field is the same at 51 Mcps as at 450 Mcps and g is nearly 2, it was concluded that there is no orbital contribution to the paramagnetism. (The value of 1.95 given for g is probably too low.)

Whereas in paramagnetic salts one may have a wide range of g-values because of orbital magnetic moment contributions, in radicals one does not have such contributions because either (*a*) the molecule has a low symmetry and therefore cannot have orbital degeneracy, or (*b*) if molecular symmetry would allow degeneracy, the Jahn–Teller effect (284) causes molecular distortion if the electron did occupy a degenerate orbital (113). Spin–orbit coupling is also very small, as is true also in aromatic molecules (358).

In 1949 the compound $ON(C_6H_5)C(CH_3)_2CH_2\overline{C(CH_3)N(C_6H_5)O}$ (referred to as Banfield and Kenyon's radical) was found to show ESR absorption at 24,000 Mcps with $g = 2.0057$ and a width reported as 42 gauss (later revised to 18.4 gauss (250, 251)). At the time, this was the sharpest known ESR line, and rough susceptibility measurements showed Curie law dependence. It had been concluded from susceptibility measurements that the paramagnetism

arises entirely from an unpaired electron and that this substance also is completely dissociated in the solid state (303). Shortly thereafter, 1,1-diphenyl-2-picrylhydrazyl was shown to have $g = 2.0036$ (251, 560) and a line width of 2.7 gauss. It was later the first radical to be observed at fields of the order of 10 gauss, where the absorption intensity is far less than in the microwave region (182). Many other radicals have since been investigated, and in addition to usually finding a g-value very near the free-electron value of 2.0023, one is struck with the relative narrowness of the lines. With paramagnetic salts which are magnetically dilute (as, for example, the alums) the line width is more commonly of the order of several hundred gauss. To achieve widths of the order of 10 gauss one uses a diamagnetic alum containing a small fraction of paramagnetic ions. Without the benefit of diamagnetic spacers such as water molecules, the exchange interaction in free radicals is large. The narrowing from an estimated 100 gauss does not occur by rapid reorientation in the solid, but rather occurs as the result of electronic exchange. When 1,1-diphenyl-2-picrylhydrazyl is dissolved in benzene, the line is broadened, contrary to the usual trend when paramagnetic substances are diluted. The line with progressive dilution becomes broader and eventually in the region of 0.002 molar splits into five components over a total range of about 50 gauss (270, 285, 306). It is to be noted that at 10^{-3} molar the separation between molecules is about 100 Å., and yet for many radicals the absorption line is even narrower than for more dilute solutions. There can be no question that spin–orbit coupling is very small, for if it were appreciable, one would expect fairly short relaxation times which would give rise to an uncertainty broadening greater than the widths of the narrow lines observed. The g-values attest to the same thing.

The radical-ion $(SO_3)_2NO^-$ is unusual, in that there is not a marked exchange narrowing so frequently found for other radicals (410). While for most free radicals the line becomes broader with dilution because of reduced exchange, the triplet lines of $(SO_3)_2NO^-$ become narrower.

1,1-Diphenyl-2-picrylhydrazyl (DPPH) has been used as a reference substance more than any other because of its stability (the decomposition is not more than several per cent per year in the dark) and because very small quantities—of the order of 10^{-11} mole—can be detected. In observing absorption lines tens of gauss wide, a small bit may be affixed to the sample tube to provide a reference marker. The detection of ESR absorption by several tenths of a gram of DPPH with a microammeter to monitor crystal detector current at 9000 Mcps was mentioned earlier. Tris(p-nitrophenyl)methyl (TpNPM) has a narrower line than DPPH and its g-value is reported to be independent of field (491), but because of its reactivity with oxygen, it is less convenient to use as a standard. Other radicals listed in table 8 have even narrower lines.

The g-factors for polycrystalline 1,1-diphenyl-2-picrylhydrazyl and tris(p-nitrophenyl)methyl do not change appreciably down to 1.6°K. (187, 512), but the line width increases at lower temperatures in a fashion reminiscent of NSR lines in solids. No antiferromagnetism was found at 1.6°K. for 1,1-diphenyl-2-picrylhydrazyl (187). The line has a Lorentz shape at 4°K. and at room tempera-

ture in low fields ($\sim$ 10 gauss) (597). This is predicted for strongly exchange-narrowed lines (8).

Free radicals have been found in partially polymerized glycol dimethacrylate at room temperature (164). Styrene polymerized with a sodium dispersion sometimes forms a red solid with persistent ESR absorption, though the experiment is not readily reproducible (343).

It is of considerable importance that calculations of unpaired electron density be carried out for a variety of radicals, as has been done for $CH_2(CH)_3CH_2$ and $CH_2(CH)_5CH_2$ (367). Nearly equal free-electron densities were found on the odd-numbered carbon atoms, while on the even-numbered atoms the density was essentially zero.

Various types of related free radicals will now be considered.

A. Semiquinones

Static magnetic susceptibility experiments and potentiometric titrations taken during the course of the slow reduction of quinones and related substances led to the discovery of semiquinones as free-radical intermediates. As an example, tetramethylquinone on reduction by glucose in pyridine shows a diminution in diamagnetic susceptibility to a minimum value and then a rise to a steady final value (366). The same system studied by ESR absorption shows thirteen hyperfine splitting lines, $(2I + 1)$, as expected from the hyperfine interaction with twelve equivalent protons (605). In alkaline alcoholic solution, one gets the same semiquinone ion from reaction of the corresponding hydroquinone with oxygen (573). The oxidation of hydroquinone proceeds too rapidly for susceptibility measurements or titrations, but an absorption due to the semiquinone ion $O{=}C_6H_4{-}O^-$ was found on making an alcoholic solution of hydroquinone slightly alkaline (573), the oxidant being oxygen. Five hyperfine splitting components appear with $g = 2.0057$ and an intensity 1:4:6:4:1, as expected if the four ring protons share equally an odd-electron contribution. This is shown in figure 21c. For phenyl-*p*-benzoquinone treated similarly one should get components of intensity 1:3:3:1 due to the three ring protons, and this trace is shown in figure 21d. In dichloroquinone, where two ring protons are present, three lines appear as expected. If aqueous alkali is added to hydroquinone a different radical appears to be formed, presumably due to the semiquinone of hydroxyquinone. Semiquinone radicals of *o*-phenanthraquinone and the benzil–benzoin system have been observed (572). In mono- or dimethyl-substituted semiquinones the interaction of the unpaired electron with methyl and ring protons has been ascertained from the measured separation of hyperfine components (573) to get an estimate of relative unpaired electron densities at the several carbon atoms. Numerous other semiquinones are currently being studied, and in some cases more than one radical intermediate is observed (605). Quinhydrones adsorbed on barium hydroxide octahydrate show ESR absorption at 90°K. (55), presumably because of removal of hydrogen ions by the solid. It is suggested that similar radical formation may occur at cell walls in biological systems.

TABLE 8

Electron spin resonance properties of free radicals

Radical (or Parent Substance)	Value of g	Width in Gauss*		Components	Separation in Gauss	References
		$\Delta H_{1/2}$	ΔH_{MS}			
Anthracene	(1?)					(325)
Anthracene negative ion (dilute solution)	2.00		10			(113)
Banfield and Kenyon's radical (s)	2.0057 ± 0.0002	18.4				(252)
	2.000		8.9			(113)
1,2-Benzanthracene negative ion (dilute solution)						(343)
Benzophenone anil sodium (dilute solution)	2.00		Several			(113)
Benzophenone sodium ketyl (in dioxane)	2.0031					(270)
p,p'-Benzhydrylyldiphenylbutane (n = 4 in formula V, p. 923)	2.0025 ± 0.0002		9.5, 14.0†			(516)
p,p'-Benzhydrylyldiphenylethane (n = 2 in formula V, p. 923)			13.0, 16.5†	Hyperfine splitting		(516)
p,p'-Benzhydrylyldiphenyl ether (formula VI, p. 923)	2.0031 ± 0.0002		7.5, 7.5†	Hyperfine splitting		(516)
p,p'-Benzhydrylyldiphenylmethane (n = 1 in formula V, p. 923)	2.0025 ± 0.0002		11.5, 10.5†	Hyperfine splitting		(516)
p,p'-Benzhydrylyldiphenylpropane (n = 3 in formula V, p. 923)	2.0025 ± 0.0002		16.0, 13.5†	Hyperfine splitting		(516)
p-Benzoquinhydrone adsorbed in $Ba(OH)_2 \cdot 8H_2O$	2.003 ± 0.001	Several				(55)
Beryllium benzoylacetonate ion (solution)				4		(411)
Bianthrone (s) (heated)	2.0036		10			(385)
p,p'-Biphenylenebis(diphenylmethyl)		15				(265)
Biphenylenetriphenylethyl (s)	2.00		5			(113)
α,γ-Bisdiphenylene-β-phenylallyl‡	2.0026	0.7	0.4			(605)
1,9-Bis(2-furyl)-5-oxo-1,3,6,8-nonatetraene	2 (and 1?)					(325)
Di(dimethylamino)diphenyl nitrogen (dilute solution)	2.00	Several				(113)
Difluorenyl nitrogen (in benzene)	2.00			10	0.9	(113, 603)
Dimesitylmethyl in benzene				2 groups	24	(287)
N,N-Dimethyl-N',N'-dideutero-p-phenylenediamine positive ion in D_2O				7 groups	8.5	(598)
2,6-Dimethyl-2,5,7-octatriene (alloöcimene)	(1?)					(325)
N,N'-Dimethyl-p-phenylenediamine positive ion (see also Wurster's Blue)				9 groups	9.5	(598)
m-Dinitrobenzene ion (dilute solution)	2.00		25§	8		(113)
Di-p-anisyl nitric oxide (s)	2.0066					(270)
	2.0063 ± 0.0005	31.4 (flat-topped)				(252)

Di-*p*-anisyl nitrogen oxide (solution)	2.0063	14				(251)
Diphenoquinone-*p*,*p*′-bisdiphenyl methide (formula II, p. 923)	2.0025 ± 0.0002		12.5, 12.5†	Hyperfine splitting		(516)
Diphenoquinone-*p*,*p*′-bisdixenyl methide (formula III, p. 923)			12.5, 12.5†			(516)
Diphenoquinone-*p*,*p*′-bisphenyl-α-naphthyl methide (formula IV, p. 923)	2.0025 ± 0.0002		12.5, 12.5†			(516)
2,2-Diphenyl-1-(2,4-dinitro-6-sulfophenyl)hydrazyl (0.002 *M* solution in dioxane)				9		(285)
1,9-Diphenyl-5-oxo-1,3,6,8-nonatetraene	2 (and 1?)					(325)
1,1-Diphenyl-2-picrylhydrazyl (s)	2.0036 ± 0.0002	2.70	1.9			(252)
1,1-Diphenyl-2-picrylhydrazyl (single crystal)	2.0035 to 2.0041					(270)
1,1-Diphenyl-2-picrylhydrazyl (0.002 *M* solution in benzene)		48§		5		(270)
Diphenylquinoxalinium chlorostannite (s)	2.0036 ± 0.0005	Weak line				(252)
Di-*p*-xenylphenylmethyl (s)	2.00	Several				(113)
20-Methylcholanthrene negative ion						(343)
N-Methyl-*p*-phenylenediamine positive ion				24	2	(598)
Naphthacene negative ion (dilute solution)	2.00		10			(113)
Naphthalene negative ion (in tetrahydrofuran)	2.00			28	1.2	(113, 587)
Nitrobenzene negative ion (dilute solution)	2.00		25§	10		(113)
2-Nitrophenanthrophenazinium chlorostannite (s)	2.0032 ± 0.0002	Weak line				(252)
Pentaphenylcyclopentadienyl (s)	1.95					(328)
Peroxylamine disulfonate ion (0.001 *M*)	2.0054	0.5		3	13	(113)
Phenanthraquinhydrone on $Ba(OH)_2 \cdot 8H_2O$						(55)
Phenanthrophenazinium chlorostannite (s)	2.0033 ± 0.0002	6.4				(252)
Phenazinium chloride (s)	2.0031 ± 0.0002	Weak line				(252)
p-Phenylenediamine (positive ion)				15	2	(598)
p-Phenylenediamine in methyl methacrylate (on illumination)						(56)
N-Picryl-9-aminocarbazyl (single crystal)	2.0024 to 2.0041			2		(118)
N-Picryl-9-aminocarbazyl (polycrystalline)	2.0036		7			(118)
N-Picryl-9-aminocarbazyl (0.002 *M* solution in benzene)				7		(285)
Porphyrexide (s)	2.0064 ± 0.0002	17.0				(252)
Porphyrindene (s)	2.001		10.7			(113)
Porphyrindene	2.0057					(270)
Porphyrindene	2.0057 ± 0.0002	25.2				(252)
Semiquinone ions	2.006					(572)
Sodium trimesitylboron (in tetrahydrofuran)				4	14	(603)
Spirocyclohexylporphyrexide	2.0065					(270)

TABLE 8—*Continued*

Radical (or Parent Substance)	Value of g	Width in Gauss*		Components	Separation in Gauss	References
		$\Delta H_{1/2}$	ΔH_{MS}			
Sulfur (liquid)	2.02	15 at 190°C. 35 at 375°C.				(178)
Tetramethylbenzidine formate (s)	2.00		3.4			(113)
Tetramethylbenzidine perchlorate	2.00		Several			(113)
Tetramethyl-*p*-phenylenediamine in methyl methacrylate (on illumination)	2.001 ± 0.002					(56)
Tetraphenylhydrazine perchlorate (dilute solution)	2.00		Several			(113)
Tetraphenylstibonium peroxylamine disulfonate (s)	2.00		100			(113)
Tetraxenyl-*p*-xylylene (formula I, p. 923)						(516)
Thymoquinhydrone on $Ba(OH)_2 \cdot 8H_2O$						(55)
1,3,5-Trinitrobenzene negative ion	2.00		25§	8		(113)
2,4,7-Trinitrofluorenone negative ion (dilute solution)	2.00		25§			(113)
Triphenylamine perchlorate (s)	2.003		2			(113)
Triphenylmethyl (0.001 *M* in benzene)				18 groups of multiple lines		(287)
Tri-*p*-anisylaminium perchlorate			0.68			(116)
Tri-*p*-aminophenylaminium perchlorate			0.33			(116)
Tris-*o*-anisylmethyl (dilute solution)	2.00					(113)
Tris-*p*-nitrophenylmethyl (s)	2.0037		0.7			(113)
Tris-*p*-xenylmethyl (s)	2.0031		5.7			(113)
Tri-*tert*-butylphenoxyl	1.99					(371)
Tri-*tert*-butylphenoxyl (s)	2.0052	7.7				(605)
Violanthrene	2.00	13				(618)
Violanthrone	2.00	15				(618)
Wurster's Blue (as ferricyanide) (s)	2.0028 ± 0.0002	3.7				(252)
Wurster's Blue (as picrate) (s)	2.0033 ± 0.0002	6.0				(252)
Wurster's Blue (in water) (*N,N,N',N'*-tetramethyl-*p*-phenylenediamine positive ion)				13 triplets	7.4	(598)
Wurster's Blue perchlorate (s)	2.003		2.7			(113)
Wurster's Red (*N,N'*-dimethyl-*p*-phenylenediamine positive ion)				27	2.8	(252)
Biological materials	2.00					(125)
Boron glass (γ-irradiated)		1–2		4	10–15	(617)
Chlorine dioxide (dilute solution)	2.00		50			(113)
H radicals in irradiated $HClO_4$, H_2SO_4, H_3PO_4	2.0022 to 2.0025			2 lines each with 2 satellites		(345, 622)
γ-Irradiated glass	2.0, 4.00		30			(122)
γ-Irradiated glass (boron-free)	2.0, 4.00					(617)

γ-Irradiated lead glass	2.00, 4.00			2		(617)
γ-Irradiated lime glass	2.00, 4.00			2		(617)
γ-Irradiated borosilicate glasses	4.00					(617)
Irradiated ice (H_2O) (hydrogen atoms)	2.0	6		2	30	(519)
Irradiated ice (D_2O) (deuterium atoms)		2		3	5	(519)
Irradiated H_2O–H_2O_2 ice (OH)				2	12–15	(519)
Irradiated amino acids (pile)				3		(123)
Potassium dissolved in liquid ammonia (25°C.) (solvated electrons)	2.0012 ± 0.0002	0.02 to 0.06				(268)
Lithium (in ethylenediamine)		0.6				(399)
Lithium (in methylamine)		0.4				(399)
Glycol dimethacrylate and methyl methacrylate		100§				(164)
Silica (vitreous)	2.004 ± 0.004					(519)
Phosphorus (atomic; gas phase)			1 gauss	2	20	(141)

* $\Delta H_{1/2}$ = full width at half-height; ΔH_{MS} = full width between points of maximum slope.

† Line widths observed immediately after the synthesis and the final value seen before complete disappearance.

‡ Tentative structure.

§ Overall width of multiple line.

The particular merit of these substances is that the hyperfine structure is readily interpretable, arising from only a small number of protons in contrast to the triphenylmethyl type of radicals or radicals containing both nitrogen and hydrogen. Triphenylmethyl shows eighteen groups of hyperfine lines (287).

Molecular complexes of aromatic diamines and quinones show ESR absorption, presumably because of charge transfer. The molar susceptibility of *N*,*N*,*N*′,*N*′-tetramethyl-*p*-phenylenediamine with tetrabromobenzoquinone was 40, the largest observed value (293).

B. Hydrocarbon negative ions

Another type of free radical is the negative ion formed by the reaction of sodium with aromatic compounds such as naphthalene:

$$C_{10}H_8 + Na \rightarrow C_{10}H_8^- + Na^+$$

This reaction is known to be slow except in good electron-transfer solvents such as 1,2-dimethoxyethane and tetrahydrofuran (495), but there was a disagreement as to whether one or two electrons were involved from as many sodium atoms.

The answer given by ESR experiments supports the one-electron process (343), and as a result of competition experiments, a scale of electronegativities has been established. For naphthalene, the reaction with a sodium dispersion in one of the above solvents proceeds essentially to completion. Now if to the naphthalene ion-radical one adds anthracene in the same concentration, one observes that equilibrium is displaced strongly in favor of the anthracene ion-radical, showing it to be the more electronegative. As a result of such competition experiments, a scale of electronegativities is being established, the order of increasing electronegativity in tetrahydrofuran being biphenyl, phenanthrene, naphthalene, anthracene, and naphthacene (600). (Benzene would appear first in the list, but there is uncertainty as to whether ESR absorption is due to $C_6H_6^-$ or an impurity.) Such an operational definition of electronegativity is appealing, for one simply asks which of two molecules in open competition is the more likely to acquire an available electron.

Recent susceptibility measurements on hydrocarbon negative ions support the idea of one-electron radicals which do not associate, though anthracene and phenanthrene are said to form divalent, diamagnetic ions also (114). Molecular orbital calculations indicate that the singly charged negative ion should be stable by about 3 e.v. to disproportionation into hydrocarbon and doubly charged ions, both in the gas phase and in solution (261).

An interesting application of the hydrocarbon radical-ion studies results from an investigation of line broadening in the presence of neutral molecules. In tetrahydrofuran the naphthalene ion, $C_{10}H_8^-$, shows a hyperfine structure of at least twenty-eight lines arising from interactions with the protons (587), but upon the addition of naphthalene the lines are broadened eventually to a single line. The transfer of an electron from an ion to a neutral molecule limits the lifetimes of the states which give rise to the hyperfine structure and hence one

gets an uncertainty-principle broadening. Mean lifetimes of the order of 10^{-6} sec. were obtained and a second-order rate constant was calculated.

C. Biradical and triplet molecules

ESR absorption with $g = 1$ has been reported in anthracene and 2,6-dimethyl-2,5,7-octatriene (325), but this result has not been confirmed. In impure anthracene one gets a resonance line with $g = 2$, but on purification the line disappears. One will be inclined to regard with suspicion the report of ESR absorption in compounds which do not theoretically justify the hope of measurable dissociation, biradical or triplet formation. Calculations (151) on conjugated systems for the energy separation ΔE between singlet and triplet states will be helpful in deciding on probabilities of ESR observation. It has been suggested that if ΔE is no larger than about 1.7 kcal, such triplet states should be detectable. In view of ESR sensitivity, this figure is probably too low. The question of a possible radical state in the Chichibabin hydrocarbon $(C_6H_5)_2CC_6H_4C_6H_4C(C_6H_5)_2$ was unmistakably settled by detection of ESR absorption (265). Early susceptibility measurements were interpreted as indicating no (less than 2 per cent) radical (372), while ortho–para conversion experiments gave 9.7 per cent (493). The ESR data are interpreted as giving 4–5 per cent radicals, in excellent agreement with the 4 per cent figure one obtains at 300°K. from the calculated (151) singlet–triplet separation of 2500 cal.

Porphyrindene (252) is of interest because it shows a greatly diminished susceptibility at low temperatures (373), being a thermally excited singlet–triplet system.

The following series of compounds:

I. $(Xe)_2CC_6H_4C(Xe)_2$ $\quad Xe = C_6H_5C_6H_4—$

II. $(C_6H_5)_2CC_6H_4C_6H_4C(C_6H_5)_2$

III. $(Xe)_2CC_6H_4C_6H_4C(Xe)_2$

IV.
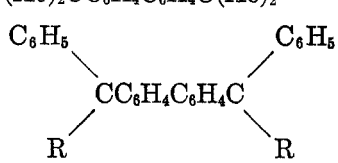
$R = \alpha$-naphthyl

V. $(C_6H_5)_2CC_6H_4(CH_2)_nC_6H_4C(C_6H_5)_2$ $\quad n = 1$ to 4

VI. $(C_6H_5)_2CC_6H_4OC_6H_4C(C_6H_5)_2$

has shown ESR absorption, with g-values and line widths listed in table 8 (516). Some of these are true biradicals, i.e., the unpaired electrons are entirely independent, whereas others have coupled electrons with spin 1. Most of these compounds were previously believed not to exist in radical form (370).

Curiously, although much effort has been expended in looking for optically excited triplet states, none has yet been reported. With the use of high-intensity flash technique possibly coupled with the use of low temperatures such triplet

states will likely be found, and the ESR measurements will be most valuable in giving quantitative as well as qualitative information on concentrations of excited molecules.

D. Radicals in Lewis acids

The literature of organic chemistry is full of references to deeply colored concentrated sulfuric acid solutions of conjugated organic compounds containing oxygen or sulfur. Similarly, many such compounds give deeply colored solutions in ether solution with aluminum chloride or upon heating with solid aluminum chloride. In a number of cases of both types of systems free radicals have been found to be present (246). Bianthrone and fluorenone show ESR absorption with aluminum chloride in anhydrous ether. Those showing ESR absorption in concentrated sulfuric acid include bianthrone, fluorenone, anthraquinone, triphenylmethyl peroxide, thiophenol, *p*-thiocresol, thio-β-naphthol, diphenyl disulfide, and diphenylene disulfide as well as numerous others. The radical concentration may be 10 per cent or more of the reacting substance.

In the case of bianthrone in sulfuric acid, it is presumed that a proton adds to one or both oxygen atoms and this ion may exist in a biradical state as follows:

$$^{+}HO(C_{14}H_8)=(C_{14}H_8)=O \rightarrow {}^{+}H\dot{O}-(C_{14}H_8)-(C_{14}H_8)-\dot{O}$$

The biradical is apparently stabilized by the proton, since there is about ten times as large a concentration of the biradical form as is estimated to be present in inert solvents at room temperature (246, 543). ESR absorption lines of thiophenols in sulfuric acid are often complex and involve more than proton addition followed by radical formation. As an example, thiophenol shows two well-resolved lines shortly after mixing with concentrated sulfuric acid (figures 21e and 21f). One line has roughly seven times the area of the other, but the weaker slowly diminishes in intensity and disappears after a number of days, while the stronger line has been observed after 22 days. This can only mean that more than one radical is present (605). The lines in other substances often show hyperfine structure due to protons and this frequently changes markedly with time, thus helping to identify the radicals responsible for them. Much quantitative work is required to identify intermediates present in strong sulfuric acid, as well as the final products.

E. Thermochromic compounds

Numerous static susceptibility measurements have shown that a variety of disulfides dissociate into radicals on heating (338, 375). Increasing conjugation lowers the temperature required for the formation of detectable radicals. In solutions of high-boiling solvents such as anisole the temperature required is considerably less than that for the solid. The radicals should and do show ESR absorption (605). Earlier, solid bianthrone had been reported to show ESR absorption on heating to 265°C., the paramagnetism persisting long after it had cooled to room temperature (385). In solvents, ESR absorption of bianthrone in biradical form was found at temperatures of 88–200°C. The *g*-factor is 2.0036.

On the basis of absorption spectra, the high-temperature form of bianthrone is concluded to be a biradical state (204, 543). Since the thermochromic absorption band in the visible region obeys Beer's law, there is no dissociation involved

Presumably in bianthrone at elevated temperatures, rotation about the central bond occurs so that the two ring systems are no longer coplanar (357). Careful detailed supporting evidence should be adduced to substantiate qualitative observations on a growing list of thermochromically paramagnetic substances. These data should include enthalpy, free-energy, and entropy changes.

Progressively increasing ESR absorption in liquid sulfur has been found in the interval 190°C. to 375°C., and is attributed to broken S—S bonds in linear polymers. A radical concentration of 10^{-5} mole/l. was found at 200°C. The line width increases from 15 to 35 gauss in the interval (178).

F. Unstable free radicals

In principle, ESR absorption should be an excellent method for directly measuring concentrations of free radicals in the course of a chemical reaction, using a stirred-flow technique if necessary. The possibility of detecting radicals of short life is contingent upon their concentration, line width, and lifetime. These factors are necessarily interrelated. At present, one is able to detect 10^{-11} mole of a radical with a 1-gauss line width. Assuming that the line width were 10–50 gauss, the lifetime should be longer than 10^{-6} sec. Using a 0.5-cc. sample, one should be able to measure absorption at 10^{-5} molar. The application to such systems remains a challenge to chemists.

XIX. COLOR CENTERS

The absorption bands of ionic crystals which contain lattice imperfections has been the subject of a large number of papers. The F-center of the alkali halides is presumably an electron trapped in an anion vacancy. To some degree this electron will be associated with an atomic orbital of each of the six alkali atoms which surround it (273, 376). It should be capable of orientation in a magnetic field to give ESR absorption and indeed it does (263, 266, 488, 550). The line in potassium chloride colored by excess potassium is broad (ΔH_{MS} = 54 gauss (307)) and is Gaussian in shape with g = 1.995 (263, 307). If its width were to be determined by dipolar interaction the width would be 0.1 gauss and the shape Lorentzian for randomly distributed F-centers (307). The effect has been observed for lithium fluoride (263, 290, 423), lithium chloride (423), potassium bromide (266, 307, 550), and sodium chloride (307, 423). A reported spectrum of nineteen lines in lithium fluoride (486) has not been verified (290, 423). Assuming that the cause of line broadening is the interaction of an F-center electron with the neighboring K^{39} and K^{41} nuclei (both of spin $\frac{3}{2}$), line widths are calculated in terms of a fractional effective s-character ξ. The latter is the ratio of the square of the wave function at a nucleus to that of a 4s-electron in a free atom. Using observed line widths, ξ appears to be about 0.6 (307). Since K^{41} has a smaller nuclear moment, it should show less hyperfine interaction and give a narrower ESR line. This is verified by experiments on $K^{41}Cl$ (99.21 per cent of

the potassium as K^{41}) irradiated with x-rays, which gives a line width of 36 gauss. If only the immediately neighboring potassium ions interacted, the line width should have been 31 gauss. Additional data on sodium chloride and potassium bromide are in agreement with the general predictions of this line-broadening mechanism. It is hoped that in cesium or rubidium halides hyperfine structure of F-centers may be resolved. Additional evidence for this line-width interpretation comes from saturation experiments (421), which give excellent agreement between observed and calculated values of absorption and dispersion of F-centers in potassium chloride. The type of broadening in the alkali halide color centers has been called inhomogeneous and arises in general from such factors as hyperfine interaction, anisotropy broadening, dipolar interaction between nuclei of different precession frequencies, and from inhomogeneities of the applied magnetic field (421). An inhomogeneously broadened line does not change shape on saturation. The more usual homogeneous broadening arises from such factors as dipolar interaction or large radiofrequency fields which change the line shape according to equation 43. It is pointed out (421) that the Kramers–Kronig relations do not hold for saturable systems, so that one cannot use them to calculate χ' from χ'' or *vice versa* when H_1 is large. Further, the thermal relaxation time t_1 was found to be 2.5×10^{-5} sec., so that relaxation broadening does not determine the line width. The g-value of 1.995 is interpreted on the same model of the excess electron shared among adjacent cations (292). Attempts have been made with partial success to compute energy levels for F-centers (142, 330).

One of the important recent advances in the field of semiconductors is the discovery of ESR absorption lines in both n- and p-type silicon (161, 162, 422, 608). At low n-type impurity concentrations the lines show the hyperfine splitting to be expected from the nuclear spin of the atom donating the electron, with the expected number of lines being observed for P ($I = \frac{1}{2}$), As ($I = \frac{3}{2}$), Sb^{121} ($I = \frac{5}{2}$), and Sb^{123} ($I = \frac{7}{2}$). At higher concentrations the lines became single and narrow, the same line having earlier been attributed to conduction electrons in silicon (422). An attempt has been made to calculate the magnitude of the splitting (348). Certain weak lines of arsenic are attributed to transitions in which the donor nucleus flips simultaneously with the electron. Li^7 in silicon gives a single line which is inhomogeneously broadened. This is interpreted as meaning that the electron spends more time with silicon than with lithium (256). An attempt has been made to treat spin–orbit coupling in such semiconductors (153).

XX. RADIATION DAMAGE

ESR absorption in strongly irradiated materials is the subject of an increasing number of investigations. A variety of borosilicate glasses showed four lines 1–2 gauss wide in a 10–15 gauss interval (617) after γ-irradiation. Boron-free glasses give a line with $g = 2.0$. The hyperfine splitting is presumably due to B^{11}, which has $I = \frac{3}{2}$, but the nature of the "color center" responsible for the absorption has not been elucidated. The liberation of alkali metal atoms has been

suggested (122). With lime-glass samples the ESR absorption was proportional to the optical density, diminishing proportionately with bleaching. This is perhaps not surprising if trapped electrons are responsible for both ESR and optical absorption. Lattice defects in neutron irradiated diamond give an ESR line with $g = 2.0028$ and an eventual width of about 100 gauss, decreasing in width with increasing temperature (197). Electron-irradiated diamond gave a similar behavior. Additional weak lines are attributed to paramagnetic impurities. X-irradiation of quartz gave a six-line pattern presumably arising from Al^{27} impurity of spin $\frac{5}{2}$ (197). X-ray irradiation of methyl methacrylate polymers gives rise to ESR absorption with a multiple line structure (487). A similar structure is observed when such polymers are irradiated with a mercury vapor lamp (164).

Irradiation of amino acids, sugars, ascorbic acid, nylon, and polythene in a pile gave rise to ESR absorption persisting for hours or days (123, 563). Three lines with a ratio of 1:2:1 and $g = 2.00$ were observed, the separation of the outer components from the central line being 20 gauss. From the similarity of the lines in polymethyl methacrylate and amino acids, it was suggested that radicals of the form

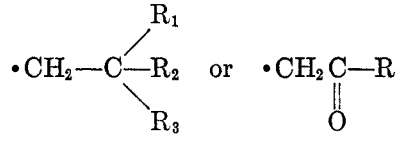

were present. The hyperfine splitting is attributed to the two protons of the methylene group. Irradiation of N^{15}-enriched compounds gave the same lines as the compounds with N^{14}, although the spins are respectively $\frac{1}{2}$ and 1. Apparently the unpaired electron density at the nitrogen nucleus must be small (563). Sucrose and various amino acids irradiated with x-rays give indefinitely stable free radicals if kept at room temperature (124).

In the irradiation of perchloric, sulfuric, and orthophosphoric acids with γ-rays, atomic hydrogen appears to be formed, since a doublet is observed with just the same splitting as for gaseous hydrogen atoms, the g-factors being 2.0023 ± 0.0002 (345). Each of the doublet lines has two satellite lines removed by just the proton resonance frequency for the applied field. The satellite lines apparently arise from the flipping of the proton dipole in conjunction with an electronic dipole. Additional evidence for this view comes from the ehancement of the satellite lines relative to the principal ones upon saturating the electronic resonance (622). Using $H_2SO_4 \cdot D_2O$, a triplet was observed with separations the same as for gaseous deuterium atoms. This behavior indicates the lack of binding of the free atoms to their neighbors. Water on γ-irradiation at 77°K. gives a symmetrical doublet with $g = 2.0$ and a separation of 30 gauss, while deuterium oxide gives a triplet of 1:2:1 ratio and 5-gauss separation (356, 519). These are due to hydrogen and deuterium atoms, respectively, but the splitting is many times smaller than for the gaseous atoms, showing considerable interaction with the surroundings. Another doublet and triplet found at 4°K. in

water and deuterium oxide is attributed to OH or OD radicals. A similar doublet is shown by H_2O_2–H_2O at 77°K. and is likewise attributed to OH. Irradiation of formic acid gives a doublet attributed to OH, while ammonia gives a doublet and a triplet, apparently from H and NH_2 (356). ESR absorption disappears on warming the samples. A number of ESR lines appear on x-irradiation of H_2S and N_2H_5Cl, but the data are insufficient for unequivocal interpretation (22).

ESR experiments thus verify the existence of "cages" (389) for free radicals. Some of these, like the H and OH radicals, require refrigeration for preservation, while others may be kept indefinitely at room temperature.

Phosphorus atoms produced by dissociation of P_4 in an arc show an ESR doublet from hyperfine splitting by the P^{31} nucleus ($I = \frac{1}{2}$). A small contribution of the excited $3s^1 3p^3 4s^1$ state to the $3s^2 3p^3$ ground state would be sufficient to give the observed 20-gauss splitting (141).

XXI. ALKALI METALS IN LIQUID AMMONIA

The narrowest ESR line yet observed ($\Delta H_{MS} = 0.02$ gauss at 24°C. at low concentrations) occurs in liquid ammonia solutions of the alkali metals sodium and potassium, with $g = 2.0012$ (264, 267). It was observed first at microwave and then later at radio frequencies (185, 268, 384). The width for potassium is nearly constant up to concentrations about 0.5 M and then increases rapidly. The signal amplitude diminishes on cooling below room temperature. The electrons given up by the sodium atoms are presumed to reside in cavities of radius about 4–5 Å. (300, 344), much smaller than the 10 Å. radius suggested earlier (390). They are supposed to be in equilibrium according to the equation (300):

$$2\epsilon \rightleftharpoons \epsilon_2 + 0.2 \text{ e.v.}$$

Here ϵ_2 represents two paired electrons within a cavity, while 2ϵ represents two electrons in separate cavities. In order to establish whether there was any unusual diamagnetism of the system, and to ascertain the cavity radius, the paramagnetic portion of the susceptibility was separately evaluated from ESR absorption intensities (268), using the Kramers–Kronig relations. Combining these data with previous static susceptibility measurements (165, 262), and correcting for the solvent, one can set the upper limit of 4 Å. to the radius of the cavity in which one or two electrons could be found (300). The susceptibility is approximately given by the relation

$$\chi = \left(\frac{N'}{n}\right)^{1/2} \frac{\mu_B^2}{kT} \exp(-W/kT)$$

where n is the number of solute atoms, N' the number of possible lattice sites, and W the difference in energy between the vacancy levels holding two electrons and one electron. The dependence of χ on the $\frac{1}{2}$-power of the solute concentration is roughly fitted by the susceptibility data (300) for potassium at 220° and 240°K. if $W = 0.1$ e.v.

The observed line widths can be made to look reasonable (268, 300), but there are too many adjustable parameters at present to give rigorous calculation. The

dipolar contribution to line width of protons to ϵ-centers, and the interaction of the latter, should be appreciable in solutions sufficiently concentrated and at a low enough temperature to give a high viscosity. However, the rotation and diffusion of ammonia molecules and the diffusion of ϵ-centers narrows the line from its dipolar width of 2.2 gauss at 0.1 M (309) to its observed value of 0.05 gauss width at 33°K., which is twice that observed at 24°K.

Numerous suggestions have been made to use these solutions for measurement of very low fields (such as that of the earth) because of the narrow line width.

Frozen solutions of metals in ammonia give ESR absorption with much wider lines, and these appear to arise from the metallic particles precipitated from solutions (160). The metals used were lithium, sodium, potassium, and cesium.

XXII. METALS

The conduction electrons at the top of the Fermi distribution displace the NSR frequency to higher values in metals as compared with salts, and they show their paramagnetism by ESR absorption (198). The paramagnetic part of the susceptibility has been measured for lithium as $2.0 \pm 0.3 \times 10^{-6}$ (489). The procedure is an interesting combination of ESR and NSR absorption. The same resonance probe used at 17 Mcps to trace out the nuclear resonance line at 6 gauss is used at 10,000 gauss, all factors except field being kept constant. The special form of the Kramers–Kronig equations

$$\chi_0 = \frac{2\gamma}{\pi\omega} \int_0^\infty \chi'' \, dH$$

was applied to get the paramagnetic susceptibility of the conduction electrons from the ratio of areas under ESR and NSR curves, using a calculated value of χ'' for Li^7 nuclei. Attempts have been made with fair success to calculate the electronic susceptibility (420). To avoid large eddy currents which would preclude observations in a tuned cavity, the samples are powdered or formed into thin films or colloidally dispersed. To date ESR absorption has been reported in lithium (103, 207, 480), beryllium (157), magnesium (480), sodium (198, 207, 340, 480, 526), aluminum (480), potassium (158, 480), bismuth (480), antimony (480), mercury (480), cadmium (480), titanium (5), vanadium (5, 480), chromium (5, 480), manganese (5, 480), niobium (5), lanthanum (5), cerium (5), cesium (158), tungsten (5, 480), tantalum (480), platinum (480), palladium (480), ruthenium (480), iridium (480), and osmium (480).

Except for lithium, sodium, beryllium, and perhaps potassium and cesium, it must be established that the observed effect was due to the metal itself rather than to glass or spurious cavity resonance (158, 207). An apparent ESR absorption from aluminum was traced to an impurity (158). The reported line widths for other metals appear unduly large. From the known sensitivity of the detection apparatus, it was estimated that in aluminum, magnesium, palladium, and tungsten the value of t_1 (which is equal to t_2 for the metals) must have been less than 5×10^{-10} sec. (158). Perhaps the best test of the genuineness of the observed metal resonances is agreement of observed with calculated line shapes. For sam-

ples which are thick compared with the depth of penetration (skin depth) of the radiofrequency field, the absorption lines are very unsymmetrical and for sufficiently long t_1 values even antisymmetrical (152). Lithium, sodium, and beryllium fit the calculated shapes very well (158). Early measurements gave 40 gauss for the line width of lithium, while the latest value is several tenths of a gauss. The relaxation times may be directly obtained from the line width, being 2.7×10^{-7} sec. for lithium, 2.8×10^{-8} sec. for beryllium, and 5×10^{-9} sec. for potassium at 4°K. The relaxation times (and therefore line widths) of lithium and beryllium are temperature-independent, while t_1 of sodium varies inversely with temperature. An estimate of t_1 for sodium (397) on a model of interaction of electrons with fields produced by translation of other electrons gives values much larger than observed (158). A spin–orbit coupling mechanism (153) predicts t_1 to decrease with increased spin–lattice coupling. One will perhaps not find ESR absorption with the heavy metals which have large spin–orbit coupling.

The g-values are very close to the free-electron value of 2.0023 (except for cesium with $g = 1.93$), being 2.0023 for lithium, 2.0032 for beryllium, and 2.0012 for sodium (158). The latter value remains constant from 4°K. to 300°K. (526). Calculations of g-values have been rather successful (23, 94, 614).

Among the narrowest ESR lines yet obtained are those found in lamellar graphite samples containing lithium, sodium, potassium, rubidium, or calcium (and in some cases ammonia) at optimum concentrations (518). The relation of the properties of these systems to those of the pure metals remains to be established.

ESR absorption has been found in graphite and graphitized materials (105, 106, 107, 241), with $g = 2.00$ and a width of $\sim$5 gauss. The number of absorbing centers in a "pure" graphite sample was found to be greater than the concentration of the impurity, so that the ESR absorption is a property of the graphite itself (241). The absorbing centers are apparently conduction electrons.

The oxidation of graphite in sulfuric acid gives rise to a new ESR line only 45 milligauss wide under most favorable conditions. Tentatively it is assigned to positive holes trapped at bisulfate ions (241).

An apparently unrelated and much broader absorption appears in coals and in carbons formed at low temperatures (48, 108, 154, 271, 272, 566). A variety of carbohydrates charred below 600°C. show a line 8 ± 2 gauss wide with $g = 2.0030 \pm 0.0003$ from 40 to 36,000 Mcps and 20° to 290°K. Heating above 600°C. destroyed the absorption. The explanation offered is that carbon rings are formed in charring and that below 600°C. a few of the rings have not been closed. About one carbon in 2000 appears to act as a free radical. The marked increase in electrical conductivity above 600°C. is adduced in support of the idea of perfection of rings by heating. Some cokes have an unexplained strong absorption at $g = 6$ (108).

XXIII. ESR AT LOW FIELDS

1,1-Diphenyl-2-picrylhydrazyl at 15 Mcps shows a Lorentz line, but as the resonant field (and frequency) are lowered, the line becomes asymmetrical. The

low-field side becomes progressively weaker and finally disappears (183, 186). The remaining portion of the line is reminiscent of non-resonant paramagnetic relaxation experiments (129, 194, 353). With the peak centered at a low value of the field, there will yet be absorption at zero field and the maximum will not coincide with the center of resonance (332). In a variation of the same experiment, one may use a fixed frequency and sweep from positive to negative field values and observe two absorption lines. As the frequency is reduced, the separation of the two peaks decreases and eventually a single peak is observed at the central position (116). If one takes the ratio of frequency to applied field, the apparent value of g increases for the peak of the (asymmetrical) line. For example, assuming $g = 2.0036$ for 1,1-diphenyl-2-picrylhydrazyl at 15 Mcps, the value increases to 2.13 at 2.5 Mcps (183). However, it is a questionable procedure to consider only the precession about the steady field when the latter is less than the line width. One approach is to consider the effect of the counter-rotating radiofrequency fields, both of which make a contribution to the line width (38). The line shape is predicted by modified Bloch equations, using for t_2 the value obtained at 15 Mcps (116).

Statistical and thermodynamic treatments of the absorption in weak fields have been proposed (183, 501).

XXIV. THE OVERHAUSER EFFECT

Many interesting radiation experiments would be possible if one could align at least 10 per cent of the nuclei in a given sample. Except at temperatures near 0°K., kT is much larger than the interaction energy of nuclei with attainable magnetic fields and hence the degree of alignment is small. However, considerable alignment may be achieved at room temperature by use of the Overhauser effect (398). One uses an atom with both a nuclear and an electronic spin moment and an appreciable interaction between them such that thermal relaxation of nuclei is principally governed by the $(\mathbf{I}\cdot\mathbf{S})$ interaction. The Hamiltonian representing this interaction may be written (406)

$$\mathcal{H} = a\mathbf{I}\cdot\mathbf{S} = aI_zS_z + \tfrac{1}{2}(I_+S_- + I_-S_+)$$

where $I_+ = I_x + iI_y$, and the other terms are similarly defined. The term in I_zS_z implies the contribution of a local field which will displace the resonant field of one dipole type by an amount which depends on the polarization of the other. This shift of resonant field of nuclei in metals from that in their compounds has been described in Part I. The second term implies non-zero values of transition probability for spin exchange between electrons and nuclei.

Assume that a nuclear dipole of spin $\frac{1}{2}$ is instantaneously antiparallel to an electronic dipole. If the nucleus flips, the coupled electron will do so also, changing the energy of the pair by $2(\mu_B - \mu_I)H$. To conserve energy, the negative of this quantity must be exchanged with the environment. The conservation of energy is made possible by a continuum of electronic levels in metals or by emission or absorption of a lattice quantum (324). In an independent process the electronic dipole will be restored to its original orientation with energy change $-2\mu_BH$ so

that the net energy change of the environment is $2\mu_I H$ (308). The Boltzmann factor governing the distribution between the states of lower and higher energy for the nucleus will be:

$$\frac{N_+}{N_-} = \exp(-2\mu_I H/kT)$$

Here N_+ and N_- refer to the number of nuclei aligned with and against the field. When a strong radiofrequency field is applied at the ESR frequency, the populations of the two electron states will be equalized and the radiofrequency field now provides the relaxation of the electronic dipole. Upon reversing the nuclear dipole the net energy change of the environment is $-2(\mu_B - \mu_I)H$. Now

$$\frac{N_+}{N_-} = \exp(-2(\mu_B - \mu_I)H/kT) \approx \exp(-2\mu_B H/kT)$$

so that the population difference of the nuclear levels is increased by the factor μ_B/μ_I. This means that the nuclei are aligned as if they possessed the electron moment μ_B instead of their thousandfold smaller value μ_I. Thus if one observes the NSR signal simultaneously, there should be a great enhancement. This effect is strikingly shown by Li^7, which shows no detectable NSR line before the saturating ESR field is turned on, but afterwards the line appears strongly (103). The enhancement of alignment was of the order of 100. The effect has also been observed with 1,1-diphenyl-2-picrylhydrazyl (39). It has been suggested that nuclear polarization might be observed with F-center saturation (324). Enhancement of proton resonance in concentrated solutions of metals in liquid ammonia is said to achieve the theoretical value (513).

When the electron spin states are equally populated, the shift of nuclear resonance frequency should be zero, while the electron resonance frequency should be displaced when the nuclei are polarized.

One major obstacle to the practical use of this effect at low temperatures is the necessity for dissipating a large amount of radiofrequency energy from the sample. A suggested application is the detection of NSR absorption from minute samples of radioactive metals (406).

The effect has been described in thermodynamic and statistical-mechanical terms (95).

XXV. MISCELLANEOUS APPLICATIONS OF ELECTRON SPIN RESONANCE

Biologists have shown considerable interest in the discovery of ESR absorption in a variety of plant and animal tissues and natural products (125). The absorption intensity is enhanced by irradiation, growth, or in some cases by heating. The absorbing centers, which appear to be free radicals, had long or indefinite lifetimes. The line width is of the order of 5–10 gauss. This work should be extended to rather less complex systems involving native preparations rather than lyophilized material. Because of the dielectric absorption of water, it will be necessary to use high-power sources, although these may cause undue heating of the samples. Nevertheless, if even a very small fraction of the biologically representative systems actually do show stable free radicals, this work will be-

come of great importance. Microwave plumbing will then become standard biological research equipment.

Free radicals have been suggested as magnetically dilute coolant substances for adiabatic demagnetization. 1,1-Diphenyl-2-picrylhydrazyl (DPPH) appears to be superior to Banfield and Kenyon's radical, because it has less exchange interaction (187, 236, 242). The Curie–Weiss Law is obeyed by both from liquid helium to room temperatures, with a Weiss constant of 0.1° for DPPH and 1.5° for the Banfield and Kenyon radical (187, 236, 512).

ESR absorption in various samples of glass has been found with g-values of approximately 2, 4, 6, and 7 (122, 482, 483, 617). Vitreous silica shows absorption with $g = 2.004$. Impurities, quadrupole interactions, hyperfine coupling with nuclei, liberation of alkali atoms, or formation of electron holes are variously invoked to explain the absorption. The last cause is doubtful, since working the glass does not change the spectrum. Studies of some glasses containing known impurities show the expected hyperfine splitting of the $g = 2$ line (482).

Hyperfine structure has been applied to the determination of dissociation of metal complexes (119). Manganous ions in very dilute solution give a characteristic six-line structure (184, 488, 551), the amplitude of which is greatly diminished on addition of complex-forming substances. Calculated dissociation constants compare favorably with those obtained by other methods. Substances used include glucose phosphates, malonic acid, glycylclycine, and histidine. The hyperfine splitting is attributed (2) to a contribution of the excited state obtained by promoting one 3s-electron to a 4s level to give $(3s)^1(3p)^6(3d)^5(4s)^1$ instead of $(3s)^2(3p)^6(3d)^5$. It is assumed that the 4s-electron is involved in complex formation and therefore cannot contribute to the splitting. Static susceptibility measurements indicate only changes in the number of 3d-electrons and indicate bond formation only when such electrons are involved. Thus by ESR absorption one has another operational criterion of covalent-bond formation.

XXVI. ELECTRON SPIN RESONANCE *vs.* STATIC SUSCEPTIBILITY MEASUREMFNTS

The advantages of electron spin resonance over static susceptibility studies are as follows:

1. In the observation of free radicals, the molecules are usually highly diamagnetic and the presence of an unpaired electron merely diminishes the observed diamagnetism, so that one must make assumptions as to the diamagnetic correction. Often this correction is made from measurements on a closely related stable molecule or from Pascal's constants. However, the diamagnetism of the free radical may be considerably enhanced by resonance effects (498, 606), so that many reported degrees of dissociation are too small. Diamagnetic corrections in some cases have been in error by at least 60 per cent (498). In looking for free radicals in concentrations of less than several per cent, one may not be able to establish even qualitatively the presence of free radicals by susceptibility methods. The observation of an absorption line or its derivative is positive evidence of the presence of paramagnetic substance, though it may be present in amounts approaching 10^{-11} mole. Table 8 includes six compounds established by ESR measurements to be radicals in contradiction of susceptibility data.

2. Not only is the observed susceptibility the sum of diamagnetic and paramagnetic terms, but the latter may be the sum of effects due to several species or to the same species in non-equivalent positions in a crystal, so that anisotropy effects may be very difficult to interpret from susceptibility measurements. Each type of center in resonance will show its own characteristic absorption independent of the presence of impurities.

3. Susceptibility measurements on a free radical can give only an effective magneton number. Resonance absorption allows g to be calculated unequivocally from the ratio of frequency to field. The contribution of orbital effects may be inferred from the g-value. Anisotropy effects are due to variations in g. The number of radicals is established by the absorption intensity.

4. Resonance absorption lines may show a hyperfine splitting by nuclei, thus leading to information about the localization of an unpaired electron.

XXVII. EXPERIMENTAL PROCEDURES

Analogues of both the nuclear absorption and the induction apparatus are in use in ESR measurements, together with special techniques of the microwave region. One may select a convenient value either of magnetic field or of frequency, but at low fields the transitions observed may be different from those at high fields. The range of frequencies used thus far is 0.8 Mcps (116) to 55,600 Mcps (395). Since the field should exceed the line width by several fold, one would hardly look for electron spin resonance in the megacycle region for a line more than 10 gauss wide. This largely restricts low-field observations to free radicals and metals. It is a simple matter to observe the absorption of a free radical in the earth's field. If $g \approx 2$ and the observation field is 20 gauss, the resonant frequency is 56 Mcps. At such frequencies all the types of nuclear resonance detection systems are applicable without modification and accurately wound solenoids or Helmholtz coils are used to provide the field. An oscillating detector suitable for use at 350 Mcps and capable of detecting 10^{14} centers has been described (356).

For observations of wide lines or weak signals, it is desirable to work in the kilogauss range. The resonant frequency given by the equation $\nu = 1.3997gH$ (Mcps) is then in the microwave region and one must use the specialized techniques appropriate to this range. The most generally used regions are the X-band (8200 to 12,400 Mcps) and the K-band (18,000 to 26,500 Mcps), since components are readily available. The internal dimensions of the wave guide are, respectively, 0.400 × 0.900 in. and 0.170 × 0.420 in. Special parts are easier to make for the X-band, but there are no compelling advantages of one over the other region.

Instead of using coil-condenser tuned circuits, one will usually make use of the microwave analogue—the resonant cavity. (Some non-resonant procedures have been used (336).) The electrical resonance frequency of the cavity is determined by its length, which will be one or two guide half-wavelengths. The "guide wavelength" λ_g will be related to the wavelength in free space λ_1 and to the wide dimension a of the wave guide by the expression (454):

$$\lambda_g = \frac{\lambda_1}{(1 - (\lambda_1/2a)^2)^{1/2}}$$

Resonant cavities are of the transmission and the reflection types, the former being shown in figures 22 and 26. The sample will be located at a point where the microwave electric field is a minimum and the magnetic field a maximum. If the sample is of large diameter so as to extend into regions of appreciable electric field or shows a high dielectric loss, the transmitted power will be greatly reduced. The signal will then be weak because of low H_1. Since the field falls off sinusoidally from the center of the wave guide, the absorption in a long sample will not be uniform throughout its length. One must carefully tune the klystron source to the electrical resonance frequency of the cavity to avoid distorting an absorption line (27). The cavity will often have a movable plunger or tuning screws for small frequency changes. Energy is coupled into and out of the cavity by irises or loops which serve as impedance-matching devices. The sensitivity is dependent upon the degree of coupling (163, 564). The transmitted power is reduced when ESR absorption occurs, the latter being equivalent to a reduction in the factor of merit, Q, of the cavity. (Q will be given by the ratio of the cavity resonance frequency to the width of the cavity resonance curve at half-height.) Reflection cavities are widely used, being especially advantageous for experiments below room temperature. The entire cavity may be immersed in a dewar and one then has heat leakage from only one arm. To further reduce heat leakage, a glass wave guide with a thin interior coating of metal may be used (595). The reflection cavity likewise has the advantage that for illumination experiments one may irradiate the sample at the end of the cavity through a window.

Since the resonant cavity and the klystron are independent and both must be tuned to the same frequency, it has not been feasible to operate at fixed field and variable frequency. The field may be varied linearly with time through the resonant value, and the power transmitted or reflected is monitored. If a sample is moderately large, is strongly paramagnetic, and its ESR absorption line is nar-

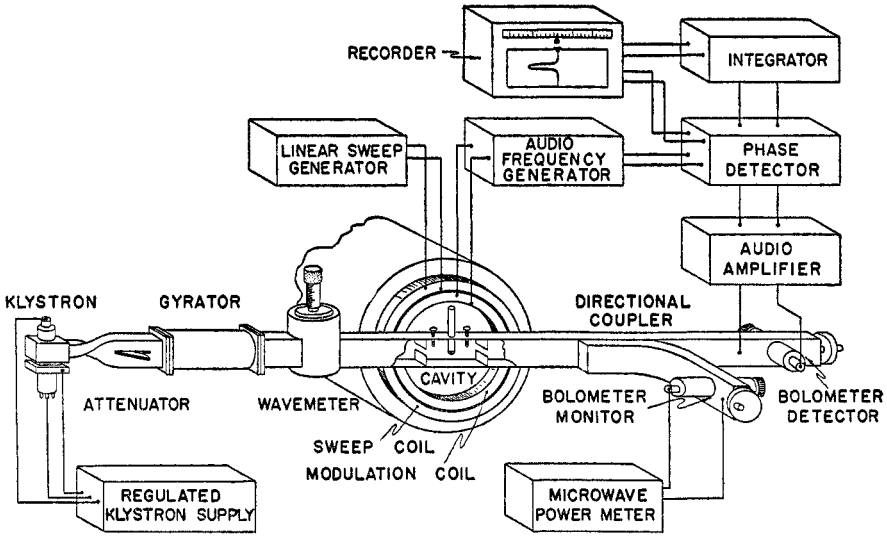

FIG. 26. Transmission cavity spectrometer

row, it is possible to reduce the transmitted power by one-half or more. Direct plotting of the output indicated by a silicon–tungsten crystal or a bolometer in terms of field strength is feasible for strong lines. Within the "square-law" region, the absorption is given directly by changes in detector current or resistance.

Just as with nuclear absorption or induction, it is desirable to balance out steady power so as to achieve high sensitivity for weak reflections at resonance. One may use a bridge with test and reference cavities in separate arms, the detected outputs being coupled to a transformer (31). If balanced initially, a signal will appear when the bridge is unbalanced by absorption. A more satisfactory bridge is the matched hybrid tee (also known as the magic tee) shown in figure 27b. Power may be fed at arm 3, and if arms 1 and 2 are perfectly matched, no power is fed to arm 4, which contains a detector. If arm 2 has a reflection cavity, arm 1 will have a matched load.

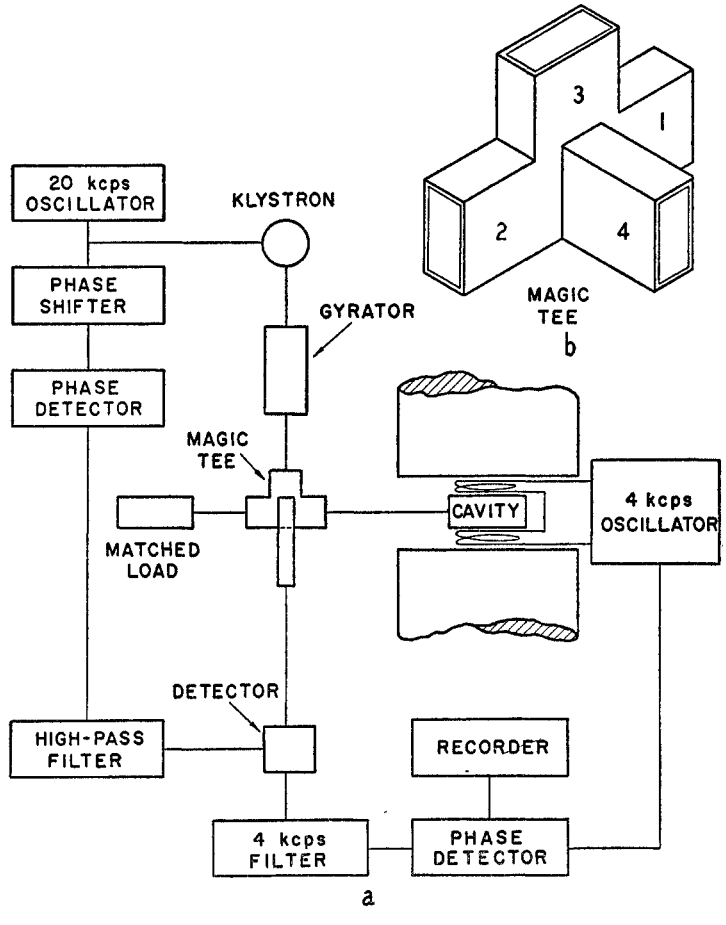

FIG. 27. (a) Reflection cavity spectrometer (287, 516); (b) hybrid or magic tee

A. Detectors

The most satisfactory detectors in the microwave region are the silicon–tungsten crystal and the bolometer. While the crystal current is linear with power below 10 microwatts, the bolometer shows nearly linear D.C. resistance with power (368). Bolometers in use include the type 821 (380, 534) or the 621 barreter (380), which have a 25-micron platinum wire heated by a constant current to such a temperature that its resistance is 200 ohms. The sensitivity is of the order of 4.5 ohms per milliwatt. With good crystal detectors, one may achieve a sensitivity of 1 microamp. per microwatt below 10 microwatts. If low audiofrequency modulation of the field is used, the crystal is at least ten times as noisy as the bolometer. However, the bolometer response falls off rapidly beyond several hundred cycles per second. It is limited to powers less than 32 milliwatts. Crystal noise is inversely proportional to frequency up to 1 Mcps (558), and has fallen nearly to the thermal level, so that crystals are excellent for the double-detection system to be described later.

B. Microwave sources

Commonly one uses klystrons, which will deliver to the cavity perhaps 25 to 150 milliwatts, depending on the loss characteristics of the sample and the nature of the detector. 2K25 klystrons have been widely used at 9000 Mcps because of their availability. These differ widely in their power output from a nominal value of 25 milliwatts to 75 milliwatts in especially good tubes. The V-260 klystron gives 125 milliwatts with excellent stability (570). The 2K33 has been widely used at 24,000 Mcps. For saturation experiments very high powers have been used (86, 514).

When impedance mismatch occurs in a wave-guide system, energy is reflected and if it is returned to the klystron without attenuation it has the effect of "pulling" the frequency. Formerly it was customary to insert an attenuator between the source and the cavity just to attenuate the reflected energy. Naturally this meant wasting most of the source power. The microwave gyrator (248) makes use of Faraday rotation of ferrite to attenuate reflected power with little forward loss. A commercial version, the "Uniline" (104), attenuates the reflected power twentyfold or more while transmitting 80 per cent in the forward direction.

Frequency drift of the klystron due to temperature or voltage variations cannot be tolerated while tracing out a line over a period of some minutes. The simplest procedure (which is surprisingly effective) is to surround the inverted klystron in an oil bath and to operate it continuously. Anode and repeller voltages must be closely regulated. Automatic stabilization of frequency may be accomplished with a reference cavity as one arm of a hybrid tee (428). A preferable procedure uses the sample cavity as a reference and frequency-modulates the klystron to eliminate distortion of lines because of dispersion (247, 285).

With the radiofrequency oscillating detector, dispersion of the sample produces no serious effects on the detected absorption line. With a microwave cavity, however, dispersion has the effect of detuning the cavity and decreasing the power

transmitted or increasing the power reflected. This gives rise to serious distortion of a wide (100 gauss) line, though its effect on narrow free-radical lines is small (333, 596). With point-by-point plotting of a line, the cavity can be retuned each time, though this is an annoyance. Slow modulation of the klystron frequency over 100 kcps insures that the cavity resonant frequency will be traversed, and the true line shape is obtained from the lower envelope of the recorded line (595).

The direct plotting of transmitted power for strongly paramagnetic substances with slow field-scanning has been mentioned. Alternatively one can frequency-modulate the klystron and measure the intensity of the reflected power, which will now be amplitude-modulated (349). However, if the absorption by the sample is weak, the signal will be obscured by noise, and some means of narrowing the band width of the system must be used. Magnetic field modulation at audio-frequencies may be used for ESR observations with oscilloscopic display if the modulation amplitude is several times the line width and the line is not too weak (64, 349). Amplifier band width should be sufficient to avoid line distortion. It is not practical to try to modulate at amplitudes much greater than perhaps 100 gauss; hence this procedure is principally used for much narrower lines. For signals which are large enough to display on an oscilloscope or recorder after amplification (and detection if necessary), any of a variety of spectrometers may be used. Except for the weakest of signals, the transmission cavity spectrometer using field modulation and a bolometer as a detector is the simplest to use. The bolometer will form one arm of a bridge, the output of which is coupled through a high-quality transformer to a low-noise preamplifier. When signals are too weak for such direct display, one will modulate at a fraction of the line width, use a phase detector with long time-constant, and record the derivative of the absorption curve.

It has been suggested (245) that the most sensitive type of spectrometer is one which uses a magic tee (or similar bridge) and reflection cavity along with a second klystron to give a convenient intermediate frequency which is then amplified (30, 247, 488, 615). The detected output has the frequency of the field modulation if such is used. Advantages claimed over the transmission cavity system are freedom from fluctuations in klystron power, greater signal-to-noise ratio for direct display, and a greater range of linearity of response (163). Reference 245 appears to be the only detailed description of a high-resolution ESR spectrometer.

An analog of the double-detection system for the 10–500 Mcps region uses simultaneous field modulation at high and low audiofrequencies (521). Amplification occurs first at the higher frequency, followed by detection and amplification of the lower. High useful sensitivity is claimed. Use of the higher frequency alone would result in distortion of narrow lines due to the same sidebands which serve a useful purpose in calibration of high-resolution spectra (301, 517).

In analogy with the radiofrequency bridge which allowed dispersion to be observed by use of phase unbalance, the microwave bridges may be similarly used (163). A second procedure involves the comparison of the amplitudes of the

signals from the test cavity at resonance and from a cavity directly coupled to it (332, 333).

A microwave analog of the nuclear induction experiments uses a cylindrical cavity and observes an induced voltage (30).

An extensive analysis of microwave ESR spectrometers treats both transmission and reflection types in quantitative fashion (163).

C. Field-dependent cavity absorption

A mystifying phenomenon is the weak and very broad ESR absorption of an empty cavity. It has been observed in many different laboratories, but no two observers seem to agree on the exact shape of the "absorption line," except that one of the peaks (if more than one is observed) is centered around a field corresponding to $g = 2$. The effect must be corrected for when making intensity measurements on broad lines, though it is often difficult to get a reproducible cavity line.

It has been found possible to eliminate the effect by use of dielectric tuning stubs inserted in the narrow face of the wave-guide cavity (409).

D. Ultimate sensitivity

The ultimate sensitivity of an ESR spectrometer may be expressed by specifying the minimum observable value of χ''. One of several calculations which have been made gives (67)

$$\chi''_{\min} = \frac{V}{\pi Q_0}\left(\frac{N'kT\Delta f}{P_1}\right)^{1/2}$$

where V is the "effective volume" of the cavity, Q_0 the factor of merit of the empty cavity, N' the noise factor and Δf the band width of the receiver, T the absolute temperature, and P_1 the power incident on the cavity. $\chi''_{\min}$ for reasonable values of these parameters at 3 cm. is about 10^{-13}. For a 3-gauss line width, this corresponds to about 6×10^{-12} mole at 300°K. for a paramagnetic substance with $S = \frac{1}{2}$, $g = 2$.

For a transmission cavity, $\chi''_{\min}$ was calculated to be 3×10^{-12} (49).

An analysis for a heterodyne detection system gives a somewhat lower figure of 4.2×10^{-14} mole minimum when all parameters are given their most favorable possible values (163). The practically attainable limit is probably closer to the 10^{-11} mole detected in a number of laboratories.

E. Determination of splitting factors

Spectroscopic splitting factors g are most commonly determined relative to the value 2.0036 for polycrystalline 1,1-diphenyl-2-picrylhydrazyl. Absolute values can be obtained by independent measurements of field and frequency if the field is homogeneous enough to warrant this procedure. Proton resonance is generally used for field measurement.

While microwave frequencies may be measured to about 0.1 per cent with a wavemeter, one is interested in at least another significant figure. Starting with

a crystal-controlled oscillator in the region 0.1–5 Mcps, one will use frequency multiplying stages to get into the region of several hundred Mcps (239, 369, 541). The output of the final stage is connected to a crystal mixer in the wave guide. Being a non-linear device, the crystal will produce harmonics which will beat with the microwave frequency. For example, the seventeenth harmonic of 540 Mcps will give a 20 Mcps beat with 9200 Mcps. The beat frequency may be accurately measured with a meter such as the General Radio 620A. Markers at intervals of perhaps 5 Mcps are sometimes used for reference.

F. Relaxation times

To get t_1, one can plot absorption amplitude as a function of microwave (or radiofrequency) power, using values large enough to produce saturation (86, 346, 514). For 1,1-diphenyl-2-picrylhydrazyl this requires about 10 watts (86). Another method compares maximum line intensities for electron and proton resonance at a single radiofrequency changing the steady field to observe the two in succession (175). t_2 may be determined from line widths, as may t_1 when the two are equal.

XXVIII. SUMMARY

An attempt has been made here to make qualitatively understandable some of the applications of nuclear and electronic spin resonance. A thorough understanding of their subtleties is not achieved by a casual approach. It represents a worthy challenge to any chemist or physicist who seeks a broad understanding of matter. The resonant techniques provide incisive probes, often to allow a direct question about molecular structure or environment to be answered in more direct fashion than by other means. These branches of spectroscopy cannot be said to supplant any other approaches, but to provide a valuable supplement.

Thanks are due to H. M. McConnell, G. E. Pake, G. K. Fraenkel, and S. I. Weissman for copies of manuscripts in advance of publication or for unpublished data, to T. L. Collins for the data of table 7, to Prof. F. Bitter for figure 20, and to Varian Associates for permission to reproduce their "*n-m-r* Table." Absorption traces were taken by R. L. Batdorf, Jean Buckley, and Juana Vivo. The drawings were made by J. Pearson. Assistance by Florence Wertz and Juana Vivo is gratefully acknowledged, as is the patience shown by typist Ronald Zillgitt.

XXIX. REFERENCES

(1) ABELL, D. F., AND KNIGHT, W. D.: Phys. Rev. **93,** 940A (1954).
(2) ABRAGAM, A., AND PRYCE, M. H. L.: Proc. Roy. Soc. (London) **A205,** 135 (1951).
(3) ALPERT, N. L.: Phys. Rev. **72,** 637 (1947).
(4) ALPERT, N. L.: Phys. Rev. **75,** 398; erratum, 1271 (1949).
(5) AL'TSCHULER, S. A., KURENEV, V. YA., AND SALIKHOV, S. G.: Doklady Akad. Nauk S.S.S.R. **84,** 677 (1952); Chem. Abstracts **46,** 10723g (1952).
(6) ANDERSON, H. L.: Phys. Rev. **76,** 1460 (1949).
(7) ANDERSON, P. W.: Bull. Am. Phys. Soc. **30,** No. 3, 23 (1955).
(8) ANDERSON, P. W., AND WEISS, P. R.: Revs. Mod. Phys. **25,** 269 (1953).
(9) ANDERSON, W. A.: Ph.D. Thesis, Stanford University, 1954.

(10) ANDERSON, W. A., AND ARNOLD, J. T.: Phys. Rev. **94,** 497 (1954).
(11) ANDREW, E. R.: J. Chem. Phys. **18,** 607 (1950).
(12) ANDREW, E. R.: Phys. Rev. **82,** 443 (1951).
(13) ANDREW, E. R.: Physica **17,** 405 (1951).
(14) ANDREW, E. R.: Phys. Rev. **91,** 425 (1953).
(15) ANDREW, E. R., AND BERSOHN, R.: J. Chem. Phys. **18,** 159 (1950).
(16) ANDREW, E. R., AND EADES, R. G.: Proc. Phys. Soc. (London) **A66,** 415 (1953).
(17) ANDREW, E. R., AND EADES, R. G.: Proc. Roy. Soc. (London) **A216,** 398 (1953).
(18) ANDREW, E. R., AND EADES, R. G.: Proc. Roy. Soc. (London) **A218,** 537 (1953).
(19) ANDREW, E. R., AND HYNDMAN, D.: Proc. Phys. Soc. (London) **A66,** 1187 (1953).
(20) ANDREW, E. R., AND RUSHWORTH, F. A.: Proc. Phys. Soc. (London) **B65,** 801 (1952).
(21) ARCHIBALD, W. J.: Am. J. Phys. **20,** 368 (1952).
(22) ARD, W. B., JR., AND GORDY, W.: Bull. Am. Phys. Soc. **30,** No. 3, 12 (1955).
(23) ARGYRES, P. N., AND KAHN, A. H.: Bull. Am. Phys. Soc. **29,** No. 7, 11 (1954).
(24) ARNOLD, J. T.: Ph.D. Thesis, Stanford University, 1954.
(25) ARNOLD, J. T., DHARMATTI, S. S., AND PACKARD, M. E.: J. Chem. Phys. **19,** 507 (1951).
(26) ARNOLD, J. T., AND PACKARD, M. E.: J. Chem. Phys. **19,** 1608 (1951).
(27) ARNOLD, R., AND KIP, M.: Phys. Rev. **75,** 1199 (1949).
(28) AYANT, Y.: Compt. rend. **236,** 198 (1953).
(29) AYANT, Y.: Compt. rend. **238,** 1876 (1954).
(30) BAGGULEY, D. M. S.: Unpublished work quoted by B. Bleaney and K. W. H. Stevens: Repts. Progr. in Phys. **16,** 124 (1953).
(31) BAGGULEY, D. M. S., AND GRIFFITHS, J. H. E.: Proc. Phys. Soc. (London) **A65,** 594 (1952).
(32) BAKER, E. B.: Rev. Sci. Instr. **25,** 390 (1954).
(33) BAKER, E. B.: Abstracts of Pittsburgh Conference on Applied Spectroscopy, 1955.
(34) BANAS, E. M., AND MROWCA, B. A.: Bull. Am. Phys. Soc. **30,** No. 2, 25 (1955).
(35) BANAS, E. M., MROWCA, B. A., AND GUTH, E.: Phys. Rev. **98,** 265A (1955).
(36) BATDORF, R. L.: Ph.D. Thesis, University of Minnesota, 1955.
(37) BECKER, G.: Z. Physik **130,** 415 (1951).
(38) BECKER, S., AND EISNER, M.: Phys. Rev. **94,** 811A (1954).
(39) BELJERS, H. G., KINT, L. VAN DER, AND WIERINGEN, J. S. VAN: Phys. Rev. **95,** 1683 (1954).
(40) BENE, G. J., DENIS, P. M., AND EXTERMANN, R. C.: Compt. rend. **231,** 1294 (1950).
(41) BENE, G. J., DENIS, P. M., AND EXTERMANN, R. C.: Arch. sci. (Geneva) **4,** 212, 266 (1951).
(42) BENE, G. J., DENIS, P. M., AND EXTERMANN, R. C.: Helv. Phys. Acta **24,** 304 (1951).
(43) BENE, G. J., DENIS, P. M., AND EXTERMANN, R. C.: Physica **17,** 308 (1951).
(44) BENE, G. J., DENIS, P. M., AND EXTERMANN, R. C.: Helv. Phys. Acta **25,** 458 (1952).
(45) BENE, G. J., DENIS, P. M., AND EXTERMANN, R. C.: Helv. Phys. Acta **26,** 267 (1953).
(46) BENE, G. J., AND EXTERMANN, R. C.: Phys. Rev. **97,** 238 (1955).
(47) BENEDEK, G. B., AND PURCELL, E. M.: J. Chem. Phys. **22,** 2003 (1954).
(48) BENNETT, J. E., INGRAM, D. J. E., AND TAPLEY, J. G.: J. Chem. Phys. **23,** 215 (1955).
(49) BERINGER, R., AND CASTLE, J. G.: Phys. Rev. **78,** 581 (1950).
(50) BERINGER, R., AND HEALD, M. A.: Phys. Rev. **95,** 1474 (1954).
(51) BERSOHN, R.: J. Chem. Phys. **20,** 1505 (1952).
(52) BERSOHN, R., AND GUTOWSKY, H. S.: J. Chem. Phys. **22,** 651 (1954).
(53) BETHE, H. A.: Ann. Physik **3,** 133 (1929).
(54) BHAR, J. N., AND BHAR, B. N.: Science and Culture (India) **18,** 86 (1952).
(55) BIJL, D., KAINER, H., AND ROSE-INNES, A. C.: Nature **174,** 830 (1954).
(56) BIJL, D., AND ROSE-INNES, A. C.: Nature **175,** 82 (1955).
(57) BITTER, F.: *Dielectric Materials and Applications,* edited by A. R. von Hippel, p. 145. Technology Press of Massachusetts Institute of Technology, New York (1954).
(58) BITTER, F.: Private communication.

(59) BITTER, F., ALPERT, N. L., POSS, H. L., LEHR, C. G., AND LIN, S. T.: Phys. Rev. **71,** 738 (1947).
(60) BITTER, F., AND REED, F. E.: Rev. Sci. Instr. **22,** 171 (1951).
(61) BLEANEY, B.: Phil. Mag. **42,** 441 (1951).
(62) BLEANEY, B.: Physica **17,** 175 (1951).
(63) BLEANEY, B.: J. Phys. Chem. **57,** 508 (1953).
(64) BLEANEY, B., AND INGRAM, D. J. E.: Nature **164,** 116 (1949).
(65) BLEANEY, B., AND SCOVIL, H. E. D.: Proc. Phys. Soc. (London) **A64,** 204 (1951).
(66) BLEANEY, B., AND STEVENS, K. W. H.: Repts. Progr. in Phys. **16,** 108 (1953).
(67) BLEANEY, B., AND STEVENS, K. W. H.: Repts. Progr. in Phys. **16,** 121 (1953).
(68) BLEANEY, B., AND STEVENS, K. W. H.: Repts. Progr. in Phys. **16,** 152 (1953).
(69) BLOCH, F.: Phys. Rev. **70,** 460 (1946).
(70) BLOCH, F.: Phys. Rev. **83,** 1062 (1951).
(71) BLOCH, F.: Science **118,** 425 (1953).
(72) BLOCH, F.: Phys. Rev. **94,** 496 (1954).
(73) BLOCH, F., AND GARBER, D. H.: Phys. Rev. **76,** 585 (1949).
(74) BLOCH, F., HANSEN, W. W., AND PACKARD, M.: Phys. Rev. **69,** 127 (1946).
(75) BLOCH, F., HANSEN, W. W., AND PACKARD, M.: Phys. Rev. **70,** 474 (1946).
(76) BLOCH, F., AND SIEGERT, A.: Phys. Rev. **57,** 522 (1940).
(77) BLOEMBERGEN, N.: *Nuclear Magnetic Relaxation,* Chap. V. Martinus Nijhoff, The Hague (1948).
(78) BLOEMBERGEN, N.: Physica **15,** 386 (1949).
(79) BLOEMBERGEN, N.: Physica **16,** 95 (1950).
(80) BLOEMBERGEN, N.: J. Appl. Phys. **23,** 1383 (1952).
(81) BLOEMBERGEN, N., AND DICKINSON, W. C.: Phys. Rev. **79,** 179 (1950).
(82) BLOEMBERGEN, N., AND POULIS, N. J.: Physica **16,** 915 (1950).
(83) BLOEMBERGEN, N., AND POUND, R. V.: Phys. Rev. **95,** 8 (1954).
(84) BLOEMBERGEN, N., PURCELL, E. M., AND POUND, R. V.: Phys. Rev. **73,** 679 (1948).
(85) BLOEMBERGEN, N., AND ROWLAND, T. J.: Acta Met. **1,** 731 (1953).
(86) BLOEMBERGEN, N., AND WANG, S.: Phys. Rev. **93,** 72 (1954).
(87) BLOOM, A. L., AND SHOOLERY, J. N.: Phys. Rev. **90,** 358 (1953).
(88) BLOOM, A. L., AND SHOOLERY, J. N.: Phys. Rev. **97,** 1261 (1955).
(89) BRADFORD, R., CLAY, C., CRAFT, A., STRICK, E., AND UNDERHILL, J.: Phys. Rev. **83,** 656 (1951).
(90) BRADFORD, R., CLAY, C., AND STRICK, E.: Phys. Rev. **84,** 157 (1951).
(91) BREIT, G.: Phys. Rev. **72,** 984 (1947).
(92) BREIT, G., AND RABI, I. I.: Phys. Rev. **38,** 2082 (1931).
(93) BROERSMA, S.: BULL. Am. Phys. Soc. **30,** No. 1, 43 (1955).
(94) BROOKS, H.: Phys. Rev. **94,** 1411A (1954).
(95) BROVETTO, P., AND FERRONI, S.: Nuovo cimento **12,** 90 (1954).
(96) BROWN, L. C., AND WILLIAMS, D.: Phys. Rev. **95,** 1110 (1954).
(97) BROWN, R. M.: Phys. Rev. **78,** 530 (1950).
(98) BROWN, R. M., AND PURCELL, E. M.: Phys. Rev. **75,** 1262 (1949).
(99) BURGESS, J. H., AND BROWN, R. M.: Rev. Sci. Instr. **23,** 334 (1952).
(100) CARR, E. F., AND KIKUCHI, C.: Phys. Rev. **78,** 470 (1950).
(101) CARR, H. Y., AND PURCELL, E. M.: Phys. Rev. **88,** 415 (1952).
(102) CARR, H. Y., AND PURCELL, E. M.: Phys. Rev. **94,** 630 (1954).
(103) CARVER, T. R., AND SLICHTER, C. P.: Phys. Rev. **92,** 212 (1953).
(104) CASCADE RESEARCH CORPORATION (Los Gatos, California).
(105) CASTLE, J. G., JR.: Phys. Rev. **92,** 1063 (1953).
(106) CASTLE, J. G., JR.: Phys. Rev. **94,** 1410 (1954).
(107) CASTLE, J. G., JR.: Phys. Rev. **95,** 846 (1954).
(108) CASTLE, J. G., JR.: Bull. Am. Phys. Soc. **30,** No. 2, 41 (1955).
(109) CHANCE, B., HUGHES, V., MACNICHOL, E. F., SAYRE, D., AND WILLIAMS, F. C.: *Wave Forms,* p. 197. McGraw-Hill Book Company, Inc., New York (1948).

(110) CHIAROTTI, G., AND GIULOTTO, L.: Nuovo cimento **8,** 595 (1951).
(111) CHIAROTTI, G., AND GIULOTTO, L.: Nuovo cimento **10,** 54 (1953).
(112) CHIAROTTI, G., AND GIULOTTO, L.: Phys. Rev. **93,** 1241 (1954).
(113) CHU, T. L., PAKE, G. E., PAUL, D. E., TOWNSEND, J., AND WEISSMAN, S. I.: J. Phys. Chem. **57,** 504 (1953).
(114) CHU, T. L., AND YU, S. C.: J. Am. Chem. Soc. **76,** 3367 (1954).
(115) CLAY, C. S., BRADFORD, R. S., AND STRICK, E.: J. Chem. Phys. **19,** 1429 (1951).
(116) CODRINGTON, R. S., OLDS, J. D., AND TORREY, H. C.: Phys. Rev. **95,** 607A (1954).
(117) COHEN-HADRIA, A., AND GABILLARD, R.: Compt. rend. **234,** 1877 (1952).
(118) COHEN, V. W., KIKUCHI, C., AND TURKEVICH, J.: Phys. Rev. **85,** 379 (1952).
(119) COHN, M., AND TOWNSEND, J.: Nature **173,** 1090 (1954).
(120) COLLINS, T. L.: Ph.D. Thesis, University of British Columbia, 1950.
(121) COLLINS, T. L.: Unpublished calculations.
(122) COMBRISSON, J., AND UEBERSFELD, J.: Compt. rend. **238,** 572 (1954).
(123) COMBRISSON, J., AND UEBERSFELD, J.: Compt. rend. **238,** 1397 (1954).
(124) COMMONER, B.: Private communication.
(125) COMMONER, B., TOWNSEND, J., AND PAKE, G. E.: Nature **174,** 689 (1954).
(126) CONGER, R. L.: J. Chem. Phys. **21,** 937 (1953).
(127) CONGER, R. L., AND SCHILBERG, L. E.: Rev. Sci. Instr. **25,** 52 (1954).
(128) CONGER, R. L., AND SELWOOD, P. W.: J. Chem. Phys. **20,** 383 (1952).
(129) COOKE, A. H.: Repts. Progr. in Phys. **13,** 276 (1950).
(130) COOKE, A. H.: Quoted by B. Bleaney and K. W. H. Stevens: Repts. Progr. in Phys. **16,** 149 (1953).
(131) COOKE, A. H., AND DRAIN, L. E.: Proc. Phys. Soc. (London) **A65,** 894 (1952).
(132) COTTS, R. M., AND KNIGHT, W. D.: Phys. Rev. **96,** 1285 (1954).
(133) DAILEY, B. P.: Ann. Rev. Phys. Chem. **4,** 425 (1953).
(134) DARBY, J. F., AND ROLLIN, B. V.: Nature **164,** 66 (1949).
(135) DARROW, K. K.: Bell System Tech. J. **32,** 74 (1953).
(136) DARROW, K. K.: Bell System Tech. J. **32,** 384 (1953).
(137) DAS, T. P., AND SAHA, A. K.: Phys. Rev. **93,** 749 (1954).
(138) DEBYE, P.: *Polar Molecules*, p. 84. The Chemical Catalog Co., Inc., New York (1929).
(139) DEELEY, C. M., LEWIS, P., AND RICHARDS, R. E.: Trans. Faraday Soc. **50,** 556 (1954).
(140) DEELEY, C. M., AND RICHARDS, R. E.: J. Chem. Soc. **1954,** 3697.
(141) DEHMELT, H. G.: Bull. Am. Phys. Soc. **30,** No. 1, 42 (1955).
(142) DEXTER, D. L.: Phys. Rev. **93,** 244 (1954).
(143) DHARMATTI, S. S., AND WEAVER, H. E., JR.: Phys. Rev. **84,** 367 (1951).
(144) DHARMATTI, S. S., AND WEAVER, H. E., JR.: Phys. Rev. **84,** 843 (1951).
(145) DHARMATTI, S. S., AND WEAVER, H. E., JR.: Phys. Rev. **87,** 675 (1952).
(146) DICK, L., FOUCHER, R., PERRIN, N., VARTAPETIAN, H., BENE, G., DENIS, P., AND EXTERMANN, R.: Compt. rend. **239,** 1376 (1954).
(147) DICKINSON, W. C.: Phys. Rev. **77,** 736 (1950).
(148) DICKINSON, W. C.: Phys. Rev. **80,** 563 (1950).
(149) DICKINSON, W. C.: Phys. Rev. **81,** 717 (1951).
(150) DRAIN, L. E.: Proc. Phys. Soc. (London) **A62,** 301 (1949).
(151) DYATKINA, M., AND SYRKIN, J.: Acta Physicochim. U.R.S.S. **21,** 23 (1946).
(152) DYSON, F. J.: Phys. Rev. **98,** 349 (1955).
(153) ELLIOTT, R. J.: Phys. Rev. **96,** 266 (1954).
(154) ETIENNE, A., AND UEBERSFELD, J.: J. chim. phys. **51,** 328 (1954).
(155) EWING, R., AND LEE, J. C.: Phys. Rev. **94,** 1411A (1954).
(156) EXTERMANN, R. C., DENIS, P., AND BENE, G.: Helv. Phys. Acta **22,** 388 (1949).
(156a) EYRING, H., WALTER, J., AND KIMBALL, G. E.: *Quantum Chemistry*, p. 151. John Wiley and Sons, Inc., New York (1944).
(157) FEHER, G., AND KIP, A. F.: Phys. Rev. **95,** 1343 (1954).
(158) FEHER, G., AND KIP, A. F.: Phys. Rev. **98,** 337 (1955).
(159) FEHER, G., AND KNIGHT, W. D.: Rev. Sci. Instr. **26,** 293 (1955).

(160) FEHER, G., AND LEVY, R. A.: Phys. Rev. **98,** 264A (1955).
(161) FLETCHER, R. C., YAGER, W. A., PEARSON, G. L., HOLDEN, A. N., READ, W. T., AND MERRITT, F. R.: Phys. Rev. **94,** 1392 (1954).
(162) FLETCHER, R. C., YAGER, W. A., PEARSON, G. L., AND MERRITT, F. R.: Phys. Rev. **95,** 844 (1954).
(163) FRAENKEL, G. K., AND HIRSHON, J. M.: To be published.
(164) FRAENKEL, G. K., HIRSHON, J. M., AND WALLING, C.: J. Am. Chem. Soc. **76,** 3606 (1954).
(165) FREED, S., AND SUGARMAN, N.: J. Chem. Phys. **11,** 354 (1943).
(166) FUJIWARA, S.: Bull. Chem. Soc. Japan **24,** 116 (1951).
(167) FUJIWARA, S., AND HAYASHI, S.: J. Chem. Soc. Japan, Pure Chem. Sect. **72,** 764 (1951).
(168) GABILLARD, R.: Compt. rend. **232,** 324 (1951).
(169) GABILLARD, R.: Compt. rend. **232,** 1477 (1951).
(170) GABILLARD, R.: Compt. rend. **232,** 1551 (1951).
(171) GABILLARD, R.: Compt. rend. **233,** 39 (1951).
(172) GABILLARD, R.: Rev. sci. **90,** 307 (1952).
(173) GABILLARD, R.: Phys. Rev. **85,** 694 (1952).
(174) GABILLARD, R.: Compt. rend. **237,** 705 (1953).
(175) GABILLARD, R., AND MARTIN, J. A.: Compt. rend. **238,** 2307 (1954).
(176) GABILLARD, R., AND SOUTIF, M.: Compt. rend. **230,** 1754 (1950).
(177) GABILLARD, R., AND SOUTIF, M.: Compt. rend. **233,** 480 (1951).
(178) GARDNER, D. M., AND FRAENKEL, G. K.: J. Am. Chem. Soc. **76,** 5891 (1954).
(179) GARDNER, J. H., AND PURCELL, E. M.: Phys. Rev. **83,** 996 (1951).
(180) GARSTENS, M. A.: Phys. Rev. **79,** 397 (1950).
(181) GARSTENS, M. A.: Phys. Rev. **81,** 288 (1951).
(182) GARSTENS, M. A.: Phys. Rev. **81,** 645 (1951).
(183) GARSTENS, M. A.: Phys. Rev. **93,** 1228 (1954).
(184) GARSTENS, M. A., AND LIEBSON, S. H.: J. Chem. Phys. **20,** 1647 (1952).
(185) GARSTENS, M. A., AND RYAN, A. H.: Phys. Rev. **81,** 888 (1951).
(186) GARSTENS, M. A., SINGER, L. S., AND RYAN, H. H.: Phys. Rev. **96,** 53 (1954).
(187) GERRITSEN, H. J., OKKES, R., GIJSMAN, H. M., AND HANDEL, J. VAN DEN: Physica **20,** 13 (1954).
(188) GINDSBERG, J., AND BEERS, Y.: Rev. Sci. Instr. **24,** 632 (1953).
(189) GIULOTTO, L.: Nuovo cimento **5,** 498 (1948).
(190) GIULOTTO, L., CHIAROTTI, G., AND CRISTIANI, G.: J. Chem. Phys. **22,** 1143 (1954).
(191) GOODEN, J. S.: Nature **165,** 1014 (1950).
(192) GORDY, W., SMITH, W. V., AND TRAMBARULO, R. F.: *Microwave Spectroscopy*, p. 213. John Wiley and Sons, Inc., New York (1953).
(193) GORTER, C. J.: *Paramagnetic Relaxation*, p. 22. Elsevier Press, Inc., New York (1947).
(194) Reference 193, p. 77.
(195) GORTER, C. J.: Experientia **9,** 161 (1953).
(196) GORTER, C. J., AND VAN VLECK, J. H.: Phys. Rev. **72,** 1128 (1947).
(197) GRIFFITHS, J. H. E., OWEN, J., AND WARD, I. M.: Nature **173,** 439 (1954).
(198) GRISWOLD, T. W., KIP, A. F., AND KITTEL, C.: Phys. Rev. **88,** 951 (1952).
(199) GRIVET, P.: Compt. rend. **233,** 397 (1951).
(200) GRIVET, P., AND AYANT, Y.: Compt. rend. **232,** 1094 (1951).
(201) GRIVET, P., GABILLARD, R., AYANT, Y., AND BASSOMPIERRE, A.: J. chim. phys. **51,** 89 (1954).
(202) GRIVET, P., SOUTIF, M., AND GABILLARD, R.: Physica **17,** 420 (1951).
(203) GROSS, E. P.: Bull. Am. Phys. Soc. **30,** No. 3, 22 (1955).
(204) GRUBB, W. T., AND KISTIAKOWSKY, G. B.: J. Am. Chem. Soc. **72,** 419 (1950).
(205) GUTOWSKY, H. S.: Phys. Rev. **83,** 1073 (1951).
(206) GUTOWSKY, H. S.: Ann. Rev. Phys. Chem. **5,** 333 (1954).
(207) GUTOWSKY, H. S., AND FRANK, P. J.: Phys. Rev. **94,** 1067 (1954).

(208) GUTOWSKY, H. S., AND FUJIWARA, S.: J. Chem. Phys. **22,** 1782 (1954).
(209) GUTOWSKY, H. S., AND HOFFMAN, C. J.: Phys. Rev. **80,** 110 (1950).
(210) GUTOWSKY, H. S., AND HOFFMAN, C. J.: J. Chem. Phys. **19,** 1259 (1951); erratum **20,** 200 (1952).
(211) GUTOWSKY, H. S., KISTIAKOWSKY, G. B., PAKE, G. E., AND PURCELL, E. M.: J. Chem. Phys. **17,** 972 (1949).
(212) GUTOWSKY, H. S., AND MCCALL, D. W.: Phys. Rev. **82,** 748 (1951).
(213) GUTOWSKY, H. S., AND MCCALL, D. W.: J. Chem. Phys. **22,** 162 (1954).
(214) GUTOWSKY, H. S., MCCALL, D. W., MCGARVEY, B. R., AND MEYER, L. H.: J. Am. Chem. Soc. **74,** 4809 (1952).
(215) GUTOWSKY, H. S., MCCALL, D. W., AND SLICHTER, C. P.: Phys. Rev. **84,** 589 (1951).
(216) GUTOWSKY, H. S., MCCALL, D. W., AND SLICHTER, C. P.: J. Chem. Phys. **21,** 279 (1953).
(217) GUTOWSKY, H. S., AND MCCLURE, R. E.: Phys. Rev. **81,** 276 (1951).
(218) GUTOWSKY, H. S., AND MCGARVEY, B. R.: J. Chem. Phys. **20,** 1472 (1952).
(219) GUTOWSKY, H. S., AND MCGARVEY, B. R.: Phys. Rev. **91,** 81 (1953).
(220) GUTOWSKY, H. S., AND MCGARVEY, B. R.: J. Chem. Phys. **21,** 1423 (1953).
(221) GUTOWSKY, H. S., AND MEYER, L. H.: J. Chem. Phys. **21,** 2122 (1953).
(222) GUTOWSKY, H. S., MEYER, L. H., AND MCCLURE, R. E.: Rev. Sci. Instr. **24,** 644 (1953).
(223) GUTOWSKY, H. S., AND PAKE, G. E.: J. Chem. Phys. **16,** 1164 (1948).
(224) GUTOWSKY, H. S., AND PAKE, G. E.: J. Chem. Phys. **18,** 162 (1950).
(225) GUTOWSKY, H. S., PAKE, G. E., AND BERSOHN, R.: J. Chem. Phys. **22,** 643 (1954).
(226) GUTOWSKY, H. S., AND SAIKA, A.: J. Chem. Phys. **21,** 1688 (1953).
(227) GVOZDOVER, S. D., AND MAGAZANIK, A. A.: Zhur. Eksptl. i Teoret. Fiz. **20,** 705 (1950).
(228) GVOZDOVER, S. D., AND POMERANTSEV, N. M.: Vestnik Moskov. Univ. **8,** No. 9, Ser. Fiz.-Mat. i Estestven. Nauk, **No. 6,** 79 (1953); Chem. Abstracts **49,** 53 (1955).
(229) HAHN, E. L.: Phys. Rev. **76,** 145 (1949).
(230) HAHN, E. L.: Phys. Rev. **77,** 297 (1950).
(231) HAHN, E. L.: Phys. Rev. **80,** 580 (1950).
(232) HAHN, E. L.: Physics Today **6,** No. 11, 4 (1953).
(233) HAHN, E. L., AND MAXWELL, D. E.: Phys. Rev. **84,** 1246 (1951).
(234) HAHN, E. L., AND MAXWELL, D. E.: Phys. Rev. **88,** 1070 (1952).
(235) HALBACH, K.: Helv. Phys. Acta **27,** 259 (1954).
(236) HANDEL, J. VAN DEN: Physica **18,** 921 (1952).
(237) HATTON, J., AND ROLLIN, B. V.: Proc. Roy. Soc. (London) **A199,** 222 (1949).
(238) HATTON, J., ROLLIN, B. V., AND SEYMOUR, E. F.: Phys. Rev. **83,** 672 (1951).
(239) HEDRICK, L. C.: Rev. Sci. Instr. **24,** 565 (1953).
(240) HEITLER, W., AND TELLER, E.: Proc. Roy. Soc. (London) **A155,** 629 (1936).
(241) HENNIG, G. R., SMALLER, B., AND YASAITIS, E. L.: Phys. Rev. **95,** 1088 (1954).
(242) HENRY, W.: Bull. Am. Phys. Soc. **29,** No. 7, 37 (1954).
(243) HERZOG, B., AND HAHN, E. L.: Bull. Am. Phys. Soc. **29,** No. 7, 11 (1954).
(244) HICKMOTT, T. W., AND SELWOOD, P. W.: J. Chem. Phys. **20,** 1339 (1952).
(245) HIRSHON, J. M., AND FRAENKEL, G. K.: Rev. Sci. Instr. **26,** 34 (1955).
(246) HIRSHON, J. M., GARDNER, D. M., AND FRAENKEL, G. K.: J. Am. Chem. Soc. **75,** 4115 (1953).
(247) HIRSHON, J. M., WHITE, R. L., AND FRAENKEL, G. K.: Rev. Sci. Instr. **23,** 772 (1952).
(248) HOGAN, C. L.: Bell System Tech. J. **31,** 1 (1952).
(249) HOLCOMB, D. F., AND NORBERG, R. E.: Phys. Rev. **93,** 919A (1954).
(250) HOLDEN, A. N., KITTEL, C., MERRITT, F. R., AND YAGER, W. A.: Phys. Rev. **75,** 1614 (1949).
(251) HOLDEN, A. N., KITTEL, C., MERRITT, F. R., AND YAGER, W. A.: Phys. Rev. **77,** 147 (1950).
(252) HOLDEN, A. N., YAGER, W. A., AND MERRITT, F. R.: J. Chem. Phys. **19,** 1319 (1951).
(253) HOLDER, B. E., AND KLEIN, M. P.: Phys. Rev. **98,** 265A (1955).

(254) HOLROYD, L. V., CODRINGTON, R. S., MROWCA, B. A., AND GUTH, E.: J. Appl. Phys. **22,** 696 (1951).
(255) HOLROYD, L. V., CODRINGTON, R. S., MROWCA, B. A., AND GUTH, E.: Rubber Chem. and Technol. **25,** 767 (1952).
(256) HONIG, A., AND KIP, A. F.: Phys. Rev. **95,** 1686 (1954).
(257) HONNOLD, V. R., MCCAFFREY, F., AND MROWCA, B. A.: J. Appl. Phys. **25,** 1219 (1954).
(258) HOOD, G. C., REDLICH, O., AND REILLY, C. A.: J. Chem. Phys. **22,** 2067 (1954).
(259) HOPKINS, N. J.: Rev. Sci. Instr. **20,** 401 (1949).
(260) HORNIG, J. F., AND HIRSCHFELDER, J. O.: J. Chem. Phys. **23,** 474 (1955).
(261) HUSH, N. S., AND BLACKLEDGE, J.: J. Chem. Phys. **23,** 514 (1955).
(262) HUSTER, E.: Ann. Physik **33,** 477 (1938).
(263) HUTCHISON, C. A., JR.: Phys. Rev. **75,** 1769 (1949).
(264) HUTCHISON, C. A., JR.: J. Phys. Chem. **57,** 546 (1953).
(265) HUTCHISON, C. A., JR., KOWALSKY, A., PASTOR, R. C., AND WHELAND, G. W.: J. Chem. Phys. **20,** 1485 (1952).
(266) HUTCHISON, C. A., JR., AND NOBLE, G. A.: Phys. Rev. **87,** 1125 (1952).
(267) HUTCHISON, C. A., JR., AND PASTOR, R. C.: Phys. Rev. **81,** 282 (1951).
(268) HUTCHISON, C. A., JR., AND PASTOR, R. C.: J. Chem. Phys. **21,** 1959 (1953).
(269) HUTCHISON, C. A., JR., AND PASTOR, R. C.: Revs. Mod. Phys. **25,** 285 (1953).
(270) HUTCHISON, C. A., JR., PASTOR, R. C., AND KOWALSKY, A. C.: J. Chem. Phys. **20,** 534 (1952).
(271) INGRAM, D. J. E., AND TAPLEY, J. G.: Phil. Mag. **45,** 1221 (1954).
(272) INGRAM, J. E., TAPLEY, J. G., JACKSON, R., BOND, R. L., AND MUNAGHAN, A. R.: Nature **174,** 797 (1954).
(273) INUI, J., AND UEMURA, Y.: Progr. Theoret. Phys. (Japan) **5,** 252, 395 (1950).
(274) ISHIGURO, E., AND KOIDE, S.: Busseiron Kenkyu **60,** 1 (1953); Chem. Abstracts **47,** 6721c (1953).
(275) ITOH, J., AND KUSAKA, R.: J. Phys. Soc. Japan **9,** 434 (1954).
(276) ITOH, J., KUSAKA, R., KIRIYAMA, R., AND YABUMOTO, S.: J. Chem. Phys. **21,** 1895 (1953).
(277) ITOH, J., KUSAKA, R., AND YAMAGATA, Y.: J. Phys. Soc. Japan **9,** 209 (1954).
(278) ITOH, J., KUSAKA, R., YAMAGATA, Y., KIRIYAMA, R., AND IBAMOTO, H.: J. Chem. Phys. **20,** 1503 (1952); erratum J. Chem. Phys. **21,** 190 (1953).
(279) ITOH, J., KUSAKA, R., YAMAGATA, Y., KIRIYAMA, R., AND IBAMOTO, H.: Physica **19,** 415 (1953).
(280) ITOH, J., KUSAKA, R., YAMAGATA, Y., KIRIYAMA, R., IBAMOTO, H., KANDA, T., AND MASUDA, Y.: J. Phys. Soc. Japan **8,** 287 (1953).
(281) ITOH, J., KUSAKA, R., YAMAGATA, Y., KIRIYAMA, R., AND IBAMOTO, H.: J. Phys. Soc. Japan **8,** 293 (1953).
(282) JACOBSOHN, B. A., AND WANGSNESS, R. K.: Phys. Rev. **73,** 942 (1948).
(283) JACOBSON, B., ANDERSON, W. A., AND ARNOLD, J. T.: Nature **173,** 772 (1954).
(284) JAHN, H. A., AND TELLER, E.: Proc. Roy. Soc. (London) **A161,** 220 (1937).
(285) JARRETT, H. S.: J. Chem. Phys. **21,** 761 (1953).
(286) JARRETT, H. S., SADLER, M. S., AND SHOOLERY, J. N.: J. Chem. Phys. **21,** 2092 (1953).
(287) JARRETT, H. S., AND SLOAN, G. J.: J. Chem. Phys. **22,** 1783 (1954).
(288) JEFFRIES, C. D.: Phys. Rev. **92,** 1262 (1953).
(289) JEFFRIES, C. D., LOELIGER, H., AND STAUB, H.: Phys. Rev. **85,** 478 (1952).
(290) JEN, C. K., AND LORD, N. W.: Phys. Rev. **96,** 1150 (1954).
(291) JONES, H., AND SCHIFF, B.: Proc. Phys. Soc. (London) **A67,** 217 (1954).
(292) KAHN, A. H., AND KITTEL, C.: Phys. Rev. **89,** 315 (1953).
(293) KAINER, H., BIJL, D., AND ROSE-INNES, A. C.: Naturwissenschaften **41,** 303 (1954).
(294) KAKIUCHI, Y., AND KOMATSU, H.: J. Phys. Soc. Japan **7,** 380 (1952).
(295) KAKIUCHI, Y., SHONO, H., KOMATSU, H., AND KIGOSHI, K.: J. Chem. Phys. **19,** 1069 (1951).

(296) KAKIUCHI, Y., SHONO, H., KOMATSU, H., AND KIGOSHI, K.: J. Phys. Soc. Japan **7,** 102 (1952).
(297) KAMBE, K., AND USUI, T.: Progr. Theoret. Phys. (Japan) **8,** 302 (1952).
(298) KAMEI, T.: Rept. Inst. Sci. and Technol., Univ. Tokyo **7,** 175 (1953).
(299) KANDA, T., MASUDA, Y., YAMAGATA, Y., AND ITOH, J.: Phys. Rev. **83,** 1066 (1951).
(300) KAPLAN, J., AND KITTEL, C.: J. Chem. Phys. **21,** 1429 (1953).
(301) KARPLUS, R.: Phys. Rev. **73,** 1027 (1948).
(302) KARPLUS, R., AND KROLL, N. M.: Phys. Rev. **77,** 536 (1950).
(303) KENYON, J., AND SUGDEN, S.: J. Chem. Soc. **1932,** 170.
(304) KETELAAR, J. A. A., AND VEDDER, W.: J. Chem. Phys. **19,** 654 (1951).
(305) KHUTSISHVILI, G. R.: Zhur. Eksptl. i Teoret. Fiz. **22,** 382 (1952).
(306) KIKUCHI, C., AND COHEN, V. W.: Phys. Rev. **93,** 394 (1954).
(307) KIP, A. F., KITTEL, C., LEVY, R. A., AND PORTIS, A. M.: Phys. Rev. **91,** 1066 (1953).
(308) KITTEL, C.: Phys. Rev. **95,** 589 (1954).
(309) KITTEL, C., AND ABRAHAMS, E.: Phys. Rev. **90,** 238 (1953).
(310) KJELDAAS, T., AND KOHN, W.: Bull. Am. Phys. Soc. **30,** No. 3, 22 (1955).
(311) KLEIN, M. P., AND HOLDER, B. E.: Phys. Rev. **98,** 265A (1955).
(312) KNIGHT, W. D.: Phys. Rev. **76,** 1259 (1949).
(313) KNIGHT, W. D.: Phys. Rev. **85,** 762 (1952).
(314) KNIGHT, W. D.: Private communication.
(315) KNIGHT, W. D., AND KITTEL, C.: Phys. Rev. **86,** 573 (1952).
(316) KNOEBEL, H. W., AND HAHN, E. L.: Rev. Sci. Instr. **22,** 904 (1951).
(317) KOENIG, S. H., PRODELL, A. G., AND KUSCH, P.: Phys. Rev. **88,** 191 (1952).
(318) KOHN, W.: Phys. Rev. **96,** 590 (1954).
(319) KOHN, W., AND BLOEMBERGEN, N.: Phys. Rev. **80,** 913 (1950).
(320) KOHN, W., AND BLOEMBERGEN, N.: Phys. Rev. **82,** 283 (1951).
(321) KOJIMA, S., AND OGAWA, S.: J. Phys. Soc. Japan **8,** 283 (1953).
(322) KOJIMA, S., OGAWA, S., AND TORIKZUKA, K.: Science of Light (Japan) **1,** No. 2, 101 (1951); Chem. Abstracts **46,** 10902 (1952).
(323) KORRINGA, J.: Physica **16,** 601 (1950).
(324) KORRINGA, J.: Phys. Rev. **94,** 1388 (1954).
(325) KOZYREV, B. M.: Doklady Akad. Nauk S.S.S.R. **81,** 427 (1951).
(326) KOZYREV, B. M.: J. chim. phys. **51,** D104 (1954).
(327) KOZYREV, B. M., AND REVKIND, A. I.: Zhur. Eksptl. i Teoret. Fiz. **27,** No. 1, 69 (1954); Phys. Abstracts **A58,** 135 (1955).
(328) KOZYREV, B. M., AND SALIKHOV, S. G.: Doklady Akad. Nauk S.S.S.R. **58,** 1023 (1947).
(329) KRAMERS, H. A.: Proc. Amsterdam Acad. Sci. **33,** 959 (1930).
(330) KRUMHANSL, J. A.: Phys. Rev. **93,** 245 (1954).
(331) KUBO, R., AND TOMITA, K.: J. Phys. Soc. Japan **9,** 888 (1954).
(332) LACROIX, R.: Helv. Phys. Acta **27,** 283 (1954).
(333) LACROIX, R., AND EXTERMANN, R. C.: Physica **17,** 427 (1951).
(334) LACROIX, R., RYTER, CH., AND EXTERMANN, R. C.: Phys. Rev. **80,** 763 (1950).
(335) LAMB, W.: Phys. Rev. **60,** 817 (1941).
(336) LANCASTER, F. W., AND GORDY, W.: J. Chem. Phys. **19,** 1181 (1951).
(337) LASAREW, B., AND SCHUBNIKOW, L.: Physik. Z. Sowjetunion **11,** 445 (1937).
(338) LECHER, H. Z.: Science **120,** 220 (1954).
(339) LEVINTHAL, E., ROGERS, E. H., AND OGG, R. A., JR.: Phys. Rev. **83,** 182 (1951).
(340) LEVY, R. A.: Phys. Rev. **98,** 264A (1955).
(341) LIDDEL, U., AND RAMSEY, N. F.: J. Chem. Phys. **19,** 1608 (1951).
(342) LINDSTRÖM, G.: Arkiv Fysik **4,** 1 (1951).
(343) LIPKIN, D., PAUL, D. E., TOWNSEND, J., AND WEISSMAN, S. I.: Science **117,** 534 (1953).
(344) LIPSCOMB, W. N.: J. Chem. Phys. **21,** 52 (1953).
(345) LIVINGSTON, R., ZELDES, H., AND TAYLOR, E. H.: Phys. Rev. **94,** 725 (1954).
(346) LLOYD, J. P., AND PAKE, G. E.: Phys. Rev. **92,** 1576 (1953).

(347) LLOYD, J. P., AND PAKE, G. E.: Phys. Rev. **94,** 579 (1954).
(348) LUTTINGER, J. M., AND KOHN, W.: Phys. Rev. **96,** 802 (1954).
(349) MALVANO, R., AND PANETTI, M.: Phys. Rev. **78,** 827 (1950).
(350) MANUS, C., BENE, G., DENIS, P., EXTERMANN, R., AND MERCIER, R.: Compt. rend. **239,** 414 (1954).
(351) MANUS, C., MERCIER, R., BENE, G. J., DENIS, P. M., AND EXTERMANN, R. C.: J. phys. radium **15,** 378 (1954).
(352) MANUS, C., MERCIER, R., DENIS, P., BENE, G., AND EXTERMANN, R.: Compt. rend. **238,** 1315 (1954).
(353) MAREL, L. A. VAN DER: Kolloid Z. **134,** 32 (1953).
(354) MASUDA, Y., AND KANDA, T.: J. Phys. Soc. Japan **8,** 432 (1953).
(355) MASUDA, Y., AND KANDA, T.: J. Phys. Soc. Japan **9,** 82 (1954).
(356) MATHESON, M. S., AND SMALLER, B.: J. Chem. Phys. **23,** 521 (1955).
(357) MATLOW, S. L.: J. Chem. Phys. **23,** 152 (1955).
(358) MCCLURE, D. S.: J. Chem. Phys. **20,** 682 (1952).
(359) MCCONNELL, H. M.: J. Chem. Phys. **23,** 760 (1955).
(360) MCCONNELL, H. M.: Submitted for publication.
(361) MCCONNELL, H. M., MCLEAN, A. D., AND REILLY, C. A.: To be published.
(362) MCGARVEY, B. R., AND GUTOWSKY, H. S.: J. Chem. Phys. **21,** 2114 (1953).
(363) MCNEIL, E. G., SLICHTER, C. P., AND GUTOWSKY, H. S.: Phys. Rev. **84,** 1245 (1951).
(364) MEYER, L. H., AND GUTOWSKY, H. S.: J. Phys. Chem. **57,** 481 (1953).
(365) MEYER, L. H., SAIKA, A., AND GUTOWSKY, H. S.: J. Am. Chem. Soc. **75,** 4567 (1953).
(366) MICHAELIS, L., SCHUBERT, M. P., REBER, R. K., KUCK, J. A., AND GRANICK, S.: J. Am. Chem. Soc. **60,** 1678 (1938).
(367) MOFFITT, W. E., AND COULSON, C. A.: Trans. Faraday Soc. **44,** 81 (1948).
(368) MONTGOMERY, C. G.: *Technique of Microwave Measurements*, pp. 161, 498. McGraw-Hill Book Company, Inc., New York (1947).
(369) Reference 368, Chap. 6.
(370) MÜLLER, E.: Fortschr. chem. Forsch. **1,** 325 (1949).
(371) MÜLLER, E., AND LEY, K.: Chem. Ber. **87,** 922 (1954).
(372) MÜLLER, E., AND MÜLLER-RODLOFF, I.: Ann. Chem. **517,** 134 (1935).
(373) MÜLLER, E., AND MÜLLER-RODLOFF, I.: Ann. Chem. **521,** 81 (1936).
(374) MÜLLER, E., AND MÜLLER-RODLOFF, I.: Chem. Ber. **69B,** 665 (1936).
(375) MUSTAFA, A., AND KAMEL, M.: Science **118,** 411 (1953).
(376) MUTO, J.: Progr. Theoret. Phys. (Japan) **4,** 243 (1949).
(377) MUTO, T., AND WATANABE, M.: Progr. Theoret. Phys. (Japan) **8,** 231 (1952).
(378) NAFE, J. E., AND NELSON, E. B.: Phys. Rev. **73,** 718 (1948).
(379) NAFE, J., AND NELSON, E.: Phys. Rev. **75,** 1194 (1949).
(380) NARDA COMPANY (Mineola, New York).
(381) NEWELL, G. F.: Phys. Rev. **80,** 476 (1950).
(382) NEWMAN, R.: J. Chem. Phys. **18,** 669 (1950).
(383) NEWMAN, R.: J. Chem. Phys. **18,** 1303 (1950); erratum **18,** 1678 (1950).
(384) NEWMAN, R., AND OGG, R. A., JR.: J. Chem. Phys. **19,** 214 (1951).
(385) NILSEN, W. G., AND FRAENKEL, G. K.: J. Chem. Phys. **21,** 1619 (1953).
(386) NORBERG, R. E.: Phys. Rev. **86,** 745 (1952).
(387) NORBERG, R. E., AND HOLCOMB, D. F.: Bull Am. Phys. Soc. **29,** No. 7, 11 (1954).
(388) NORBERG, R. E., AND SLICHTER, C. P.: Phys. Rev. **83,** 1074 (1951).
(389) NORMAN, I., AND PORTER, G.: Nature **174,** 508 (1954).
(390) OGG, R. A., JR.: J. Am. Chem. Soc. **68,** 155 (1946).
(391) OGG, R. A., JR.: J. Chem. Phys. **22,** 560 (1954).
(392) OGG, R. A., JR.: J. Chem. Phys. **22,** 1933 (1954).
(393) OGG, R. A., JR., AND RAY, J. D.: J. Chem. Phys. **22,** 147 (1954).
(394) O'MEARA, J. P., AND ROLLWITZ, W. L.: Abstracts of Papers Presented at the 124th Meeting of the American Chemical Society, Chicago, Illinois, September, 1953, p. 13D.

(395) ONO, K.: Rept. Inst. Sci. Technol. Univ. Tokyo **7,** 209 (1953); Chem. Abstracts **48,** 6822g (1954).
(396) ONO, K., ABE, H., SHIMADA, J., AND SHONO, H.: J. Phys. Soc. Japan **9,** 376 (1954).
(397) OVERHAUSER, A. W.: Phys. Rev. **89,** 689 (1953).
(398) OVERHAUSER, A. W.: Phys. Rev. **92,** 411 (1953).
(399) PACKARD, M. E.: Rev. Sci. Instr. **19,** 435 (1948).
(400) PACKARD, M. E.: Phys. Rev. **78,** 83 (1950).
(401) PACKARD, M. E., AND VARIAN, R.: Phys. Rev. **93,** 941A (1954).
(402) PACKARD, M. E., AND WEAVER, H. E., JR.: Phys. Rev. **88,** 163A (1952).
(403) PAKE, G. E.: J. Chem. Phys. **16,** 327 (1948).
(404) PAKE, G. E.: Am. J. Phys. **18,** 438, 473 (1950).
(405) PAKE, G. E.: J. chim. phys. **50,** C104 (1953).
(406) PAKE, G. E.: Ann. Rev. Nuc. Sci. **4,** 33 (1954).
(407) PAKE, G. E., AND GUTOWSKY, H. S.: Phys. Rev. **74,** 979 (1948).
(408) PAKE, G. E., AND PURCELL, E. M.: Phys. Rev. **74,** 1184 (1948).
(409) PAKE, G. E., AND SANDS, R. H.: Personal communication.
(410) PAKE, G. E., TOWNSEND, J., AND WEISSMAN, S. I.: Phys. Rev. **85,** 682 (1952).
(411) PAKE, G. E., WEISSMAN, S. I., AND TOWNSEND, J.: Discussions Faraday Soc., April 4–6, 1955.
(412) PENROSE, R. P.: Nature **163,** 992 (1949).
(413) PERLMAN, M. M., AND BLOOM, M.: Phys. Rev. **88,** 1290 (1952).
(414) PETCH, H. E., CRANNA, N. G., AND VOLKOFF, G. M.: Can. J. Phys. **31,** 837 (1953).
(415) PETCH, H. E., SMELLIE, D. W. L., AND VOLKOFF, G. M.: Phys. Rev. **84,** 602 (1951).
(416) PETCH, H. E., VOLKOFF, G. M., AND CRANNA, N. G.: Phys. Rev. **88,** 1201 (1952).
(417) PETER, BROTHER SIMON: Ph.D. Thesis, University of California, Berkeley, 1953.
(418) PETER, BROTHER SIMON: Phys. Rev. **93,** 940A (1954).
(419) PETERSON, S. W., AND LEVY, H.: J. Chem. Phys. **20,** 204 (1952).
(420) PINES, D.: Phys. Rev. **95,** 1090 (1954).
(421) PORTIS, A. M.: Phys. Rev. **91,** 1071 (1953).
(422) PORTIS, A. M., KIP, A. F., KITTEL, C., AND BRATTAIN, W. H.: Phys. Rev. **90,** 988 (1953).
(423) PORTIS, A. M., AND SHALTIEL, D.: Phys. Rev. **98,** 264A (1955).
(424) POULIS, N. J.: Physica **16,** 373 (1950).
(425) POULIS, N. J.: Physica **17,** 392 (1951).
(426) POULIS, N. J., AND HARDEMAN, G. E. G.: Physica **18,** 201, 315, 429 (1952).
(427) POULIS, N. J., AND HARDEMAN, G. E. G.: J. chim. phys. **50,** C110 (1953).
(428) POUND, R. V.: Rev. Sci. Instr. **17,** 490 (1946).
(429) POUND, R. V.: Phys. Rev. **72,** 527 (1947).
(430) POUND, R. V.: Phys. Rev. **73,** 523 (1948).
(431) POUND, R. V.: Phys. Rev. **79,** 685 (1950).
(432) POUND, R. V.: Phys. Rev. **81,** 156 (1951).
(433) POUND, R. V.: Progr. in Nuc. Phys. **2,** 21 (1952).
(434) POUND, R. V.: J. Phys. Chem. **57,** 743 (1953).
(435) POUND, R. V., AND KNIGHT, W. D.: Rev. Sci. Instr. **21,** 219 (1950).
(436) POWLES, J. G., AND GUTOWSKY, H. S.: J. Chem. Phys. **21,** 1695 (1953).
(437) POWLES, J. G., AND GUTOWSKY, H. S.: J. Chem. Phys. **21,** 1704 (1953).
(438) PRATT, L., AND RICHARDS, R. E.: Trans. Faraday Soc. **49,** 744 (1953).
(439) PRATT, L., AND RICHARDS, R. E.: Trans. Faraday Soc. **50,** 670 (1954).
(440) PRINGLE, G. E.: Acta Cryst. **7,** 716 (1954).
(441) PROCTOR, W. G.: Phys. Rev. **79,** 35 (1950).
(442) PROCTOR, W. G., AND YU, F. C.: Phys. Rev. **76,** 1728 (1949).
(443) PROCTOR, W. G., AND YU, F. C.: Phys. Rev. **77,** 717 (1950).
(444) PROCTOR, W. G., AND YU, F. C.: Phys. Rev. **81,** 20 (1951).
(445) PRYCE, M. H. L., AND STEVENS, K. W. H.: Proc. Phys. Soc. (London) **A63,** 36 (1950).
(446) PURCELL, E. M.: Science **107,** 433 (1948).

(447) PURCELL, E. M.: Physica **17,** 282 (1951).
(448) PURCELL, E. M.: Science **118,** 431 (1953).
(449) PURCELL, E. M.: Am. J. Phys. **22,** 1 (1954).
(450) PURCELL, E. M., AND POUND, R. V.: Phys. Rev. **81,** 279 (1951).
(451) PURCELL, E. M., TORREY, H. C., AND POUND, R. V.: Phys. Rev. **69,** 37 (1946).
(452) QUINN, W. E., AND BROWN, R. M.: J. Chem. Phys. **21,** 1605 (1953).
(453) RABI, I. I., RAMSEY, N. F., AND SCHWINGER, J.: Revs. Mod. Phys. **26,** 167 (1954).
(454) RAGAN, G. L.: *Microwave Transmission Circuits,* p. 48. McGraw-Hill Book Company, Inc., New York (1948).
(455) RAMSEY, N.: Phys. Rev. **78,** 699 (1950).
(456) RAMSEY, N. F.: Phys. Rev. **86,** 243 (1952).
(457) RAMSEY, N. F.: *Nuclear Moments,* p. 15. John Wiley and Sons, Inc., New York (1953).
(458) RAMSEY, N. F.: *Nuclear Moments.* John Wiley and Sons, Inc., New York (1953).
(459) RAMSEY, N. F.: Phys. Rev. **91,** 303 (1953).
(460) RAMSEY, N. F., AND PURCELL, E. M.: Phys. Rev. **85,** 143 (1952).
(461) REDFIELD, A. G.: Bull. Am. Phys. Soc. **30,** No. 1, 43 (1955).
(462) REIF, F., AND PURCELL, E. M.: Phys. Rev. **91,** 631 (1953).
(463) REILLY, C. A., MCCONNELL, H. M., AND MEISENHEIMER, R. G.: Phys. Rev. **98,** 264A (1955).
(464) RICHARDS, R. E., AND SMITH, J. A. S.: Trans. Faraday Soc. **47,** 1261 (1951); erratum **48,** 675 (1952).
(465) RICHTER, H. L., JR., HUMPHREY, F. B., AND YOST, D. M.: Rev. Sci. Instr. **25,** 190 (1954).
(466) ROBERTS, A.: Rev. Sci. Instr. **18,** 845 (1947).
(467) ROCHOW, E. G., AND LECLAIR, H. G.: J. Inorg. Phys. Chem. **1,** 92 (1955).
(468) RODIER, G.: Compt. rend. **232,** 513 (1951).
(469) ROGERS, E. H., AND STAUB, H. H.: Phys. Rev. **76,** 585 (1949).
(470) ROLLIN, B. V., AND HATTON, J.: Phys. Rev. **74,** 346 (1948).
(471) ROSE, M. E.: Phys. Rev. **53,** 715 (1938).
(472) ROSS, I. M., AND JOHNSON, F. B.: Nature **167,** 286 (1951).
(473) ROYDEN, V.: Phys. Rev. **96,** 543 (1954).
(474) RUDDERMAN, M. A., AND KITTEL, C.: Phys. Rev. **96,** 99 (1954).
(475) RUSHWORTH, F. A.: J. Chem. Phys. **20,** 920 (1952).
(476) RUSHWORTH, F. A.: Proc. Roy. Soc. (London) **A222,** 526 (1954).
(477) SACHS, A. M., AND TURNER, E. H.: Quoted by E. M. Purcell: Physica **17,** 282 (1951).
(478) SACHS, A. M., TURNER, E. H., AND PURCELL, E. M.: Phys. Rev. **76,** 466 (1949).
(479) SAIKA, A., AND SLICHTER, C. P.: J. Chem. Phys. **22,** 26 (1954).
(480) SALIKHOV, S. G.: Izvest. Akad. Nauk S.S.S.R., Ser. Fiz. **16,** 748 (1952); Chem. Abstracts **47,** 9693f (1953).
(481) SALPETER, E. E.: Proc. Phys. Soc. (London) **A63,** 337 (1949).
(482) SANDS, R. H.: Phys. Rev. **98,** 266A (1955).
(483) SANDS, R. H., TOWNSEND, J., AND HOOD, H. P.: Phys. Rev. **95,** 607 (1954).
(484) SANFORD, R. L.: *Permanent Magnets,* National Bureau of Standards Circular C448 (1944).
(485) SCHNEIDER, E. E.: Proc. Phys. Soc. (London) **61,** 569 (1948).
(486) SCHNEIDER, E. E.: Phys. Rev. **93,** 919 (1954).
(487) SCHNEIDER, E. E., DAY, M. J., AND STEIN, G.: Nature **168,** 645 (1951).
(488) SCHNEIDER, E. E., AND ENGLAND, T. S.: Physica **17,** 221 (1951).
(489) SCHUMACHER, R. T., CARVER, T. R., AND SLICHTER, C. P.: Phys. Rev. **95,** 1089 (1954).
(490) SCHUSTER, N. A.: Rev. Sci. Instr. **22,** 254 (1951).
(491) SCHUSTER, N. A.: Ph.D. Thesis, Washington University, 1951.
(492) SCHUSTER, N. A., AND PAKE, G. E.: Phys. Rev. **81,** 886 (1951).
(493) SCHWAB, G. M., AND AGLIARDI, N.: Chem. Ber. **73,** 95 (1940).
(494) SCHWINGER, J.: Phys. Rev. **76,** 790 (1949).

(495) SCOTT, N. D., WALKER, J. F., AND HANSLEY, V. L.: J. Am. Chem. Soc. **58,** 2442 (1936).
(496) SEGALL, H., AND ASTON, J. G.: J. Chem. Phys. **23,** 528 (1955).
(497) SEGLEKEN, W. G., AND TORREY, H. C.: Bull. Am. Phys. Soc. **30,** No. 2, 14 (1955).
(498) SELWOOD, P. W., AND DOBRES, R. M.: J. Am. Chem. Soc. **72,** 3860 (1950).
(499) SELWOOD, P. W., AND SCHROYER, F. K.: Discussions Faraday Soc. **8,** 337 (1950).
(500) SEYMOUR, E. F. W.: Proc. Phys. Soc. (London) **A66,** 85 (1953).
(501) SHAPOSHNIKOV, I. G.: Zhur. Eksptl. i Teoret. Fiz. **17,** 824 (1947).
(502) SHAW, T. M., AND ELSKEN, R. H.: J. Chem. Phys. **21,** 565 (1953).
(503) SHAW, T. M., AND ELSKEN, R. H.: J. Appl. Phys. **26,** 313 (1955).
(504) SHAW, T. M., ELSKEN, R. H., AND KUNSMAN, C. H.: J. Assoc. Offic. Agr. Chemists **36,** 1070 (1953).
(505) SHAW, T. M., ELSKEN, R. H., AND PALMER, K. J.: Phys. Rev. **85,** 762A (1952).
(506) SHERIFF, R. E., AND WILLIAMS, D.: Phys. Rev. **82,** 651 (1951).
(507) SHERMAN, C.: Phys. Rev. **93,** 1429 (1954).
(508) SHONO, H.: Rept. Inst. Sci. and Technol., Univ. Tokyo **6,** 201 (1952).
(509) SHOOLERY, J. N.: J. Chem. Phys. **21,** 1899 (1953).
(510) SHOOLERY, J. N.: Anal. Chem. **26,** 1400 (1954).
(511) SHULMAN, R. G., MAYS, J. M., AND MCCALL, D. W.: Bull. Am. Phys. Soc. **30,** No. 1, 43 (1955).
(512) SINGER, L. S., AND SPENCER, E. G.: J. Chem. Phys. **21,** 939 (1953).
(513) SLICHTER, C. P.: Quoted by G. E. Pake: Ann. Rev. Nuc. Sci. **4,** 33 (1954).
(514) SLICHTER, C. P., AND PURCELL, E. M.: Phys. Rev. **76,** 466A (1949).
(515) SLICHTER, W. P., AND MAYS, J. M.: Bull. Am. Phys. Soc. **30,** No. 2, 36 (1955).
(516) SLOAN, G. J.: Ph.D. Thesis, University of Michigan, 1953.
(517) SMALLER, B.: Phys. Rev. **83,** 812 (1951).
(518) SMALLER, B., HENNIG, G. R., AND YASAITIS, E. L.: Phys. Rev. **97,** 239 (1955).
(519) SMALLER, B., MATHESON, M. S., AND YASAITIS, E. L.: Phys. Rev. **94,** 202 (1954).
(520) SMALLER, B., AND YASAITIS, E. L.: J. Chem. Phys. **21,** 1905 (1953).
(521) SMALLER, B., AND YASAITIS, E. L.: Rev. Sci. Instr. **24,** 991 (1953).
(522) SMALLER, B., YASAITIS, E. L., AVERY, E. C., AND HUTCHISON, D. A.: Phys. Rev. **88,** 414 (1952).
(523) SMITH, J. A. S.: Quart. Revs. (London) **7,** 279 (1953).
(524) SMITH, J. A. S., AND RICHARDS, R. E.: Trans. Faraday Soc. **48,** 307 (1952).
(525) SOGO, P. B., AND JEFFRIES, C. D.: Phys. Rev. **98,** 265A (1955).
(526) SOLT, J. H., JR., AND STRANDBERG, M. W. P.: Phys. Rev. **95,** 607A (1954).
(527) SOMMERS, H. S., WEISS, P. R., AND HALPERN, W.: Rev. Sci. Instr. **22,** 612 (1951).
(528) SOUTIF, M.: Rev. sci. **89,** 203 (1951).
(529) SOUTIF, M., AYANT, Y., AND DREYFUS, B.: J. chim. phys. **50,** C107 (1953).
(530) SOUTIF, M., DREYFUS, B., AND AYANT, Y.: Compt. rend. **233,** 395 (1951).
(531) SOUTIF, M., AND GABILLARD, R.: Physica **17,** 319 (1951).
(532) SPENCE, R. D., GUTOWSKY, H. S., AND HOLM, C. H.: J. Chem. Phys. **21,** 1891 (1953).
(533) SPENCE, R. D., MOSES, H. A., AND JAIN, P. L.: J. Chem. Phys. **21,** 380 (1953).
(534) SPERRY GYROSCOPE COMPANY (Great Neck, New York).
(535) SPOONER, R. B., AND SELWOOD, P. W.: J. Am. Chem. Soc. **71,** 2184 (1949).
(536) STRICK, E., BRADFORD, R., CLAY, C., AND CRAFT, A.: Phys. Rev. **84,** 363 (1951).
(537) SUGAWARA, T., MASUDA, Y., KANDA, T., AND KANDA, E.: Phys. Rev. **95,** 1355 (1954).
(538) SURYAN, G.: Current Sci. (India) **18,** 203 (1949).
(539) SURYAN, G.: Phys. Rev. **80,** 119 (1950).
(540) SURYAN, G.: Proc. Indian Acad. Sci. **A33,** 107 (1951).
(541) TAKAHASHI, I., OKAYA, A., AND OGAWA, T.: Bull. Inst. Chem. Research, Kyoto Univ. **27,** 56 (1951); Chem. Abstracts **48,** 8655i (1954).
(542) TAYLOR, K.: Nature **172,** 722 (1953).
(543) THEILACKER, W., KORTÜM, G., AND FRIEDHEIM, G.: Chem. Ber. **83,** 508 (1950).
(544) THOMAS, H. A.: Phys. Rev. **80** 901 (1950).

(545) THOMAS, H. A.: Electronics **25,** No. 1, 114 (1952).
(546) THOMAS, H. A., DRISCOLL, R. L., AND HIPPLE, J. A.: J. Research Natl. Bur. Standards **44,** 569 (1950).
(547) THOMAS, H. A., DRISCOLL, R. L., AND HIPPLE, J. A.: Phys. Rev. **78,** 787 (1950).
(548) THOMAS, H. A., AND HUNTOON, R. D.: Rev. Sci. Instr. **20,** 516 (1949).
(549) THOMAS, J. T., ALPERT, N. L., AND TORREY, H. C.: J. Chem. Phys. **18,** 1511 (1950).
(550) TINKHAM, M., AND KIP, A. F.: Phys. Rev. **83,** 657 (1951).
(551) TINKHAM, M., WEINSTEIN, R., AND KIP, A. F.: Phys. Rev. **84,** 848 (1951).
(552) TOMITA, K.: Phys. Rev. **89,** 429 (1953).
(553) TOMITA, K., AND MANNARI, I.: Progr. Theoret. Phys. (Japan) **10,** 367 (1953).
(554) TORREY, H. C.: Phys. Rev. **76,** 1059 (1949).
(555) TORREY, H. C.: Phys. Rev. **85,** 365 (1952).
(556) TORREY, H. C.: Phys. Rev. **92,** 962 (1953).
(557) TORREY, H. C.: Phys. Rev. **96,** 690 (1954).
(558) TORREY, H. C., AND WHITMER, C. A.: *Crystal Rectifiers*, p. 189. McGraw-Hill Book Company, Inc., New York (1948).
(559) TOWNES, C. H., HERRING, C., AND KNIGHT, W. D.: Phys. Rev. **77,** 852 (1950).
(560) TOWNES, C. H., AND TURKEVICH, J.: Phys. Rev. **77,** 148 (1950).
(561) TOWNSEND, J., WEISSMAN, S. I., AND PAKE, G. E.: Phys. Rev. **89,** 606 (1953).
(562) TUTTLE, W. N.: Proc. Inst. Radio Engrs. **28,** 23 (1940).
(563) UEBERSFELD, J.: Compt. rend. **239,** 240 (1954).
(564) UEBERSFELD, J.: J. phys. radium **16,** 78 (1955).
(565) UEBERSFELD, J., AND COMBRISSON, J.: J. phys. radium **14,** 104 (1953).
(566) UEBERSFELD, J., ETIENNE, A., AND COMBRISSON, J.: Nature **174,** 614 (1954).
(567) VAN VLECK, J. H.: *Electric and Magnetic Susceptibilities*, Chap. 10. Oxford University Press, London (1932).
(568) VAN VLECK, J. H.: *Electric and Magnetic Susceptibilities*, Chap. 12. Oxford University Press, London (1932).
(569) VAN VLECK, J. H.: Phys. Rev. **74,** 1168 (1948).
(570) VARIAN ASSOCIATES (Palo Alto, California).
(571) VARIAN ASSOCIATES: Publication 142, Palo Alto, California (1955).
(572) VENKATARAMAN, B., AND FRAENKEL, G. K.: Abstracts of Papers Presented at the 126th Meeting of the American Chemical Society, New York City, September, 1954, p. 22R.
(573) VENKATARAMAN, B., AND FRAENKEL, G. K.: J. Chem. Phys. **23,** 588 (1955).
(574) VERBRUGGE, F.: Am. J. Phys. **21,** 603 (1953).
(575) VERBRUGGE, F., AND HENRY, R. L.: Phys. Rev. **83,** 211 (1951).
(576) VOLKOFF, G. M.: Can. J. Phys. **31,** 820 (1953).
(577) VOLKOFF, G. M., AND LAMARCHE, G.: Can. J. Phys. **32,** 493 (1954).
(578) VOLKOFF, G. M., PETCH, H. E., AND SMELLIE, D. W. L.: Can. J. Phys. **30,** 270 (1952).
(579) WALCHLI, H. E.: Phys. Rev. **90,** 331 (1953).
(580) WALCHLI, H. E.: "A Table of Nuclear Moment Data," Publication ORNL-1469, Oak Ridge National Laboratory (1953).
(581) WALCHLI, H. E., AND MORGAN, H. W.: Phys. Rev. **87,** 541 (1952).
(582) WALLER, I.: Z. Physik **79,** 370 (1932).
(583) WALLMAN, H., MACNEE, A. B., AND GADSDEN, C. P.: Proc. Inst. Radio Engrs. **36,** 700 (1948).
(584) WALSH, J. L., BERGER, A. G., ROGERS, J. V., AND KNIGHT, W. D.: Phys. Rev. **98,** 265A (1955).
(585) WANGSNESS, R. K.: Am. J. Phys. **21,** 274 (1953).
(586) WANGSNESS, R. K., AND BLOCH, F.: Phys. Rev. **89,** 728 (1953).
(587) WARD, R. L., AND WEISSMAN, S. I.: J. Am. Chem. Soc. **76,** 3612 (1954).
(588) WARING, C. E., SPENCER, R. H., AND CUSTER, R. L.: Rev. Sci. Instr. **23,** 497 (1952).
(589) WASHINGTON UNIVERSITY DEPARTMENT OF PHYSICS: Final ONR Report, NR 310-802 (1954).

(590) WATKINS, G. D.: Ph.D. Thesis, Harvard University, 1951.
(591) WATKINS, G. D., AND POUND, R. V.: Phys. Rev. **85,** 1062 (1952).
(592) WAUGH, J. S., HUMPHREY, F. B., AND YOST, D. M.: J. Phys. Chem. **57,** 486 (1953).
(593) WAUGH, J. S., SHOOLERY, J. N., AND YOST, D. M.: Rev. Sci. Instr. **23,** 441 (1952).
(594) WEAVER, H. E., JR.: Phys. Rev. **89,** 923 (1953).
(595) WEIDNER, R. T., AND WHITMER, C. A.: Rev. Sci. Instr. **23,** 75 (1952).
(596) WEIDNER, R. T., AND WHITMER, C. A.: J. Chem. Phys. **20,** 749 (1952).
(597) WEIDNER, R. T., AND WHITMER, C. A.: Phys. Rev. **91,** 1279 (1953).
(598) WEISSMAN, S. I.: J. Chem. Phys. **22,** 1135 (1954).
(599) WEISSMAN, S. I.: J. Chem. Phys. **22,** 1378 (1954).
(600) WEISSMAN, S. I.: Private communication.
(601) WEISSMAN, S. I., AND BANFILL, D.: J. Am. Chem. Soc. **75,** 2534 (1953).
(602) WEISSMAN, S. I., AND SOWDEN, J. C.: J. Am. Chem. Soc. **75,** 503 (1953).
(603) WEISSMAN, S. I., TOWNSEND, J., PAUL, D. E., AND PAKE, G. E.: J. Chem. Phys. **21,** 2227 (1953).
(604) WERTZ, J. E.: To be published.
(605) WERTZ, J. E., AND VIVO, J. L.: To be published.
(606) WHELAND, G. W.: *Advanced Organic Chemistry,* p. 696. John Wiley and Sons, Inc., New York (1949).
(607) WHITE, H. E.: *Introduction to Atomic Spectra,* p. 157. McGraw-Hill Book Company, Inc., New York (1934).
(608) WILLENBROCK, F. K., AND BLOEMBERGEN, N.: Phys. Rev. **91,** 1281 (1953).
(609) WILLIAMS, D.: Physica **17,** 454 (1951).
(610) WILLIAMS, R. B.: Abstracts, Pittsburgh Conference on Applied Spectroscopy (1955).
(611) WILSON, C. W., III, AND PAKE, G. E.: J. Polymer Sci. **10,** 503 (1953).
(612) WIMETT, T. F.: Phys. Rev. **91,** 476A (1953).
(613) WINTER, J., SALMON, J., MANUS, C., BENE, G., DENIS, P., AND EXTERMANN, R.: Compt. rend. **239,** 803 (1954).
(614) YAFET, Y.: Phys. Rev. **85,** 478 (1952).
(615) YAGER, W. A., GALT, J. K., MERRITT, F. R., AND WOOD, E. A.: Phys. Rev. **80,** 744 (1950).
(616) YASAITIS, E., AND SMALLER, B.: Phys. Rev. **82,** 750 (1951).
(617) YASAITIS, E. L., AND SMALLER, B.: Phys. Rev. **92,** 1068 (1953)
(618) YOKOZAWA, Y., AND TATSUZAKI, L.: J. Chem. Phys. **22,** 2087 (1954).
(619) ZAVOISKY, E.: J. Phys. (U.S.S.R.) **9,** 245, 447 (1945).
(620) ZAVOISKY, E. K.: J. Phys. (U.S.S.R.) **10,** 170, 197 (1946).
(621) ZAVOISKY, E. K.: Doklady Akad. Nauk S.S.S.R. **57,** 887 (1947); Chem. Zentr. (Russian Zone Ed.) **1949, I,** 170.
(622) ZELDES, H., AND LIVINGSTON, R.: Phys. Rev. **96,** 1702 (1954).
(623) ZENER, C.: Phys. Rev. **81,** 440 (1951).
(624) ZENER, C., AND HEIKES, R. R.: Revs. Mod. Phys. **25,** 191 (1953).
(625) ZIEL, A. VAN DER: *Noise,* p. 343. Prentice-Hall, Inc., New York (1954).
(626) ZIMMERMAN, J. R.: J. Chem. Phys. **21,** 1605 (1953).
(627) ZIMMERMAN, J. R.: J. Chem. Phys. **22,** 950 (1954).

XXX. LIST OF RECURRING SYMBOLS

c = speed of light
DPPH = 1,1-diphenyl-2-picrylhydrazyl
e = electronic charge
E = energy
ESR = electron spin resonance
g = defined by $h\nu = g\mu_n H_z$ or $h\nu = g\mu_B H_z$

$g_{\|}$, $g_{\perp}$ = g-components parallel and perpendicular to axis of symmetry
H = magnetic field
H_1 = amplitude of rotating radiofrequency field
H_c = resonant field for observed compound
H_r = resonant field for reference compound
H_x, H_y = x- and y-field components
H_z = applied steady magnetic field
H_{eff} = sum of H_z plus local fields
H_{loc} = local (internal) field
$\mathcal{H}$ = Hamiltonian
ΔH, $\Delta H_{1/2}$ = field deviation from center of resonance; line width at half-height
ΔH_{MS} = separation in gauss of points of maximum slope
I = nuclear spin
$\mathbf{I}$ = nuclear spin operator
J = total angular momentum quantum number
J_{ik} = coupling constant
k = Boltzmann constant
kcps = Kilocycles per second
L = torque; orbital angular momentum quantum number
m = mass
M = magnetic quantum number
Mcps = Megacycles per second
$\mathfrak{M}$ = magnetic moment per unit volume (magnetic polarization)
$\mathfrak{M}_0$ = equilibrium moment in z-direction
$\mathfrak{M}_x$, $\mathfrak{M}_y$, $\mathfrak{M}_z$ = components of macroscopic magnetic moment
N = number of dipoles per cm.^{3}
NSR = nuclear spin resonance
p = angular momentum
$\mathcal{P}$ = radiofrequency energy absorbed per cm.^{3} sec.
Q = quality factor of tuned circuit
q = charge
r = radius
$\mathbf{r}$ = radius vector
r_{jk} = interatomic distance
S = spin quantum number
$\mathbf{S}$ = spin operator
t = time
t_1 = thermal relaxation time
t_2 = dipole–dipole relaxation time
T = absolute temperature
v = velocity
V = electrostatic potential
W = energy
α = demagnetizing factor for shape of sample

γ = magnetogyric (gyromagnetic) ratio
θ = angle
μ = magnetic moment
μ_B = Bohr magneton
μ_I = nuclear magnetic moment
μ_n = nuclear magneton
μ_{eff} = effective Bohr magneton number
ν = frequency
ν_0 = resonant frequency
$\Delta\nu = \nu - \nu_0$
σ = shielding constant
τ_c = correlation time
χ = volume susceptibility (may be complex)
χ' = real component of high-frequency susceptibility
χ'' = out-of-phase component of high-frequency susceptibility
χ_0 = static volume susceptibility
ψ = wave function
ω = angular frequency
ω_0 = angular velocity of precession; resonant angular frequency
$\Delta\omega = \omega - \omega_0$